Stretch, stiffness, sensing, signaling & speed

STRETCH, STIFFNESS, SENSING, SIGNALING *& SPEED*

Mechanical activation of Cardiac Fibroblasts

Meike Ploeg

Stretch, Stiffness, Sensing, Signaling & Speed:

Mechanical Activation of Cardiac Fibroblasts

Meike Ploeg

Colofon

STRETCH, STIFFNESS, SENSING, SIGNALING & SPEED
Mechanical activation of Cardiac Fibroblasts
Meike Ploeg

ISBN: 978-94-6458-835-4

Printing: Ridderprint, www.ridderprint.nl
Cover art, layout and design: Elisa Calamita, www.elisacalamita.com

STRETCH, STIFFNESS, SENSING, SIGNALING & SPEED

Mechanical activation of Cardiac Fibroblasts

PROEFSCHRIFT

ter verkrijging van de graad van doctor aan de Universiteit Maastricht,

op gezag van de Rector Magnificus, Prof. dr. Pamela Habibović

volgens het besluit van het College van Decanen,

in het openbaar te verdedigen

op dinsdag 24 januari 2023 om 13.00 uur

door

Meike Christianne Ploeg,

Geboren op 6 februari 1993, te Zeewolde, Nederland

Promotors
Prof. dr. F.W. Prinzen
Dr. F.A. van Nieuwenhoven

Beoordelingscommissie
Prof. dr. U. Schotten (voorzitter)
Dr. W.M. Blankesteijn
Prof. Dr. M.J.T.H. Goumans (Leids Universitair Medisch Centrum)
R. Peyronnet, PhD (University of Freiburg, Germany)
Prof. Dr. B.L.M. Schroen

Table of contents

General introduction

1

The healthy heart

The human heart consists of two atria and two ventricles. The atria are the upper receiving chambers, collecting venous blood. The ventricles comprise most of the heart's tissue volume and lie below the atria [1]. The ventricles pump blood to the other organs and itself in order to provide sufficient oxygen and metabolites to maintain organ function. It does so by generating force through contraction, providing pressure to pump blood through the arteries [2, 3]. Under physiological conditions, the heart is filled during diastole [4] causing stretching of cardiomyocytes (CMs)[5] and other cardiac cell types (preload)[6, 7]. During systole, ventricular pressure has to overcome diastolic pulmonary and aortic artery pressure (afterload) to open the pulmonary and aortic valves, respectively [4, 8].

Alterations in both preload and afterload lead to changes in cardiac structure, at the macroscopic, microscopic and molecular levels. Such changes are often referred to as cardiac remodeling. Cardiac remodeling can be defined as changes in structural, contractile and electrical processes that manifest clinically as changes in size, shape and function of the heart driven by a change in cardiac load or injury, ultimately leading to heart failure [9, 10].

Cardiovascular diseases and heart failure

Cardiovascular Diseases are a set of heterogeneous diseases affecting heart and circulatory system [11-13]. It has been and still is the leading cause of death worldwide [14, 15]. It is estimated that by the year 2030, 23.6 million people will die of Cardiovascular Diseases each year [12, 13].

Heart failure is the third most prevalent Cardiovascular Disease in the United States [16, 17]. In the Netherlands, there are 250,000 patients with heart failure, accounting for around 19% of all cardiac deaths [18]. Heart failure is also costly, due to frequent hospitalizations. In 2020 on average 80 patients per day were admitted to the hospital due to heart failure [18]. Heart failure develops secondary to diseases like myocardial infarction, valvular disease or chronic high blood pressure [9, 19, 20]. Important factors in the development of heart failure are the changes in the composition of the myocardium like changes in the myocytes and in the interstitial tissue [21, 22]. Better insight in these "remodeling" processes will contribute to better treatment of heart failure.

Myocardial remodeling

Myocardial tissue largely consists of CMs, cardiac fibroblasts (CFs), endothelial cells and vascular smooth muscle cells [23, 24]. CMs are rhythmically contracting cells that are aligned into fiber-like structures [25, 26]. Although CMs generate the contraction of the

heart, CFs produce the components of the cardiac extracellular matrix (ECM) [27-31] and are therefore important for maintaining the integrity of the heart [32, 33]. The cardiac ECM consists of structural matrix proteins like collagens (mainly of collagen type 1) [32, 34], elastin, laminins and fibronectin [33-35]. Besides structural matrix proteins the ECM also contains matricellular proteins: a group of ECM-regulatory proteins that includes proteins like connective tissue growth factor (CTGF/CCN2), thrombospondins and tenascins [33, 36]. Moreover, recently our research group discovered cartilage intermediate layer protein 1 (Cilp1) as matricellular protein in the cardiac ECM [37]. In addition to producing ECM proteins and matricellular proteins, CFs also produce matrix metalloproteinases (MMPs) and tissue inhibitors of MMPs (TIMPs), the balance of which can modulate the degradation of the ECM [32, 38], resulting in control over the cardiac ECM turnover [33, 38]. Moreover, CFs are activated in response to injury, then called myofibroblasts [39, 40], and participate as key players in the wound healing response [30, 41-43].

Cardiac remodeling processes can serve as physiological adaptation of the heart to maintain its function in abnormal loading conditions like pressure and volume overload [9, 19], exercise or pregnancy [44, 45]. However, such adaptations can also become maladaptive. The transition from adaptive to maladaptive remodeling is difficult to predict or identify since the occurrence and time course can vary [9]. Maladaptive changes are often associated with the expansion and/or reorganization of the ECM and molecular changes affecting contractile function [10, 46, 47]. Such maladaptive remodeling then worsens the mechanical performance of the heart, thus creating a vicious circle, aggravating heart failure [9, 10].

There is considerable evidence that cardiac remodeling is determined by a combination of mechanical, neurohumoral, and local autocrine/paracrine factors [9]. The neurohumoral factors, stem from the physiological regulation of blood pressure and volume: the sympathetic nervous system (SNS) and renin-angiotensin-aldosterone system (RAAS) [48]. Activation of the SNS increases in heart rate, contractility and vascular tone [48, 49]. Activation of RAAS also results in vasoconstriction and an increase in blood volume [48, 50]. The vasoconstriction and increased blood volume will also further enhance venous return to the heart and causes increased filling of the ventricles and stretch of the myocardium [48]. Chronic activation of the SNS and RAAS leads to structural and functional changes within the myocardium, resulting in cardiac remodeling [50-53].

In response to wall stretch cardiac tissues produce natriuretic peptides [54-58]. Atrial natriuretic peptide (ANP, encoded by the NPPA gene) and brain natriuretic peptide (BNP, encoded by the NPPB gene) [59, 60] are mainly found in the atria and ventricles respectively, but have been found in other tissues as well [61-64]. The third natriuretic peptide is C-type natriuretic peptide (CNP, encoded by the

NPPC gene) and is mainly produced in endothelial tissue [61, 65]. *In vitro* studies have shown increased expression of ANP and BNP in CMs after mechanical stimulation in the form of

cyclic stretch [66, 67]. It has been suggested that natriuretic peptides, but BNP specifically, prevents development of cardiac fibrosis by serving as an antifibrotic signal to CFs during cardiac remodeling [68].

Cardiac fibrosis

Cardiac fibrosis develops as a consequence of pathological conditions, like cardiac overload or myocardial infarction [69]. Cardiac fibrosis starts with the differentiation of CFs towards myofibroblast as a critical event [34, 70, 71]. Myofibroblasts are characterized by the synthesis of α-smooth muscle actin (α-SMA), transcribed from the Acta2 gene, and organized in stress fibers. Myofibroblasts have active migratory, proliferative and secretory properties [72]. The differentiation of CFs to myofibroblasts is controlled by the joint action of growth factors like transforming growth factor (TGFb1), specialized ECM proteins like the fibronectin, and the mechanical microenvironment [72, 73]. Moreover, myofibroblasts exhibit increased fibrillar collagen synthesis within the ECM leading to alterations in matrix composition and structure [33] and cell-perceived ECM stiffening [74, 75]. Together, these alterations in the matrix composition and structure, the induction of growth factors and cytokines, increased mechanical stress, and the release of neurohormonal factors all contribute to myofibroblasts differentiation [34, 69]. Eventually leading towards increased ECM stiffness [76, 77]. After myocardial injury, the myofibroblasts stay within the myocardial scar in a state referred to as the matrifibrocyte [78]. The formation of fibrotic tissue following MI has a functional purpose of healing the myocardium and replacement of dead cells [79], thereby preventing further damage. However, as a consequence of fibrosis, conduction propagation is disturbed [80-82], myocardial tissue becomes stiffer [76, 77], which then causes impaired cardiac filling [83-85], while the replacement of CMs by CFs reduces contractility [85], ultimately leading towards impaired cardiac function [34, 86, 87]. However, an impaired healing process, by inhibition of the immune response or TGFβ1, has more detrimental consequences, such as ventricular rupture or left ventricular dilatation [88-90] . Therefore, balance is key when it comes to the fibrotic response.

In conclusion, CFs are quiescent cells under physiological conditions, but become activated and go through different states of differentiation and adaptation following cardiac injury or overload (figure 1). Upon injury, they become activated, at which they elongate and begin to express αSMA. As time of injury progresses, the myofibroblast differentiated state is maximal, with high levels of αSMA protein in elongated processes within these cells. Finally, these fibroblasts stop proliferating and lose αSMA expression as they further differentiate into the matrifibrocyte within the scar region [78]. With the use of single-cell transcriptomics different populations of fibroblasts have been identified [91, 92]. More specifically, such sub-populations of CFs have been identified as key drivers in fibrosis [93]. These studies show the complexity and diversity of CFs and their role in fibrosis. In the present thesis, we focus on the activation of CFs by mechanical stimulation.

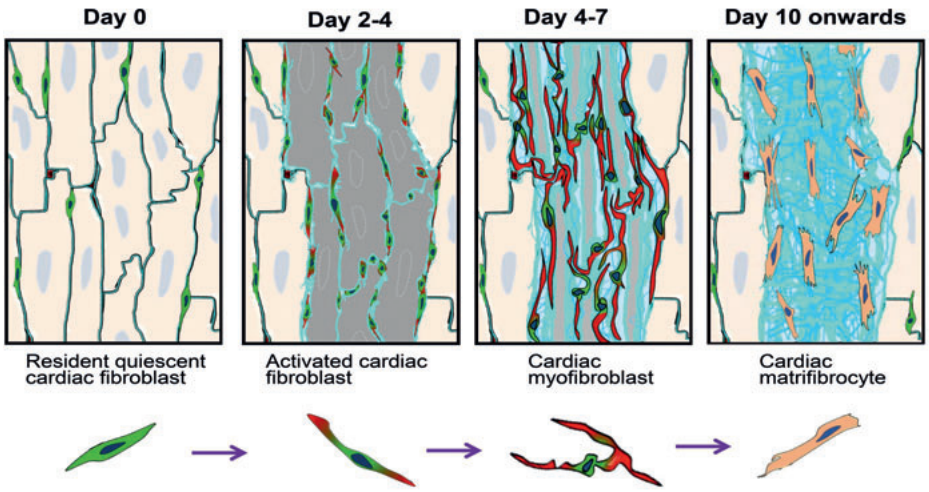

Figure 1. Different stages of CF activation. Quiescent CFs (green) reside in the interstitial space, surrounded by CMs (beige) within the ECM. After myocardial injury CMs die (grey) and CFs become activated (red) and start producing αSMA protein and ECM products (aqua). Over time debris from CMs is cleared and CFs are differentiated towards myofibroblasts (red-green) implementing αSMA proteins into stress fibers. More ECM product is formed as replacement in the healing process (stripes in the aqua area). Eventually myofibroblasts stop proliferating and lose αSMA expression, then differentiate towards matrifibrocytes (brown), which stay within the healed scar. Figure from Fu et al. [78]

Cardiac fibroblast mechanosensing

Besides the above described functions in cardiac ECM organization, CFs have an important role as intermediate sensor and amplifier of signals from immune cells and CMs, through the production of autocrine and paracrine mediators such as cytokines, growth factors, prostaglandins, and nitric oxide [41, 94-96]. Communication between CFs and other cardiac cells happens through direct cell-cell contacts, soluble paracrine factors and ECM-mediated interactions [27, 97, 98].

Complex and dynamic crosstalk between the different cell types and the ECM is important for cardiac function [27, 99]. CFs are able to sense increased mechanical loads in order to respond to changes in load. Every heart beat generates load changes, resulting in changes in load with a frequency in the order of 1 Hz in humans [100]. However, load also fluctuates due to changes in physical activity (in order to minutes – hours) and due to diseases, such as hypertension and valvular disease, that last for many days to years. The exact mechanical signals are not entirely clear, but stretch of the cells as well as stiffness of the surrounding ECM are important for CF function [100, 101]. Mechanical forces are interpreted by cells via mechanotransduction: the conversion of mechanical stimuli into biochemical activity [6, 102]. There are four different pathways by which gene expression might be regulated through mechanical signals. The first pathway is initiated when mechanical force leads to

ECM activation converting the mechanical signal into a biochemical signal, already in the ECM which acts downstream via cell surface proteins. Secondly, signaling happens via direct mechanical activation of cell surface transmembrane proteins, which convert the mechanical signal into intracellular biochemical signals at the level of the plasma membrane. Thirdly, mechanical signaling might travel via the cytoskeleton and finally, mechanical signaling can directly affect the nucleus (figure 2) [6]. Moreover, mechanical stress can induce the synthesis and/or secretion of a growth factor that indirectly regulates CF gene expression via an auto- or paracrine feedback loop [103].

Cell–matrix adhesion contacts form the physical link between the ECM and the cell via the cytoskeleton [103, 104].The main receptors that connect the cytoskeleton to the ECM are integrins [105], which transmit the tractional forces developed in the cytoskeleton to the ECM and vice versa [102, 106]. Besides this communicating role, integrins can also regulate signaling pathways, converting the mechanical stimulus into a biochemical signal [102, 107]. Integrins are also involved in the release from TGFβ from its binding complex in response to cell traction forces [108, 109]. TGFβ can be stored within the ECM which upon mechanical stimulation can be rapidly activated and released [6]. Toll-like receptors (TLRs) are another group of receptors activated by mechanical stress [110]. Danger-associated molecular patterns (DAMPs) are endogenous molecules, such as heat shock proteins [111] or ECM-derived molecules like tenascin C [112], capable of activating TLRs. Results obtained in the pressure overloaded heart suggest the release of DAMPs in the mechanically stressed heart [113, 114].

Besides these membrane receptors, also ion-channels can be mechanosensitive. Mechanical cues can lead to opening of so-called stretch-activated ion channels, such as Piezo1 [115]. Piezo1 is a calcium (Ca^{2+})-permeable, transmembrane nonselective cation channel, which can be activated by mechanical forces, such as stretch [115, 116]. Structurally three Piezo1 proteins together from a trimer, which together appears like a propeller blade with an ionic pore in the middle. The trimer perforates the cell membrane into the cytosol [117], which is thought to be critical in force sensing [118, 119]. Increased membrane tension, induced by stretch, opens Piezo1 channel to allow permeation of cations, including calcium [120-122]. Calcium fulfills an important role in CFs, controlling ECM synthesis and cell proliferation [123, 124] but is also involved in CFs activation towards myofibroblasts [125]. Recently it has been shown that both human and mouse CFs express functional Piezo1 channels, which are indeed mechanosensitive and that activation of Piezo1 induces expression and secretion of IL-6 [126]. Gain-of-function Piezo1 mutation causes activation of hypertrophic and fibrotic signals in the myocardium, leading to pathological cardiac remodeling in mice [127].

From the surface molecules, like integrins, mechanotransduction is propagated via the cytoskeleton. The cytoskeleton is the dynamic structural network providing shape and stability, enables cell function and is the physical connection within the cell [128]. The cytoskeleton experiences isometric tension, under influence of ECM stiffness, resulting in an interaction between cytoskeleton stiffness and ECM stiffness [129]. The family of small

Rho GTPases, like RhoA, are an example of mechanotransduction pathways communicating from the surface via the cytoskeleton. By the interaction of RhoA with Rho kinase (ROCK), the latter becomes activated resulting in phosphorylation of several downstream targets, which among others are involved in stress fiber formation [130].

Signals reach the nucleus via specialized proteins that are part of the linker nucleoskeleton and cytoskeleton (LINC) complex spanning the nuclear envelope [131] and eventually leading to gene transcription. Disruption of the LINC complex resulted in loss of the stiffness-sensing ability of CFs. No response on nuclear shape was detected whereas intact LINC complex shows that the nuclear shape is affected by substrate stiffness: round on soft substrates and flattened on stiff substrates [132]. Substrate stiffness also affected CFs responses, including motility and migration speed [132].

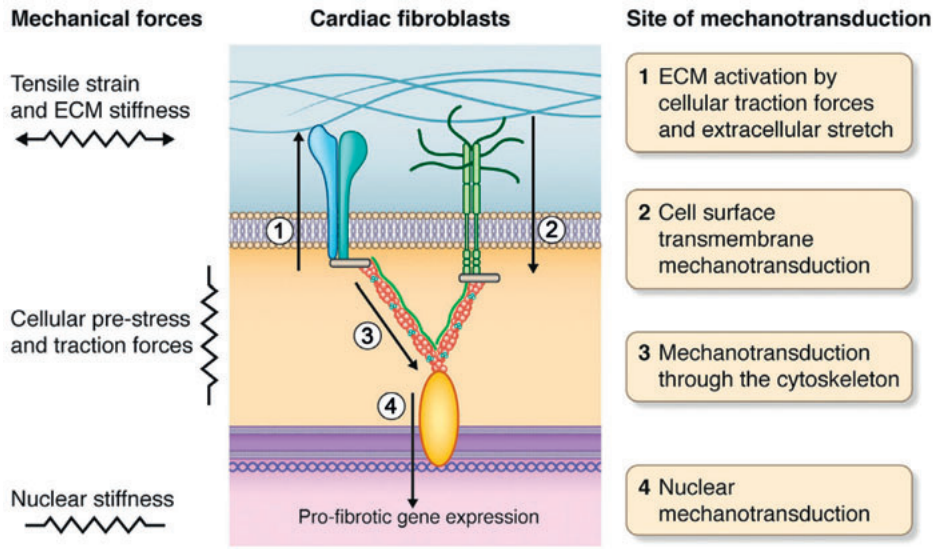

Figure 2. Mechanical signaling in CFs occurs at different levels eventually leading to pro-fibrotic gene expression. Figure from Herum et al. [6]

The information mentioned above shows how much is already known about mechanotransduction on a cellular level, however, the recent discovery of Piezo1 shows that there is still much unknown. Most information was gained from *in vitro* studies, since these allow for research on a specific cell type and in more detail. However, within myocardial tissue it is difficult to distinguish between the role of CFs and other cells. For the purpose of the specific role of CFs in mechanical stimulation, an *in vitro* model is most suitable. Here, we chose for a combination of *in vitro* 2D monolayer experiments and development of a 3D model of cells within a collagen 1 matrix to answer our research questions. Ultimately using an *in vivo* model to look at the broader picture of fibrosis.

Aim of the thesis

The general aim of this thesis is to investigate mechanisms of mechanosensing on activation of CFs. To gain further insight in these mechanisms, we have studied the following specific research questions:

- What is the role of the mechanosensitive ion channel piezo1 on stretch-induced expression of BNP and CILP1 in CFs?
- What is the influence of duration and amplitude of mechanical stimulation on CF activation?
- How do substrate stiffness and 3D culture conditions influence CF activation?
- What are the mechanisms leading to progressive changes in left atrial structure, including fibrosis, and function after chronic mitral regurgitation?

Stretch, stiffness, sensing, signaling & speed is the title of this thesis, reflecting the different aspects of mechanical activation in CFs investigated in this thesis. Figure 3 [133] visualizes the different research questions of this thesis.

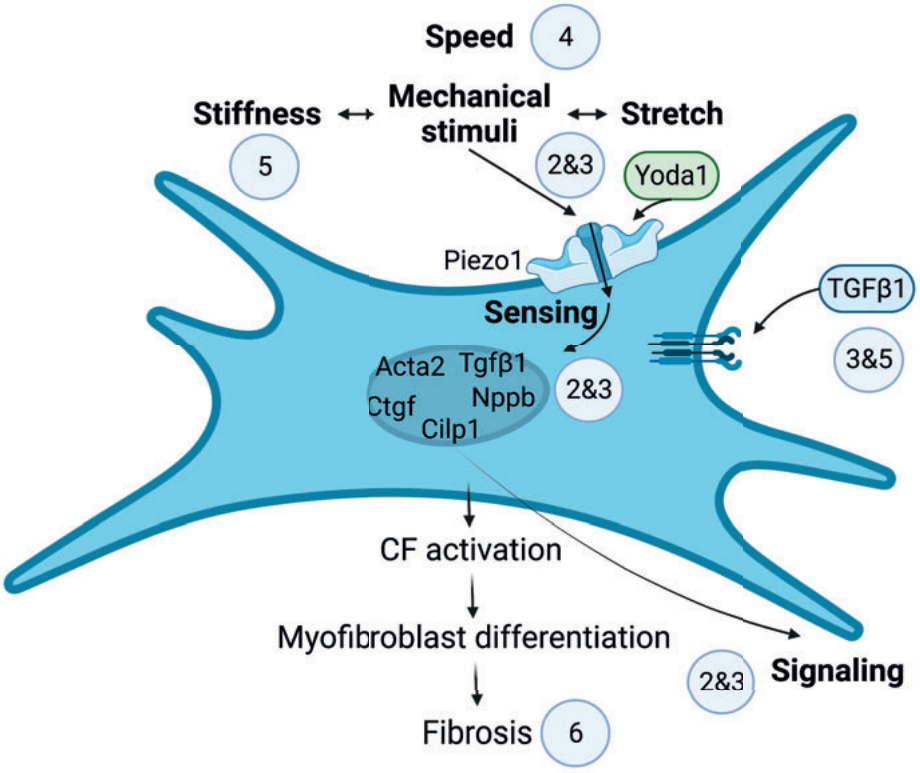

Figure 3. Visual summary of the different research questions aimed to answer in this thesis related to mechanical activation of CFs. The spheres implicate the number of the chapter in which the research question is answered.

Outline of the thesis

After this general introduction, chapter 2 and 3 describe studies investigating the effect of cyclic *stretch* on the expression of Nppb (chapter 2) and Cilp1 (chapter 3) and the role of mechanotransducer Piezo1 in *sensing* and *signaling*. Thereto CFs were exposed to mechanical stimulation in the form of 10% cyclic *stretch* at a frequency of 1 Hz, or the piezo1-agonist Yoda1.

Chapter 4 focusses on the effect of relatively short periods of *stretch* variation on the *speed* of CF activation in order to find the minimal stimulus necessary to initiate processes towards CF activation and differentiation.

Chapter 5 describes the development of a potentially more physiologically relevant *in vitro* model for studying the effect of *stiffness*, and *stretch* on CF function. Stiffness is an important mechanical stimulus for CFs.

Chapter 6 describes a combined animal and computer modeling study on the effect of long-lasting *stretch*, induced by mitral regurgitation in canine hearts, to investigate mechanisms of the progressive changes to left atrial structure, including fibrosis, and function.

In the final chapter, general discussion (chapter 7), the studies performed are put into broader perspective and suggestions for future investigations are made.

References

1. Marieb EN, Hoehn K. Human Anatomy and Physiology. San Francisco, CA: Pearson; 2013.
2. Ahmad F, Seidman JG, Seidman CE. The Genetic Basis for Cardiac Remodeling. Annual Review of Genomics and Human Genetics. 2005;6(1):185-216.
3. Jalil J. Structural vs. contractile protein remodeling and myocardial stiffness in hypertrophied rat left ventricle. Journal of Molecular and Cellular Cardiology. 1988;20(12):1179-87.
4. Zimmermann WH. Biomechanical regulation of in vitro cardiogenesis for tissue-engineered heart repair. Stem Cell Res Ther. 2013;4(6):137.
5. Toischer K, Rokita AG, Unsold B, Zhu W, Kararigas G, Sossalla S, et al. Differential cardiac remodeling in preload versus afterload. Circulation. 2010;122(10):993-1003.
6. Herum KM, Lunde IG, McCulloch AD, Christensen G. The Soft- and Hard-Heartedness of Cardiac Fibroblasts: Mechanotransduction Signaling Pathways in Fibrosis of the Heart. J Clin Med. 2017;6(5).
7. Zhang X, Kim TH, Thauland TJ, Li H, Majedi FS, Ly C, et al. Unraveling the mechanobiology of immune cells. Curr Opin Biotechnol. 2020;66:236-45.
8. RC T, MN L. Cardiac Responses to Increased Afterload. State-of-the-art Review. Hypertension. 1982;4(3):8-18.
9. Cohn JN, Ferrari R, Sharpe N. Cardiac remodeling—concepts and clinical implications: a consensus paper from an international forum on cardiac remodeling. Journal of the American College of Cardiology. 2000;35(3):569-82.
10. Segura AM, Frazier OH, Buja LM. Fibrosis and heart failure. Heart Fail Rev. 2014;19(2):173-85.
11. CDC. U.S. Department of Health and Human Services Centers for Disease Control and Prevention. Million hearts: strategies to reduce the prevalence of leading cardiovascular disease risk factors--United States. MMWR Morb Mortal Wkly Rep. 2011;60(36):1248-51.
12. Francula-Zaninovic S, Nola IA. Management of Measurable Variable Cardiovascular Disease' Risk Factors. Curr Cardiol Rev. 2018;14(3):153-63.
13. Kralj V, Biloš IB. Morbidity and mortality from cardiovascular diseases. Cardiologia Croatica. 2013;8(10-11).
14. Roth GA, Abate D, Abate KH, Abay SM, Abbafati C, Abbasi N, et al. Global, regional, and national age-sex-specific mortality for 282 causes of death in 195 countries and territories, 1980–2017: a systematic analysis for the Global Burden of Disease Study 2017. The Lancet. 2018;392(10159):1736-88.
15. Saglietto A, Manfredi R, Elia E, D'Ascenzo F, GM DEF, Biondi-Zoccai G, et al. Cardiovascular disease burden: Italian and global perspectives. Minerva Cardiol Angiol. 2021;69(3):231-40.
16. Rosamond W, Flegal K, Friday G, Furie K, Go A, Greenlund K, et al. Heart disease and stroke statistics--2007 update: a report from the American Heart Association Statistics Committee and Stroke Statistics Subcommittee. Circulation. 2007;115(5):e69-171.
17. Velagaleti RS, Vasan RS. Heart failure in the twenty-first century: is it a coronary artery disease or hypertension problem? Cardiol Clin. 2007;25(4):487-95; v.
18. Koop Y, Wimmers RH, Vaartjes I, Bots ML. Hart- en vaatziekten in Nederland 2021, cijfers over ziekte en sterte. Nederlandse Hartstichting. 2021.
19. Sabbah HN, Goldstein S. Ventricular remodelling: consequences and therapy. European Heart Journal. 1993;14(Suppl C):24–9.
20. Michaelides A, Ryan JM, VanFossen D, Pozderac R, Boudoulas H. Exercise-induced QRS prolongation in patients with coronary artery disease: A marker of myocardial ischemia. American Heart Journal. 1993;126(6):1320-5.
21. Borbely A, Falcao-Pires I, van Heerebeek L, Hamdani N, Edes I, Gavina C, et al. Hypophosphorylation of the Stiff N2B titin isoform raises cardiomyocyte resting tension in failing human myocardium. Circ Res. 2009;104(6):780-6.

22. Hochman-Mendez C, Curty E, Taylor DA. Change the Laminin, Change the Cardiomyocyte: Improve Untreatable Heart Failure. Int J Mol Sci. 2020;21(17).
23. Frangogiannis NG. The extracellular matrix in myocardial injury, repair, and remodeling. J Clin Invest. 2017;127(5):1600-12.
24. Saucerman JJ, Tan PM, Buchholz KS, McCulloch AD, Omens JH. Mechanical regulation of gene expression in cardiac myocytes and fibroblasts. Nat Rev Cardiol. 2019;16(6):361-78.
25. Ariyasinghe NR, Lyra-Leite DM, McCain ML. Engineering cardiac microphysiological systems to model pathological extracellular matrix remodeling. Am J Physiol Heart Circ Physiol. 2018;315(4):H771-H89.
26. Walker CA, Spinale FG. The structure and function of the cardiac myocyte: A review of fundamental concepts. The Journal of Thoracic and Cardiovascular Surgery. 1999;118(2):375-82.
27. Li Y, Asfour H, Bursac N. Age-dependent functional crosstalk between cardiac fibroblasts and cardiomyocytes in a 3D engineered cardiac tissue. Acta Biomater. 2017;55:120-30.
28. Porter KE, Turner NA. Cardiac fibroblasts: at the heart of myocardial remodeling. Pharmacol Ther. 2009;123(2):255-78.
29. Kohl P, Gourdie RG. Fibroblast-myocyte electrotonic coupling: does it occur in native cardiac tissue? J Mol Cell Cardiol. 2014;70:37-46.
30. Camelliti P, Borg TK, Kohl P. Structural and functional characterisation of cardiac fibroblasts. Cardiovasc Res. 2005;65(1):40-51.
31. M E. Cardiac Fibroblasts: Function, Regulation of Gene Expression, and Phenotypic Modulation. Basic Res Cardiol. 1992;87:183-9.
32. Fan D, Takawale A, Lee J, Kassiri Z. Cardiac fibroblasts, fibrosis and extracellular matrix remodeling in heart disease. Fibrogenesis Tissue Repair. 2012;5(1):15.
33. van Nieuwenhoven FA, Turner NA. The role of cardiac fibroblasts in the transition from inflammation to fibrosis following myocardial infarction. Vascul Pharmacol. 2013;58(3):182-8.
34. Li L, Zhao Q, Kong W. Extracellular matrix remodeling and cardiac fibrosis. Matrix Biol. 2018;68-69:490-506.
35. Kielty CM, Sherratt MJ, Shuttleworth CA. Elastic fibres. J Cell Sci. 2002;115(Pt 14):2817-28.
36. Frangogiannis NG. Matricellular proteins in cardiac adaptation and disease. Physiol Rev. 2012;92(2):635-88.
37. van Nieuwenhoven FA, Munts C, Op 't Veld RC, Gonzalez A, Diez J, Heymans S, et al. Cartilage intermediate layer protein 1 (CILP1): A novel mediator of cardiac extracellular matrix remodelling. Sci Rep. 2017;7(1):16042.
38. Moore L, Fan D, Basu R, Kandalam V, Kassiri Z. Tissue inhibitor of metalloproteinases (TIMPs) in heart failure. Heart Fail Rev. 2012;17(4-5):693-706.
39. Powell DW, Mifflin RC, Valentich JD, Crowe SE, Saada JI, West AB. Myofibroblasts. I. Paracrine cells important in health and disease. Am J Physiol. 1999;277(1):C1-9.
40. Tsuruda T, Boerrigter G, Huntley BK, Noser JA, Cataliotti A, Costello-Boerrigter LC, et al. Brain natriuretic Peptide is produced in cardiac fibroblasts and induces matrix metalloproteinases. Circ Res. 2002;91(12):1127-34.
41. Brown RD, Ambler SK, Mitchell MD, Long CS. The cardiac fibroblast: therapeutic target in myocardial remodeling and failure. Annu Rev Pharmacol Toxicol. 2005;45:657-87.
42. Banerjee I, Yekkala K, Borg TK, Baudino TA. Dynamic interactions between myocytes, fibroblasts, and extracellular matrix. Ann N Y Acad Sci. 2006;1080:76-84.
43. Pedrotty DM, Klinger RY, Kirkton RD, Bursac N. Cardiac fibroblast paracrine factors alter impulse conduction and ion channel expression of neonatal rat cardiomyocytes. Cardiovasc Res. 2009;83(4):688-97.
44. Chung E, Leinwand LA. Pregnancy as a cardiac stress model. Cardiovascular Research. 2014;101(4):561-70.
45. Gibb AA, Hill BG. Metabolic Coordination of Physiological and Pathological Cardiac Remodeling. Circ Res. 2018;123(1):107-28.

46. Leonard BL, Smaill BH, LeGrice IJ. Structural remodeling and mechanical function in heart failure. Microsc Microanal. 2012;18(1):50-67.
47. Mann DL, Bristow MR. Mechanisms and models in heart failure: the biomechanical model and beyond. Circulation. 2005;111(21):2837-49.
48. Hartupee J, Mann DL. Neurohormonal activation in heart failure with reduced ejection fraction. Nature Reviews Cardiology. 2016;14(1):30-8.
49. Mann DL. Innate Immunity and the Failing Heart. Circulation Research. 2015;116(7):1254-68.
50. Jackson G, Gibbs CR, Davies MK, Lip GY. ABC of heart failure: Pathophysiology. British Medical Journal. 2000;320(7228):167-70.
51. Triposkiadis F, Karayannis G, Giamouzis G, Skoularigis J, Louridas G, Butler J. The sympathetic nervous system in heart failure physiology, pathophysiology, and clinical implications. J Am Coll Cardiol. 2009;54(19):1747-62.
52. Leenen FH. Brain mechanisms contributing to sympathetic hyperactivity and heart failure. Circ Res. 2007;101(3):221-3.
53. Kemp CD, Conte JV. The pathophysiology of heart failure. Cardiovascular Pathology. 2012;21(5):365-71.
54. Kinnunen P, Vuolteenaho O, Ruskoaho H. Mechanisms of Atrial and Brain Natriuretic Peptide Release From Rat Ventricular Myocardium: Effect of Stretching. Endocrinology. 1993;132(5):1961-70.
55. Toth M, Vuorinen KH, Vuolteenaho O, Hassinen IE, Uusimaa PA, Leppaluoto J, et al. Hypoxia stimulates release of ANP and BNP from perfused rat ventricular myocardium. Am J Physiol. 1994;266(4 Pt 2):H1572-80.
56. Zois NE, Bartels ED, Hunter I, Kousholt BS, Olsen LH, Goetze JP. Natriuretic peptides in cardiometabolic regulation and disease. Nat Rev Cardiol. 2014;11(7):403-12.
57. Fu S, Ping P, Wang F, Luo L. Synthesis, secretion, function, metabolism and application of natriuretic peptides in heart failure. J Biol Eng. 2018;12:2.
58. Jarai R, Kaun C, Weiss TW, Speidl WS, Rychli K, Maurer G, et al. Human cardiac fibroblasts express B-type natriuretic peptide: fluvastatin ameliorates its up-regulation by interleukin-1alpha, tumour necrosis factor-alpha and transforming growth factor-beta. J Cell Mol Med. 2009;13(11-12):4415-21.
59. Del Ry S, Cabiati M, Lionetti V, Emdin M, Recchia FA, Giannessi D. Expression of C-type natriuretic peptide and of its receptor NPR-B in normal and failing heart. Peptides. 2008;29(12):2208-15.
60. Maisel AS, Duran JM, Wettersten N. Natriuretic Peptides in Heart Failure: Atrial and B-type Natriuretic Peptides. Heart Fail Clin. 2018;14(1):13-25.
61. Forte M, Madonna M, Schiavon S, Valenti V, Versaci F, Zoccai GB, et al. Cardiovascular Pleiotropic Effects of Natriuretic Peptides. Int J Mol Sci. 2019;20(16).
62. He XL, Dukkipati A, Garcia KC. Structural determinants of natriuretic peptide receptor specificity and degeneracy. J Mol Biol. 2006;361(4):698-714.
63. Matsuo A, Nagai-Okatani C, Nishigori M, Kangawa K, Minamino N. Natriuretic peptides in human heart: Novel insight into their molecular forms, functions, and diagnostic use. Peptides. 2019;111:3-17.
64. Potter LR, Yoder AR, Flora DR, Antos LK, Dickey DM. Natriuretic peptides: their structures, receptors, physiologic functions and therapeutic applications. Handb Exp Pharmacol. 2009(191):341-66.
65. Moyes AJ, Chu SM, Aubdool AA, Dukinfield MS, Margulies KB, Bedi KC, et al. C-type natriuretic peptide co-ordinates cardiac structure and function. Eur Heart J. 2020;41(9):1006-20.
66. Blaauw E, van Nieuwenhoven FA, Willemsen P, Delhaas T, Prinzen FW, Snoeckx LH, et al. Stretch-induced hypertrophy of isolated adult rabbit cardiomyocytes. Am J Physiol Heart Circ Physiol. 2010;299(3):H780-7.
67. Ovchinnikova E, Hoes M, Ustyantsev K, Bomer N, de Jong TV, van der Mei H, et al. Modeling Human Cardiac Hypertrophy in Stem Cell-Derived Cardiomyocytes. Stem Cell Reports. 2018;10(3):794-807.
68. Tamura N, Ogawa Y, Chusho H, Nakamura K, Nakao K, Suda M, et al. Cardiac fibrosis in mice lacking brain natriuretic peptide. Proc Natl Acad Sci U S A. 2000;97(8):4239-44.
69. Kong P, Christia P, Frangogiannis NG. The pathogenesis of cardiac fibrosis. Cell Mol Life Sci. 2014;71(4):549-74.

70. Wang J, Chen H, Seth A, McCulloch CA. Mechanical force regulation of myofibroblast differentiation in cardiac fibroblasts. Am J Physiol Heart Circ Physiol. 2003;285(5):H1871-81.
71. Hinz B. The myofibroblast: paradigm for a mechanically active cell. J Biomech. 2010;43(1):146-55.
72. Hinz B. Formation and function of the myofibroblast during tissue repair. J Invest Dermatol. 2007;127(3):526-37.
73. Tomasek JJ, Gabbiani G, Hinz B, Chaponnier C, Brown RA. Myofibroblasts and mechano-regulation of connective tissue remodelling. Nat Rev Mol Cell Biol. 2002;3(5):349-63.
74. Yong KW, Li Y, Huang G, Lu TJ, Safwani WK, Pingguan-Murphy B, et al. Mechanoregulation of cardiac myofibroblast differentiation: implications for cardiac fibrosis and therapy. Am J Physiol Heart Circ Physiol. 2015;309(4):H532-42.
75. MacKenna D, Summerour SR, Villarreal FJ. Role of mechanical factors in modulating cardiac fibroblast function and extracellular matrix synthesis. Cardiovascular Research. 2000;46(2):257-63.
76. Herum KM, Choppe J, Kumar A, Engler AJ, McCulloch AD. Mechanical regulation of cardiac fibroblast profibrotic phenotypes. Mol Biol Cell. 2017;28(14):1871-82.
77. Lopez B, Querejeta R, Gonzalez A, Larman M, Diez J. Collagen cross-linking but not collagen amount associates with elevated filling pressures in hypertensive patients with stage C heart failure: potential role of lysyl oxidase. Hypertension. 2012;60(3):677-83.
78. Fu X, Khalil H, Kanisicak O, Boyer JG, Vagnozzi RJ, Maliken BD, et al. Specialized fibroblast differentiated states underlie scar formation in the infarcted mouse heart. J Clin Invest. 2018;128(5):2127-43.
79. Frangogiannis NG. The mechanistic basis of infarct healing. Antioxid Redox Signal. 2006;8(11-12):1907-39.
80. Verheule S, Schotten U. Electrophysiological Consequences of Cardiac Fibrosis. Cells. 2021;10(11).
81. Burstein B, Nattel S. Atrial fibrosis: mechanisms and clinical relevance in atrial fibrillation. J Am Coll Cardiol. 2008;51(8):802-9.
82. Peschar M, Vernooy K, Vanagt WY, Reneman RS, Vos MA, Prinzen FW. Absence of reverse electrical remodeling during regression of volume overload hypertrophy in canine ventricles. Cardiovasc Res. 2003;58(3):510-7.
83. Douglas PS, Tallant B. Hypertrophy, fibrosis and diastolic dysfunction in early canine experimental hypertension. Journal of the American College of Cardiology. 1991;17(2):530-6.
84. Ellims AH, Shaw JA, Stub D, Iles LM, Hare JL, Slavin GS, et al. Diffuse myocardial fibrosis evaluated by post-contrast t1 mapping correlates with left ventricular stiffness. J Am Coll Cardiol. 2014;63(11):1112-8.
85. Thune JJ, Solomon SD. Left ventricular diastolic function following myocardial infarction. Curr Heart Fail Rep. 2006;3(4):170-4.
86. Krenning G, Zeisberg EM, Kalluri R. The origin of fibroblasts and mechanism of cardiac fibrosis. J Cell Physiol. 2010;225(3):631-7.
87. Gyongyosi M, Winkler J, Ramos I, Do QT, Firat H, McDonald K, et al. Myocardial fibrosis: biomedical research from bench to bedside. Eur J Heart Fail. 2017;19(2):177-91.
88. Heymans S, Luttun A, Nuyens D, Theilmeier G, Creemers E, Moons L, et al. Inhibition of plasminogen activators or matrix metalloproteinases prevents cardiac rupture but impairs therapeutic angiogenesis and causes cardiac failure. Nat Med. 1999;5(10):1135-42.
89. Savvatis K, Pappritz K, Becher PM, Lindner D, Zietsch C, Volk HD, et al. Interleukin-23 deficiency leads to impaired wound healing and adverse prognosis after myocardial infarction. Circ Heart Fail. 2014;7(1):161-71.
90. Frantz S, Hu K, Adamek A, Wolf J, Sallam A, Maier SK, et al. Transforming growth factor beta inhibition increases mortality and left ventricular dilatation after myocardial infarction. Basic Res Cardiol. 2008;103(5):485-92.
91. Krstevski C, Cohen CD, Dona MSI, Pinto AR. New perspectives of the cardiac cellular landscape: mapping cellular mediators of cardiac fibrosis using single-cell transcriptomics. Biochem Soc Trans. 2020;48(6):2483-93.

92. Tallquist MD. Cardiac Fibroblast Diversity. Annu Rev Physiol. 2020;82:63-78.
93. McLellan MA, Skelly DA, Dona MSI, Squiers GT, Farrugia GE, Gaynor TL, et al. High-Resolution Transcriptomic Profiling of the Heart During Chronic Stress Reveals Cellular Drivers of Cardiac Fibrosis and Hypertrophy. Circulation. 2020;142(15):1448-63.
94. Fujiu K, Nagai R. Fibroblast-mediated pathways in cardiac hypertrophy. J Mol Cell Cardiol. 2014;70:64-73.
95. Kamo T, Akazawa H, Komuro I. Cardiac nonmyocytes in the hub of cardiac hypertrophy. Circ Res. 2015;117(1):89-98.
96. Bageghni SA, Hemmings KE, Zava N, Denton CP, Porter KE, Ainscough JFX, et al. Cardiac fibroblast-specific p38alpha MAP kinase promotes cardiac hypertrophy via a putative paracrine interleukin-6 signaling mechanism. FASEB J. 2018;32(9):4941-54.
97. Zhang P, Su J, Mende U. Cross talk between cardiac myocytes and fibroblasts: from multiscale investigative approaches to mechanisms and functional consequences. Am J Physiol Heart Circ Physiol. 2012;303(12):H1385-96.
98. Ogle BM, Bursac N, Domian I, Huang NF, Menasche P, Murry CE, et al. Distilling complexity to advance cardiac tissue engineering. Sci Transl Med. 2016;8(342):342ps13.
99. Baudino TA, Carver W, Giles W, Borg TK. Cardiac fibroblasts: friend or foe? Am J Physiol Heart Circ Physiol. 2006;291(3):H1015-26.
100. van Putten S, Shafieyan Y, Hinz B. Mechanical control of cardiac myofibroblasts. J Mol Cell Cardiol. 2016;93:133-42.
101. Emig R, Zgierski-Johnston CM, Timmermann V, Taberner AJ, Nash MP, Kohl P, et al. Passive myocardial mechanical properties: meaning, measurement, models. Biophys Rev. 2021;13(5):587-610.
102. Katsumi A, Orr AW, Tzima E, Schwartz MA. Integrins in mechanotransduction. J Biol Chem. 2004;279(13):12001-4.
103. Chiquet M, Renedo AS, Huber F, Flück M. How do fibroblasts translate mechanical signals into changes in extracellular matrix production? Matrix Biology. 2003;22(1):73-80.
104. Ingber DE, Dike L, Hansen L, Karp S, Liley H, Maniotis A, et al. Cellular Tensegrity: Exploring How Mechanical Changes in the Cytoskeleton Regulate Cell Growth, Migration, and Tissue Pattern during Morphogenesis. International Review of Cytology. 1994;150:173-224.
105. Schroer AK, Merryman WD. Mechanobiology of myofibroblast adhesion in fibrotic cardiac disease. Journal of Cell Science. 2015;128(10):1865–75.
106. Huang S, Ingber DE. The structural and mechanical complexity of cell-growth control. Nat Cell Biol. 1999;1(5):E131-8.
107. Schwartz MA, Assoian RK. Integrins and cell proliferation: regulation of cyclin-dependent kinases via cytoplasmic signaling pathways. J Cell Sci. 2001;114(Pt 14):2553-60.
108. Henderson NC, Arnold TD, Katamura Y, Giacomini MM, Rodriguez JD, McCarty JH, et al. Targeting of alphav integrin identifies a core molecular pathway that regulates fibrosis in several organs. Nat Med. 2013;19(12):1617-24.
109. Wipff PJ, Rifkin DB, Meister JJ, Hinz B. Myofibroblast contraction activates latent TGF-beta1 from the extracellular matrix. J Cell Biol. 2007;179(6):1311-23.
110. Bryant CE, Gay NJ, Heymans S, Sacre S, Schaefer L, Midwood KS. Advances in Toll-like receptor biology: Modes of activation by diverse stimuli. Crit Rev Biochem Mol Biol. 2015;50(5):359-79.
111. Quintana FJ, Cohen IR. Heat shock proteins as endogenous adjuvants in sterile and septic inflammation. J Immunol. 2005;175(5):2777-82.
112. Maqbool A, Spary EJ, Manfield IW, Ruhmann M, Zuliani-Alvarez L, Gamboa-Esteves FO, et al. Tenascin C upregulates interleukin-6 expression in human cardiac myofibroblasts via toll-like receptor 4. World J Cardiol. 2016;8(5):340-50.
113. Waehre A, Vistnes M, Sjaastad I, Nygard S, Husberg C, Lunde IG, et al. Chemokines regulate small leucine-rich proteoglycans in the extracellular matrix of the pressure-overloaded right ventricle. J Appl Physiol (1985). 2012;112(8):1372-82.

114. Strand ME, Herum KM, Rana ZA, Skrbic B, Askevold ET, Dahl CP, et al. Innate immune signaling induces expression and shedding of the heparan sulfate proteoglycan syndecan-4 in cardiac fibroblasts and myocytes, affecting inflammation in the pressure-overloaded heart. FEBS J. 2013;280(10):2228-47.
115. Coste B, Mathur J, Schmidt M, Earley TJ, Ranade S, Petrus MJ, et al. Piezo1 and Piezo2 are essential components of distinct mechanically activated cation channels. Science. 2010;330(6000):55-60.
116. Coste B, Xiao B, Santos JS, Syeda R, Grandl J, Spencer KS, et al. Piezo proteins are pore-forming subunits of mechanically activated channels. Nature. 2012;483(7388):176-81.
117. Guo YR, MacKinnon R. Structure-based membrane dome mechanism for Piezo mechanosensitivity. Elife. 2017;6.
118. Beech DJ, Kalli AC. Force Sensing by Piezo Channels in Cardiovascular Health and Disease. Arterioscler Thromb Vasc Biol. 2019;39(11):2228-39.
119. Haselwandter CA, MacKinnon R. Piezo's membrane footprint and its contribution to mechanosensitivity. Elife. 2018;7.
120. Cox CD, Bae C, Ziegler L, Hartley S, Nikolova-Krstevski V, Rohde PR, et al. Removal of the mechanoprotective influence of the cytoskeleton reveals PIEZO1 is gated by bilayer tension. Nat Commun. 2016;7:10366.
121. Lewis AH, Grandl J. Mechanical sensitivity of Piezo1 ion channels can be tuned by cellular membrane tension. Elife. 2015;4.
122. Chen X, Wanggou S, Bodalia A, Zhu M, Dong W, Fan JJ, et al. A Feedforward Mechanism Mediated by Mechanosensitive Ion Channel PIEZO1 and Tissue Mechanics Promotes Glioma Aggression. Neuron. 2018;100(4):799-815 e7.
123. Martin TP, Lawan A, Robinson E, Grieve DJ, Plevin R, Paul A, et al. Adult cardiac fibroblast proliferation is modulated by calcium/calmodulin-dependent protein kinase II in normal and hypertrophied hearts. Pflugers Arch. 2014;466(2):319-30.
124. Zhang X, Zhang T, Wu J, Yu X, Zheng D, Yang F, et al. Calcium sensing receptor promotes cardiac fibroblast proliferation and extracellular matrix secretion. Cell Physiol Biochem. 2014;33(3):557-68.
125. Adapala RK, Thoppil RJ, Luther DJ, Paruchuri S, Meszaros JG, Chilian WM, et al. TRPV4 channels mediate cardiac fibroblast differentiation by integrating mechanical and soluble signals. J Mol Cell Cardiol. 2013;54:45-52.
126. Blythe NM, Muraki K, Ludlow MJ, Stylianidis V, Gilbert HTJ, Evans EL, et al. Mechanically activated Piezo1 channels of cardiac fibroblasts stimulate p38 mitogen-activated protein kinase activity and interleukin-6 secretion. J Biol Chem. 2019;294(46):17395-408.
127. Bartoli F, Evans EL, Blythe NM, Stewart L, Chuntharpursat-Bon E, Debant M, et al. Global PIEZO1 Gain-of-Function Mutation Causes Cardiac Hypertrophy and Fibrosis in Mice. Cells. 2022;11(7).
128. Ingber DE, Wang N, Stamenovic D. Tensegrity, cellular biophysics, and the mechanics of living systems. Rep Prog Phys. 2014;77(4):046603.
129. Wang N, Tolic-Norrelykke IM, Chen J, Mijailovich SM, Butler JP, Fredberg JJ, et al. Cell prestress. I. Stiffness and prestress are closely associated in adherent contractile cells. Am J Physiol Cell Physiol. 2002;282(3):C606-16.
130. Maekawa M, Ishizaki T, Boku S, Watanabe N, Fujita A, Iwamatsu A, et al. Signaling from Rho to the actin cytoskeleton through protein kinases ROCK and LIM-kinase. Science. 1999;285(5429):895-8.
131. Crisp M, Liu Q, Roux K, Rattner JB, Shanahan C, Burke B, et al. Coupling of the nucleus and cytoplasm: role of the LINC complex. J Cell Biol. 2006;172(1):41-53.
132. Lovett DB, Shekhar N, Nickerson JA, Roux KJ, Lele TP. Modulation of Nuclear Shape by Substrate Rigidity. Cell Mol Bioeng. 2013;6(2):230-8.
133. Created with BioRender.com.

Piezo1 mechanosensitive ion channel mediates stretch-induced Nppb expression in adult rat cardiac fibroblasts.

Meike C. Ploeg[1], Chantal Munts[1], Frits W. Prinzen[1], Neil A. Turner[2,3], Marc van Bilsen[1] and Frans A. van Nieuwenhoven[1]

[1] Department of Physiology, Cardiovascular Research Institute Maastricht (CARIM), Maastricht University, the Netherlands; [2] Discovery and Translational Science Department, Leeds Institute of Cardiovascular and Metabolic Medicine, School of Medicine, University of Leeds, Leeds, LS2 9JT, UK; [3] Multidisciplinary Cardiovascular Research Centre, University of Leeds, Leeds, LS2 9JT, UK.

Cells. 2021 Jul 9;10(7):1745.

2

Abstract

Background: In response to stretch, cardiac tissue produces natriuretic peptides, which have been suggested to have beneficial effects in heart failure patients. In the present study, we explored the mechanism of stretch-induced brain natriuretic peptide (Nppb) expression in cardiac fibroblasts.

Methods and results: Primary adult rat cardiac fibroblasts subjected to 4 h or 24 h of cyclic stretch (10% 1 Hz) showed a 6.6-fold or 3.2-fold ($p < 0.05$) increased mRNA expression of Nppb, as well as induction of genes related to myofibroblast differentiation. Moreover, BNP protein secretion was upregulated 5.3-fold in stretched cardiac fibroblasts. Recombinant BNP inhibited TGFβ1-induced Acta2 expression. Nppb expression was >20-fold higher in cardiomyocytes than in cardiac fibroblasts, indicating that cardiac fibroblasts were not the main source of Nppb in the healthy heart. Yoda1, an agonist of the Piezo1 mechanosensitive ion channel, increased Nppb expression 2.1-fold ($p < 0.05$) and significantly induced other extracellular matrix (ECM) remodeling genes. Silencing of Piezo1 reduced the stretch-induced Nppb and Tgfβ1 expression in cardiac fibroblasts.

Conclusion: Our study identifies Piezo1 as mediator of stretch-induced Nppb expression, as well as other remodeling genes, in cardiac fibroblasts.

Introduction

Mechanical factors influence the form and function of cells [1-4]. Specifically in the heart, mechanical signals include the forces of cyclic contraction and relaxation of the myocardial walls and the hemodynamic load leading to stretch of the cardiac chambers during the filling phase, and increased wall stress during the contraction phase [5]. These factors are known to regulate myocardial function, gene expression and structural appearance [6, 7].

Cardiovascular tissue is composed of cardiomyocytes, fibroblasts, vascular and immune cells which reside within the myocardial extracellular matrix (ECM) [8]. The ECM provides structure, transmits mechanical forces and modulates cell function [8, 9]. Cardiac fibroblasts play an important role in the regulation of the ECM, by synthesizing structural ECM proteins (i.e collagens), ECM degrading matrix metalloproteinases (MMPs and TIMPs)[10], growth factors such as transforming growth factor β1 (TGFβ1) and matricellular proteins like tenascin C (TNC) [11] and connective tissue growth factor (CTGF) [12]. Matricellular proteins gain increasing attention for their significant role in cardiac remodeling [11]. In response to injury, cardiac fibroblasts become activated and differentiate to so called myofibroblasts [10, 13]. These myofibroblasts have special morphological and functional characteristics, like the expression of alpha smooth muscle actin (aSMA, encoded by ACTA2 gene) [10, 14]. TGFβ1 is known as established stimulus for myofibroblast differentiation [15, 16]. Even though myofibroblast differentiation is an essential process in normal wound healing, it can result in pathological fibrosis in cases of prolonged injury or loss of regulatory mechanisms [8]. Besides biochemical factors, mechanical cues like mechanical strain and ECM stiffness also play an important role in regulating myofibroblast differentiation [17, 18]. Cardiac fibroblasts express a number of different mechanosensitive ions channels that are coupled to alteration of cellular phenotype and function [19].

Cardiovascular tissues can produce natriuretic peptides in response to wall stretch [20-24]. There are three types of natriuretic peptides: atrial natriuretic peptide (ANP, encoded by NPPA gene), brain natriuretic peptide (BNP, encoded by NPPB gene), and C-type natriuretic peptide (CNP, encoded by NPPC gene) [25, 26]. ANP and BNP are found in multiple tissues, but they are produced primarily in the cardiac atria or ventricles, respectively [27-30]. CNP is mainly produced in the endothelium [27, 31]. Cyclic stretch induced increased Nppa and Nppb expression in adult rabbit cardiomyocytes [32] and human embryonic stem cell–derived cardiomyocytes (hESC-CMs)[33].

BNP inhibits collagen production and fibroblast proliferation [10], and the TGFβ-activation of pro-fibrotic and inflammatory genes in cultured human cardiac fibroblasts [34]. Nppb knock out mice subjected to pressure overload by aortic constriction show increased fibrosis as well as increased mRNA levels of Tgfβ3 and Col1a1 [35]. The beneficial effects of BNP in the heart has led to pharmacotherapy aimed at increasing BNP signaling in heart failure patients [36, 37].

While it is generally accepted that cardiomyocytes produce BNP [32, 38-42], some studies show that it is also synthesized by cardiac fibroblasts [10, 24, 38, 43]. A recent paper found that stretch of human cardiac fibroblasts increased NPPB expression [43]. However, the mechanism of stretch-induced NPPB expression in cardiac fibroblasts is unknown. Blythe and colleagues very recently identified the presence of Piezo1 as a functional Ca^{2+}-permeable mechanosensitive ion channel in both murine and human cardiac fibroblasts [44]. Therefore, we hypothesized that stretch-induced NPPB expression by cardiac fibroblasts is mediated by the mechanosensitive ion channel Piezo1.

Materials & methods

Isolation of cardiac fibroblasts

Cardiac fibroblasts were isolated from cardiac ventricles (combined left and right) of adult surplus rats (*n* = 31) from any age, weight, sex or breed. Most of the rats used were either from the Lewis or Wistar strain and aged between 5 and 52 weeks. Rat cardiac ventricular fibroblasts were isolated and cultured as previously described [9, 45, 46] in Dulbecco's modified eagles medium (DMEM; no. 22320, Gibco, Invitrogen, Breda, the Netherlands) supplemented with 10% (v/v) fetal bovine serum (FBS, Gibco), gentamicin (50 µg/ml, Gibco), 1% (v/v) Insulin-Transferrin-Selenium-Sodium Pyruvate (ITS-A, Gibco) and basic fibroblast growth factor (1 ng/ml, Gibco) ("CF culture medium"). The vast majority of these cells are fibroblast-like cells and these primary fibroblasts were used between passage 1–3. Cardiomyocytes were isolated from the left ventricle of adult male Sprague Dawley rats (*n* = 6 age 10–20 weeks) essentially as described previously [32, 47]. Experiments were performed with approval of the Animal Ethical Committee of Maastricht University (DEC-2007-116, July 31, 2007) and conform to the national legislation for the protection of animals used for scientific purposes.

Experimental stretch protocols

Cardiac fibroblasts (10,000 cells/cm^2) were plated on bioflex plates (6-well Bioflex plates, precoated with collagen-I, Flexcell Dunn Labortechnik, Asbach, Germany) in CF culture medium. The next day, CF culture medium was replaced by DMEM supplemented with gentamicin (50 µg/ml, Gibco). After 24 h, cardiac fibroblasts were subjected to 10% cyclic (1 Hz) equibiaxial stretch, (Flexcell FX-4000 strain unit, Dunn Labortechnik) for 4 h, 6 h or 24 h. Control, non-stretched cells were subjected to identical conditions however, without stretch being applied.

Experimental stimuli

To determine regulation and effects of BNP, cardiac fibroblasts (10,000 cells/cm^2) were serum-starved for 24 hours before incubation with TGFβ1 (1 ng/ml, R&D systems, Minneapolis, USA), Yoda1 (10 µM, Tocris, Bristol, UK) and BNP (1 µM, R&D systems) for 4 h or 24 h.

Gene expression analysis

Total RNA was isolated from cells using an RNA isolation kit (Omega Biotek, Norcross, USA) and reversed transcribed into cDNA using the iScript cDNA synthesis kit (Biorad, Hercules, USA) according to the manufacturer's instructions. Real-time PCR was performed on an iCycler accompanied by the My IQ single color real-time PCR detection system using iQ SYBR-Green Supermix (Biorad) [9]. Gene expression levels of Alpha-smooth muscle actin (Acta2), Connective tissue growth factor (Ctgf), Transforming growth factor beta 1 (Tgfβ1), Tenascin C (Tnc), Piezo1, Atrial Natriuretic peptide (Nppa), C-Type natriuretic peptide (Nppc) and Brain Natriuretic Peptide (Nppb) were normalized using the housekeeping gene Cyclophilin-A (Cyclo), and their relative expression was calculated using the comparative threshold cycle (Ct) method by calculating $2^{\Delta Ct}$ (e.g. $2^{(\text{Cyclophilin Ct} - \text{BNP Ct})}$). The gene expression values were multiplied by 1000 (formula $1000 * 2^{\Delta Ct}$), to enhance readability. The sequences of the specific primers used are provided below (table 1).

Table 1. Gene-specific primer sequences used for quantitative real-time PCR

Gene	Forward primer	Reverse Primer
Alpha-smooth muscle actin (Acta2)	AAGGCCAACCGGGAGAAAAT	AGTCCAGCACAATACCAGTTGT
Connective tissue growth factor (Ctgf)	CACAGAGTGGAGCGCCTGTTC	GATGCACTTTTTGCCCTTCTTAATG
Transforming growth factor, beta 1 (Tgfβ1)	GCACCATCCATGACATGAAC	GCTGAAGCAGTAGTTGGTATC
Tenascin C (Tnc)	TCTGTCCTGGACTGCTGATG	TGGCCTCTCTGAGACCTGTT
Piezo1	TTGCGTACGTTCACGAAGGA	TTCGCTCACGTAAAGCTGGT
Atrial Natriuretic peptide (Nppa)	ATCACCAAGGGCTTCTTCCT	TGTTGGACACCGCACTGTAT
C-Type natriuretic peptide (Nppc)	ACAAAGGCGGCAACAAGAAG	GCAGTTCCCAATCCGCCG
Brain Natriuretic Peptide (Nppb)	AGACAGCTCTCAAAGGACCA	CTATCTTCTGCCCAAAGCAG
Cyclophilin-A (Cyclo)	CAAATGCTGGACCAAACACAA	TTCACCTTCCCAAAGACCACAT

BNP ELISA

Conditioned media were collected after the 24 h stretch-experiments and stored at −80 ◦C for subsequent analysis. The conditioned media were concentrated (approximately 10-fold) using Amicon Ultra 3k devices (Merck-Millipore, Burlington, MA, USA) and the concentration of BNP was determined by ELISA (ab108815, Abcam, Cambridge, UK) according to the manufacturer's instructions.

Gene silencing

Cardiac fibroblasts (10,000 cells/cm^2) were plated on bioflex plates (6-well Bioflex plates, precoated with collagen-I, Flexcell Dunn Labortechnik) in CF culture medium and transfected with 10 nM Piezo1-specific Silencer Select Pre-Designed siRNA (4390771, siRNA s107968, Life Technologies, Carlsbad, USA) or Silencer Select Negative Control No. 1 siRNA (4390843, Life Technologies) using Lipofectamine RNAiMAX reagent (Life Technologies) in Opti-MEM

(Gibco) according to the manufacturer's instructions. After 72h cells were exposed to the stretch protocol described above.

Statistics

Data are presented as mean or individual data points and were analyzed with Wilcoxon matched pairs test or Friedman test, with Dunn selected columns posthoc test where appropriate. Differences were considered statistically significant when $p<0.05$.

Results

Mechanical Stretch Induces BNP Expression in Cardiac Fibroblasts

Cardiac fibroblasts exposed to cyclic stretch (10%, 1 Hz) for 4 h showed a significant increase in mRNA expression of Tgfβ1, Tnc, Ctgf and Acta2 compared to non-stretched controls (figure 1A). After 24 h of cyclic stretch the effect remained for in Tgfβ1, Ctgf and Acta2 (figure 1B). Interestingly, Nppb mRNA expression was significantly upregulated by 6.6-fold after 4 h stretch (figure 1A) and 3.2-fold after 24 h stretch (figure 1B) compared to non-stretched controls. BNP-protein secretion was upregulated by 5.3-fold in stretched cells compared to non-stretched cells, measured from conditioned media after 24 h stretch (Figure 1C). mRNA expression of Nppa and Nppc were below the detection limit. Cyclic stretch did not influence the mRNA expression of the mechanosenstive ion channel Piezo1 after 4 h (Figure 1A) or 24 h (Figure 1B).

Recombinant BNP Inhibits Profibrotic Gene Expression in Cardiac Fibroblasts

To confirm the anti-fibrotic effect of BNP [34], cardiac fibroblasts were stimulated with recombinant BNP with or without TGFβ1 for 4 h or 24 h. The expression of Acta2 and Ctgf in cardiac fibroblasts was investigated by RT-qPCR. Acta2 showed a significant reduction in expression after the addition of BNP, with and without TGFβ1 after 4 h (figure 2A). This effect was not maintained after 24 h (figure 2B). A similar trend was observed for Ctgf, but this failed to reach statistical significance.

Both cardiomyocytes and cardiac fibroblasts express Nppb

To investigate the relative mRNA expression of Nppb by cardiac fibroblasts compared to cardiomyocytes, we performed RT-qPCR on adult rat cardiomyocytes and cardiac fibroblasts. Cardiac fibroblasts showed 300-fold lower expression of Myh7 (myocyte marker) (Figure 3B) and 500-fold higher expression of Col1a1 compared to cardiomyocytes (Figure 3C). The Nppb expression in cardiomyocytes was 20-fold higher compared to cardiac fibroblasts, indicating that fibroblasts are not the main source of myocardial Nppb expression, at least under basal conditions (Figure 3A).

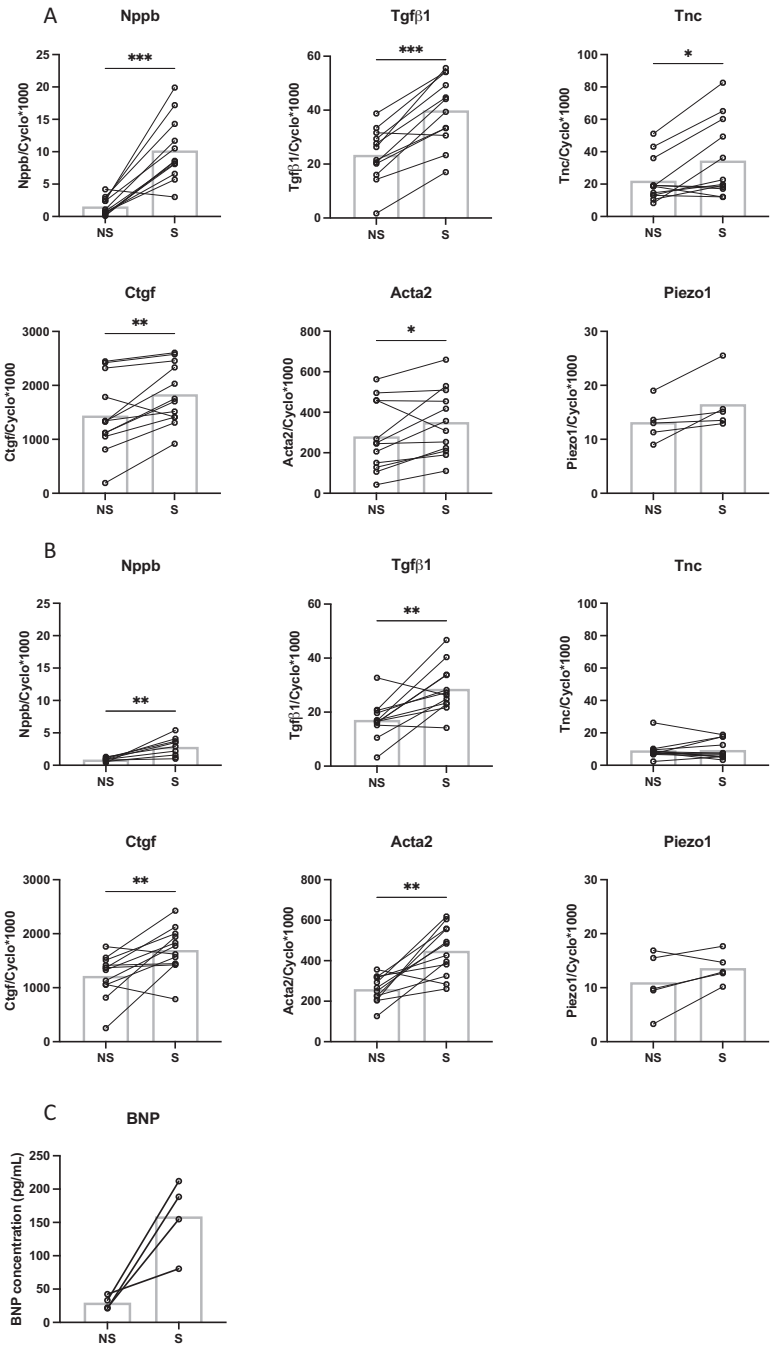

Figure 1. Relative mRNA expression levels of Nppb, Tgfβ1, Tnc, Ctgf, Acta2, and Piezo1 in cardiac fibroblasts exposed to 10% 1 Hz cyclic stretch (S) or non-stretched (NS) conditions for 4 h (n = 5–12) (A) or 24 h (n = 5–12) (B). BNP-protein concentration in conditioned media from stretched and non-stretched cardiac fibroblasts (n = 4) (C). * $p < 0.05$; ** $p < 0.01$; *** $p < 0.001$. Bar indicates mean.

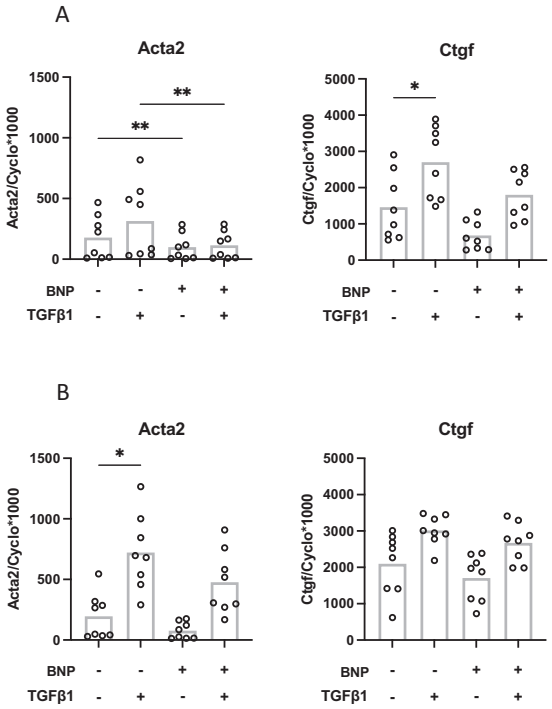

Figure 2. Relative mRNA expression levels of Ctgf and Acta2 in cardiac fibroblasts exposed to recombinant BNP and/or TGFβ1 after 4 h (A) and 24 h (B) (n=8) *p<0.05; ** p<0.01. Bar indicates mean.

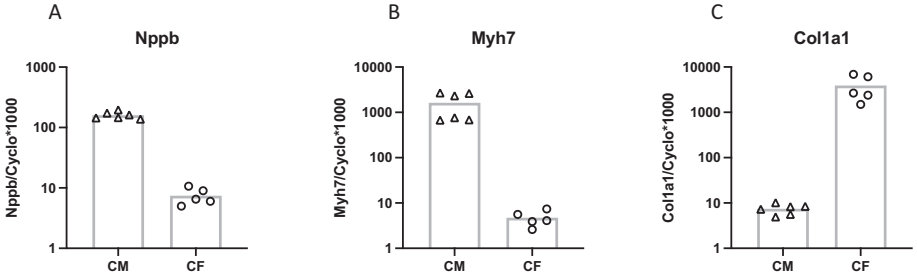

Figure 3. Relative mRNA expression levels of Nppb (a), Myh7 (b) and Col1a1 (c) in cardiomyocytes (CM) (n=6) and cardiac fibroblasts (CF) (n=5) (presented on a logarithmic scale). Bar indicates mean.

Stretch-Induced Nppb and Tgfβ1 Expression Are Mediated by Piezo1

To gain insight into the functional role of Piezo1 activation in cardiac fibroblasts, we first investigated the effect of the Piezo1 agonist Yoda1. Treatment of unstretched fibroblasts with 10 μM Yoda1 for 4 h significantly increased mRNA expression of Tgfβ1, Tnc and Nppb (figure 4A). Yoda1 stimulation also gave a significant increased expression of Piezo1 mRNA.

Next the effect of siRNA-mediated Piezo1 silencing was explored. Piezo1 silencing was successful in reducing the expression of Piezo1 by approximately 80% (figure 4B). Piezo1 silencing increased the expression of Ctgf under non-stretched conditions, and the Tnc and Acta2 expression levels under stretch. The stretch-induced increase in Tgfβ1 expression was absent following Piezo1-silencing (figure 4B). Piezo1 silencing also prevented stretch-induced Nppb expression, supporting the hypothesis that stretched induced Nppb expression is Piezo1 mediated.

Discussion

The present study identifies Piezo1 as the mechanosensitive ion channel responsible for the stretch-induced Nppb and Tgfβ1 expression in cardiac fibroblasts. Our study also confirms the finding of Watson and colleagues of stretch-induced Nppb upregulation in human ventricular cardiac fibroblasts [43] and the anti-fibrotic effect of BNP [10, 34].

Natriuretic peptides are thought to be part of a potentially beneficial counter-regulatory system in heart failure [48]. BNP might prevent the development of cardiac fibrosis by serving as a cardiomyocyte-derived antifibrotic signal to cardiac fibroblasts during the process of cardiac remodeling [35]. However, others have shown Nppb expression by fibroblasts [10, 38, 49]. We confirmed the expression of Nppb in cardiac fibroblasts, on mRNA as well as protein level in response to cyclic stretch. Although expression levels of Nppb in our isolated cardiac fibroblasts were lower then found in isolated cardiomyocytes, it is important to note that the cells were derived from healthy animals. Furthermore, the locally produced BNP by cardiac fibroblasts might still have important autocrine or paracrine functions. Cyclic stretch also upregulated the mRNA expression of Tgfβ1, Tnc, Ctgf and Acta2 after 4 h, which was maintained for all but Tnc after 24 h. Together, these genes are all related to myofibroblast differentiation and cardiac remodeling [10-12, 14-16]. Their upregulation gives some implications on the process of myofibroblast differentiation being started or already ongoing. Cyclic stretch did not affect the mRNA expression of Piezo1, after 4 h or 24 h.

The antifibrotic effect of BNP has been shown previously [34], which we confirmed specifically for myofibroblast differentiation related gene Acta2. Therefore, it is possible that BNP produced by fibroblasts acts as a local autocrine/paracrine factor modulating cardiac fibroblast activation and tissue remodeling within the heart [50]. Differences between 4 h and 24 h incubation with BNP and/or TGFβ1 in our cell culture experiments might be due to the relative short half-life of both BNP and TGFβ1. Therefore, both products are degraded within hours and their effects might be stronger at 4 h as compared to 24 h.

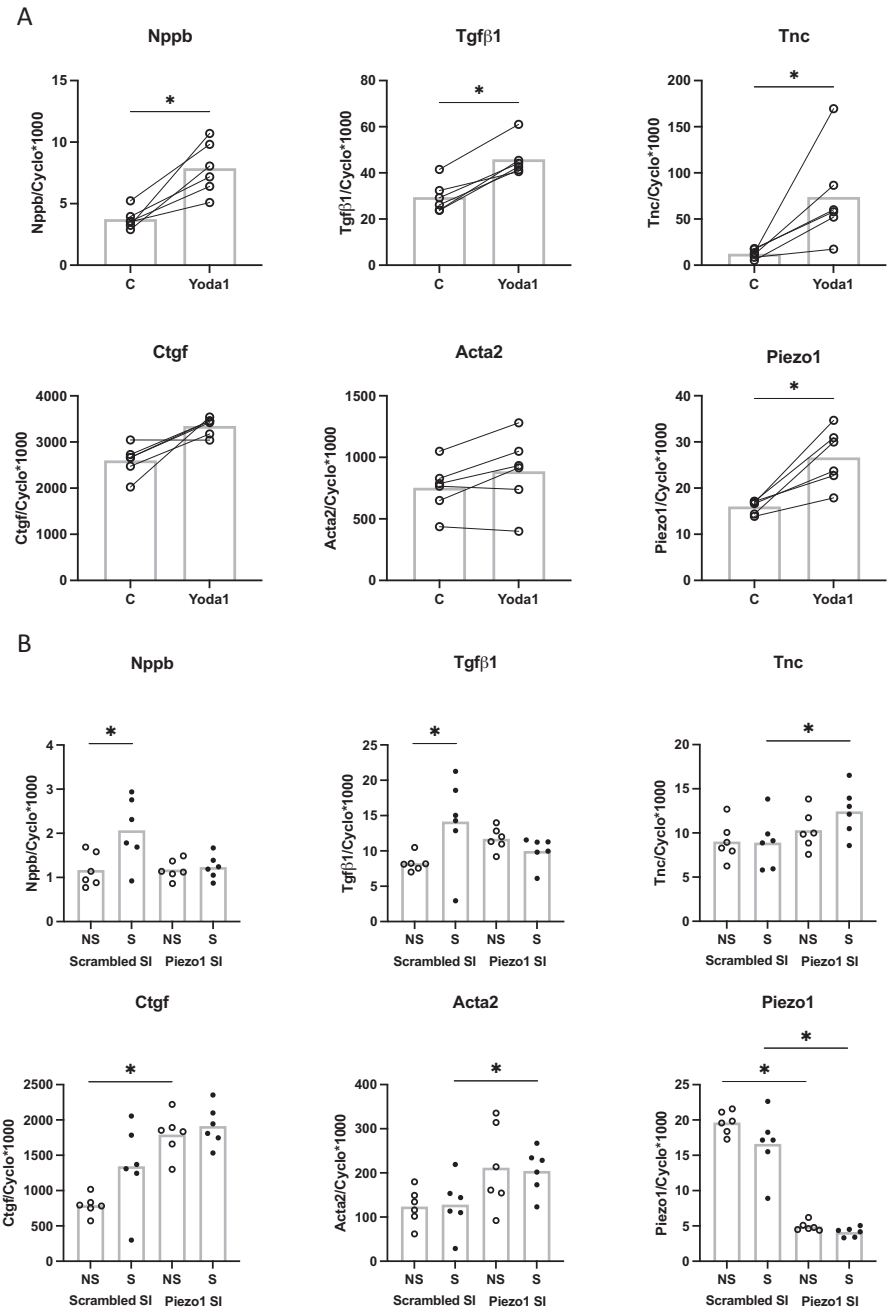

Figure 4. Relative mRNA expression levels of Nppb, Tgfβ1, Tnc, Ctgf, Acta2, and Piezo1 in cardiac fibroblasts after stimulation with Piezo1 agonist Yoda1 after 4 h (n = 6) (A). Relative mRNA expression of Nppb, Tgfβ1, Tnc, Ctgf, Acta2, and Piezo1 in cardiac fibroblasts exposed to 10% 1 Hz cyclic stretch for 6 h (S) or non-stretched (NS) conditions after transfection with either control siRNA (Scrambled SI) or Piezo1-specific siRNA (Piezo1 SI) (n = 6) (B) * $p < 0.05$. Bar indicates mean.

The well-known Piezo1 agonist Yoda1 increased the mRNA expression on Nppb, Tgfβ1, Tnc and Piezo1. For Nppb, Tgfβ1 and Tnc this is in accordance with the results of 4 h and 24 h of cyclic stretch, activating the Piezo1 mechanosensitive ion channel. The effect of Yoda1 on Piezo1 expression levels is unexpected as previous experiments showed no effect of 24 h Yoda1 stimulation on Piezo1 expression levels in murine cardiac fibroblasts [44]. The induction of Piezo1 expression by its agonist Yoda1 implies a positive feedback loop, which merits further investigation. In contrast to Yoda1, cyclic stretch did not affect Piezo1 mRNA expression. A possible explanation for the difference between the cyclic stretch and Yoda1, might be that Yoda1 is a stronger stimulus than stretch. On the other hand, stretch significantly increased the mRNA expression of Acta2 and Ctgf after 4 h, but Yoda1 does not. This might be due to the low numbers of cardiac fibroblast isolations (n = 6) used in the Yoda1 experiment; Although no statistically significant difference was found, Yoda1 increased both Ctgf (p = 0.06) and Acta2 (p = 0.1) mRNA levels, which fits with the results from the stretch experiments.

Silencing Piezo1 increased the mRNA expression levels Ctgf in non-stretched cells and of Tnc and Acta2 in stretched cells. It is possible that the Piezo1 channel is active under control conditions, and inhibits the expression of these genes. However, this would contradict our observation that Yoda1 (which activates Piezo1) stimulated Tnc expression. Possibly, silencing of Piezo1 led to cellular compensatory mechanisms that indirectly affected the expression of these genes. Obviously, the mechanisms by which Piezo1-silencing affected Ctgf, Tnc and Acta2 are not clear and further studies are warranted to investigate this mechanism. Previously, our colleagues from the Leeds group showed that IL-6 expression and secretion in cardiac fibroblasts was inhibited by Piezo1 silencing, indicating a role for Piezo1 signaling in the expression of this pro-inflammatory gene [44]. Interestingly, this was depending on substrate stiffness and/or composition as the effect was absent when cells were cultured on regular non-coated cell culture plates (rigid plastic) [18, 44]. Stiffness of standard plastic culture plates are estimated in the gigapascal (GPa) range [51]. The Bioflex plates we have used for the stretch experiment have a stiffness 1000 times less (~1 megapascal, MPa) than those standard culture plates. However, the stiffness of healthy myocardial tissue is estimated to be 10 kilopascal (kPa) [51-53], making myocardial tissue stiffness 100 times less than the Bioflex plates. Therefore, even though the Bioflex plates are softer than regular culture plates, they are still stiff compared to healthy myocardial tissue. Of note, the stiffness of fibrotic myocardium is estimated at 20–100 kPa [51-53]. It has also been shown previously that Piezo1 reacts to stiffness, in both stem cells [54] and atrial fibroblasts [55].

In the present study, we did not investigate the mechanism of Piezo1-induced effects on gene expression. However, the Leeds group has reported on how Il-6 expression is linked to Piezo1 [44]. They suggest an important role for the p38 MAPK pathway in Piezo1- induced Il-6 gene expression, in which p38 activation was depending on extracellular Ca2+. A similar activation pathway might be the case for Nppb or Tgfβ1, but the mechanism of Piezo1 activation on Nppb or Tgfβ1 expression requires further research.

In conclusion, the present study shows that both stretch-induced Nppb and Tgfβ1 expression in adult rat cardiac fibroblasts is mediated by the mechanosensitive ion channel Piezo1. Furthermore, BNP protein levels were upregulated in stretched cardiac fibroblasts and recombinant BNP inhibited TGFβ1-induced Acta2 expression in cardiac fibroblasts. Together, these results indicate that Piezo1 is an important mechanosensitive ion channel mediating stretch-induced activation of cardiac fibroblasts.

References

1. Hoffman BD, Grashoff C, Schwartz MA. Dynamic molecular processes mediate cellular mechanotransduction. Nature. 2011;475(7356):316-23.
2. Orr AW, Helmke BP, Blackman BR, Schwartz MA. Mechanisms of mechanotransduction. Dev Cell. 2006;10(1):11-20.
3. Chen CS. Mechanotransduction - a field pulling together? J Cell Sci. 2008;121(Pt 20):3285-92.
4. Geiger B, Spatz JP, Bershadsky AD. Environmental sensing through focal adhesions. Nat Rev Mol Cell Biol. 2009;10(1):21-33.
5. Zimmermann WH. Biomechanical regulation of in vitro cardiogenesis for tissue-engineered heart repair. Stem Cell Res Ther. 2013;4(6):137.
6. Grossman W, Jones D, McLaurin LP. Wall stress and patterns of hypertrophy in the human left ventricle. Journal of Clinical Investigation. 1975;56(1):56-64.
7. Toischer K, Rokita AG, Unsold B, Zhu W, Kararigas G, Sossalla S, et al. Differential cardiac remodeling in preload versus afterload. Circulation. 2010;122(10):993-1003.
8. Frangogiannis NG. The extracellular matrix in myocardial injury, repair, and remodeling. J Clin Invest. 2017;127(5):1600-12.
9. van Nieuwenhoven FA, Munts C, Op 't Veld RC, Gonzalez A, Diez J, Heymans S, et al. Cartilage intermediate layer protein 1 (CILP1): A novel mediator of cardiac extracellular matrix remodelling. Sci Rep. 2017;7(1):16042.
10. Tsuruda T, Boerrigter G, Huntley BK, Noser JA, Cataliotti A, Costello-Boerrigter LC, et al. Brain natriuretic Peptide is produced in cardiac fibroblasts and induces matrix metalloproteinases. Circ Res. 2002;91(12):1127-34.
11. Imanaka-Yoshida K. Tenascin-C in cardiovascular tissue remodeling: from development to inflammation and repair. Circ J. 2012;76(11):2513-20.
12. Daniels A, van Bilsen M, Goldschmeding R, van der Vusse GJ, van Nieuwenhoven FA. Connective tissue growth factor and cardiac fibrosis. Acta Physiol (Oxf). 2009;195(3):321-38.
13. Powell DW, Mifflin RC, Valentich JD, Crowe SE, Saada JI, West AB. Myofibroblasts. I. Paracrine cells important in health and disease. Am J Physiol. 1999;277(1):C1-9.
14. van den Borne SW, Diez J, Blankesteijn WM, Verjans J, Hofstra L, Narula J. Myocardial remodeling after infarction: the role of myofibroblasts. Nat Rev Cardiol. 2010;7(1):30-7.
15. Tarbit E, Singh I, Peart JN, Rose'Meyer RB. Biomarkers for the identification of cardiac fibroblast and myofibroblast cells. Heart Fail Rev. 2019;24(1):1-15.
16. Swaney JS, Roth DM, Olson ER, Naugle JE, Meszaros JG, Insel PA. Inhibition of cardiac myofibroblast formation and collagen synthesis by activation and overexpression of adenylyl cyclase. Proc Natl Acad Sci U S A. 2005;102(2):437-42.
17. Hinz B. The myofibroblast: paradigm for a mechanically active cell. J Biomech. 2010;43(1):146-55.
18. Yong KW, Li Y, Huang G, Lu TJ, Safwani WK, Pingguan-Murphy B, et al. Mechanoregulation of cardiac myofibroblast differentiation: implications for cardiac fibrosis and therapy. Am J Physiol Heart Circ Physiol. 2015;309(4):H532-42.
19. Stewart L, Turner NA. Channelling the Force to Reprogram the Matrix: Mechanosensitive Ion Channels in Cardiac Fibroblasts. Cells. 2021;10(5).
20. Kinnunen P, Vuolteenaho O, Ruskoaho H. Mechanisms of Atrial and Brain Natriuretic Peptide Release From Rat Ventricular Myocardium: Effect of Stretching. Endocrinology. 1993;132(5):1961-70.
21. Toth M, Vuorinen KH, Vuolteenaho O, Hassinen IE, Uusimaa PA, Leppaluoto J, et al. Hypoxia stimulates release of ANP and BNP from perfused rat ventricular myocardium. Am J Physiol. 1994;266(4 Pt 2):H1572-80.
22. Zois NE, Bartels ED, Hunter I, Kousholt BS, Olsen LH, Goetze JP. Natriuretic peptides in cardiometabolic regulation and disease. Nat Rev Cardiol. 2014;11(7):403-12.

23. Fu S, Ping P, Wang F, Luo L. Synthesis, secretion, function, metabolism and application of natriuretic peptides in heart failure. J Biol Eng. 2018;12:2.
24. Jarai R, Kaun C, Weiss TW, Speidl WS, Rychli K, Maurer G, et al. Human cardiac fibroblasts express B-type natriuretic peptide: fluvastatin ameliorates its up-regulation by interleukin-1alpha, tumour necrosis factor-alpha and transforming growth factor-beta. J Cell Mol Med. 2009;13(11-12):4415-21.
25. Del Ry S, Cabiati M, Lionetti V, Emdin M, Recchia FA, Giannessi D. Expression of C-type natriuretic peptide and of its receptor NPR-B in normal and failing heart. Peptides. 2008;29(12):2208-15.
26. Maisel AS, Duran JM, Wettersten N. Natriuretic Peptides in Heart Failure: Atrial and B-type Natriuretic Peptides. Heart Fail Clin. 2018;14(1):13-25.
27. Forte M, Madonna M, Schiavon S, Valenti V, Versaci F, Zoccai GB, et al. Cardiovascular Pleiotropic Effects of Natriuretic Peptides. Int J Mol Sci. 2019;20(16).
28. He XL, Dukkipati A, Garcia KC. Structural determinants of natriuretic peptide receptor specificity and degeneracy. J Mol Biol. 2006;361(4):698-714.
29. Matsuo A, Nagai-Okatani C, Nishigori M, Kangawa K, Minamino N. Natriuretic peptides in human heart: Novel insight into their molecular forms, functions, and diagnostic use. Peptides. 2019;111:3-17.
30. Potter LR, Yoder AR, Flora DR, Antos LK, Dickey DM. Natriuretic peptides: their structures, receptors, physiologic functions and therapeutic applications. Handb Exp Pharmacol. 2009(191):341-66.
31. Moyes AJ, Chu SM, Aubdool AA, Dukinfield MS, Margulies KB, Bedi KC, et al. C-type natriuretic peptide co-ordinates cardiac structure and function. Eur Heart J. 2020;41(9):1006-20.
32. Blaauw E, van Nieuwenhoven FA, Willemsen P, Delhaas T, Prinzen FW, Snoeckx LH, et al. Stretch-induced hypertrophy of isolated adult rabbit cardiomyocytes. Am J Physiol Heart Circ Physiol. 2010;299(3):H780-7.
33. Ovchinnikova E, Hoes M, Ustyantsev K, Bomer N, de Jong TV, van der Mei H, et al. Modeling Human Cardiac Hypertrophy in Stem Cell-Derived Cardiomyocytes. Stem Cell Reports. 2018;10(3):794-807.
34. Kapoun AM, Liang F, O'Young G, Damm DL, Quon D, White RT, et al. B-type natriuretic peptide exerts broad functional opposition to transforming growth factor-beta in primary human cardiac fibroblasts: fibrosis, myofibroblast conversion, proliferation, and inflammation. Circ Res. 2004;94(4):453-61.
35. Tamura N, Ogawa Y, Chusho H, Nakamura K, Nakao K, Suda M, et al. Cardiac fibrosis in mice lacking brain natriuretic peptide. Proc Natl Acad Sci U S A. 2000;97(8):4239-44.
36. Ichiki T, Dzhoyashvili N, Burnett JC, Jr. Natriuretic peptide based therapeutics for heart failure: Cenderitide: A novel first-in-class designer natriuretic peptide. Int J Cardiol. 2019;281:166-71.
37. Jhund PS, McMurray JJ. The neprilysin pathway in heart failure: a review and guide on the use of sacubitril/valsartan. Heart. 2016;102(17):1342-7.
38. Makino N, Sugano M, Satoh S, Oyama J, Maeda T. Peroxisome Proliferator-Activated Receptor-γ Ligands Attenuate Brain Natriuretic Peptide Production and Affect Remodeling in Cardiac Fibroblasts in Reoxygenation After Hypoxia. Cell Biochemistry and Biophysics. 2006;44(1):065-72.
39. Morita E, Yasue H, Yoshimura M, Ogawa H, Jougasaki M, Matsumura T, et al. Increased plasma levels of brain natriuretic peptide in patients with acute myocardial infarction. Circulation. 1993;88(1):82-91.
40. Nishikimi T, Yoshihara F, Morimoto A, Ishikawa K, Ishimitsu T, Saito Y, et al. Relationship Between Left Ventricular Geometry and Natriuretic Peptide Levels in Essential Hypertension. Hypertension. 1996;28(1):22-30.
41. Koglin J, Pehlivanli S, Schwaiblmair M, Vogeser M, Cremer P, vonScheidt W. Role of brain natriuretic peptide in risk stratification of patients with congestive heart failure. Journal of the American College of Cardiology. 2001;38(7):1934-41.
42. Nishikimi T, Maeda N, Matsuoka H. The role of natriuretic peptides in cardioprotection. Cardiovasc Res. 2006;69(2):318-28.
43. Watson CJ, Phelan D, Xu M, Collier P, Neary R, Smolenski A, et al. Mechanical stretch up-regulates the B-type natriuretic peptide system in human cardiac fibroblasts: a possible defense against transforming growth factor-beta mediated fibrosis. Fibrogenesis Tissue Repair. 2012;5(1):9.

44. Blythe NM, Muraki K, Ludlow MJ, Stylianidis V, Gilbert HTJ, Evans EL, et al. Mechanically activated Piezo1 channels of cardiac fibroblasts stimulate p38 mitogen-activated protein kinase activity and interleukin-6 secretion. J Biol Chem. 2019;294(46):17395-408.
45. Turner NA, Porter KE, Smith WHT, White HL, Ball SG, Balmforth AJ. Chronic β2-adrenergic receptor stimulation increases proliferation of human cardiac fibroblasts via an autocrine mechanism. Cardiovascular Research. 2003;57(3):784-92.
46. van Nieuwenhoven FA, Hemmings KE, Porter KE, Turner NA. Combined effects of interleukin-1α and transforming growth factor-β1 on modulation of human cardiac fibroblast function. Matrix Biology. 2013;32(7-8):399-406.
47. Blaauw E, Lorenzen-Schmidt I, Babiker FA, Munts C, Prinzen FW, Snoeckx LH, et al. Stretch-induced upregulation of connective tissue growth factor in rabbit cardiomyocytes. J Cardiovasc Transl Res. 2013;6(5):861-9.
48. McMurray JJ, Packer M, Desai AS, Gong J, Lefkowitz MP, Rizkala AR, et al. Dual angiotensin receptor and neprilysin inhibition as an alternative to angiotensin-converting enzyme inhibition in patients with chronic systolic heart failure: rationale for and design of the Prospective comparison of ARNI with ACEI to Determine Impact on Global Mortality and morbidity in Heart Failure trial (PARADIGM-HF). Eur J Heart Fail. 2013;15(9):1062-73.
49. Calderone A, Bel-Hadj S, Drapeau J, El-Helou V, Gosselin H, Clement R, et al. Scar myofibroblasts of the infarcted rat heart express natriuretic peptides. J Cell Physiol. 2006;207(1):165-73.
50. Kuhn M, Volker K, Schwarz K, Carbajo-Lozoya J, Flogel U, Jacoby C, et al. The natriuretic peptide/guanylyl cyclase--a system functions as a stress-responsive regulator of angiogenesis in mice. J Clin Invest. 2009;119(7):2019-30.
51. Herum KM, Lunde IG, McCulloch AD, Christensen G. The Soft- and Hard-Heartedness of Cardiac Fibroblasts: Mechanotransduction Signaling Pathways in Fibrosis of the Heart. J Clin Med. 2017;6(5).
52. Berry MF, Engler AJ, Woo YJ, Pirolli TJ, Bish LT, Jayasankar V, et al. Mesenchymal stem cell injection after myocardial infarction improves myocardial compliance. Am J Physiol Heart Circ Physiol. 2006;290(6):H2196-203.
53. Engler AJ, Carag-Krieger C, Johnson CP, Raab M, Tang HY, Speicher DW, et al. Embryonic cardiomyocytes beat best on a matrix with heart-like elasticity: scar-like rigidity inhibits beating. J Cell Sci. 2008;121(Pt 22):3794-802.
54. Chen X, Wanggou S, Bodalia A, Zhu M, Dong W, Fan JJ, et al. A Feedforward Mechanism Mediated by Mechanosensitive Ion Channel PIEZO1 and Tissue Mechanics Promotes Glioma Aggression. Neuron. 2018;100(4):799-815 e7.
55. Emig R, Knodt W, Krussig MJ, Zgierski-Johnston CM, Gorka O, Gross O, et al. Piezo1 Channels Contribute to the Regulation of Human Atrial Fibroblast Mechanical Properties and Matrix Stiffness Sensing. Cells. 2021;10(3).

Involvement of Piezo1 in the mechanoregulation of cartilage intermediate layer protein 1 (CILP1) in cardiac fibroblasts.

Meike C. Ploeg[1], Chantal Munts[1], Frits W. Prinzen[1], Neil A. Turner[2,3], Marc van Bilsen[1] and Frans A. van Nieuwenhoven[1]

[1] Department of Physiology, Cardiovascular Research Institute Maastricht (CARIM), Maastricht University, the Netherlands; [2] Discovery and Translational Science Department, Leeds Institute of Cardiovascular and Metabolic Medicine, School of Medicine, University of Leeds, Leeds, LS2 9JT, UK; [3] Multidisciplinary Cardiovascular Research Centre, University of Leeds, Leeds, LS2 9JT, UK.

3

Abstract

Background: cartilage intermediate layer protein 1 (CILP1) is a matricellular protein expressed by cardiac fibroblasts (CFs) that recently gained interest as a marker and pathogenic factor in cardiac disease. Here, we investigate the regulation of Cilp1 gene expression in CFs by cyclic stretch and the involvement of mechanosensitive ion channel Piezo1 as mechanotransducer in this process.

Methods: Primary adult rat CFs were exposed to 10% cyclic stretch (1 Hz) for 4 h or 24 h, using the Flexcell system. Moreover, Cilp1 gene expression in CF was investigated after stimulation with TGFβ1 or Piezo1 agonist Yoda1 by qRT-PCR. Finally, the effect of silencing of Piezo1 using siRNA on Cilp1 regulation by stretch was determined.

Results: 4 h 10% cyclic stretch did not alter Cilp1 mRNA expression. However, 24 h 10% cyclic stretch significantly reduced Cilp1 mRNA levels. Stimulation of CFs with TGFβ1 increased expression of Cilp1 after 4 h, but not after 24 h. Stimulation with Yoda1 resulted in a downregulation of Cilp1 after 4 h, and silencing of Piezo1 significantly induced Cilp1 mRNA expression.

Conclusion: Cilp1 mRNA expression is downregulated by 24 h of cyclic stretch in rat CFs and Piezo1 is most likely involved as mechanotransducer in this process.

Introduction

Cardiac fibroblasts (CFs) play an important role in the regulation of the extracellular matrix (ECM), by synthesizing structural ECM proteins (i.e collagens), ECM degrading matrix metalloproteinases (MMPs), their inhibitors (TIMPs)[1], growth factors such as transforming growth factor β1 (TGFβ1) and matricellular proteins like tenascin C (TNC) and connective tissue growth factor (CTGF) [2]. Recently, our group has identified cartilage intermediate layer protein 1 (CILP1) as a novel mediator of cardiac ECM remodeling [3]. We and others showed that CILP1 inhibits TGFβ activity [3, 4] in vitro, indicating an antifibrotic role for CILP1. Although we showed that the main source of cardiac CILP1 expression are cardiac fibroblasts [3], others found CILP1 predominantly in cardiomyocytes [5].

The proposed anti-fibrotic role of CILP1 was supported by mouse studies where myocardial CILP1 knockdown aggravated, whereas CILP1 overexpression attenuated ventricular remodeling and dysfunction after transverse aortic constriction [5]. By contrast, Zhang and coworkers showed very recently that fibrosis-related gene expression was attenuated in Cilp1 knock out mice post myocardial infarction compared to wild type hearts, suggesting Cilp1 has an adverse role in pathological cardiac remodeling [6]. Although the association with myocardial remodeling is very strong and convincing, the exact role of CILP1 is still under debate. Increased levels of circulating CILP1 [7] and CILP1 expression [8] have been found in heart failure patients. Moreover, CILP1 was shown to be a novel independent prognostic predictor in chronic heart failure [9] and as a biomarker of right- and left ventricular pathological remodeling in patients with pulmonary hypertension [7] and ischemic cardiomyopathy [10].

It has been previously shown that CILP1 expression is decreased in human nucleus pulposus cells after being exposed to mechanical stimulation in the form of cyclic tensile strain, the opposite was found when human nucleus pulposus were exposed to compressive loading [11]. This data indicates mechanosensitivity of CILP1 in human nucleus pulposus cells.

We and others have previously shown the involvement of Piezo1 as Ca^{2+}-permeable mechanosensitive ion channel in mechanical stimulation of cardiac fibroblasts [12, 13]. Pharmacological or genetic modulation of Piezo1 activity could be used to gain insight in the functional role of Piezo1 [14]. Yoda1 was developed as functional agonist of Piezo1 [15].

Here, we investigate the effect of mechanical stimulation in the form of cyclic stretch on Cilp1 expression in primary rat ventricular CFs and the role of Piezo1 in stretch induced Cilp1 expression.

Materials & Methods

Experiments performed in this chapter are identical to the ones performed in chapter 2.

Isolation of cardiac fibroblasts
CFs were isolated from cardiac ventricles of adult surplus rats from any age, weight, sex or breed (n=31). Most of the rats used were either from the Lewis or Wistar strain and aged between 5 and 52 weeks. Rat cardiac ventricular fibroblasts were isolated and cultured as previously described [3, 16, 17] in Dulbecco's modified eagles medium (DMEM; no. 22320, Gibco, Invitrogen, Breda, the Netherlands) supplemented with 10% (vol/vol) fetal bovine serum (FBS, Gibco), gentamicin (50 µg/ml, Gibco), 1% (vol/vol) Insulin-Transferrin-Selenium-Sodium Pyruvate (ITS-A, Gibco) and basic fibroblast growth factor (1 ng/ml, Gibco) ("CF culture medium"). These primary fibroblasts were used between passage 1-3.

Experimental stretch protocols
CFs (10,000 cells/cm^2) were plated on bioflex plates (6-well Bioflex plates, precoated with collagen-I, Flexcell Dunn Labortechnik, Asbach, Germany) in CF culture medium. The next day, CF culture medium was replaced by DMEM supplemented with gentamicin (50 µg/ml, Gibco). After 24 h, cardiac fibroblasts were subjected to 10% cyclic (1 Hz) equibiaxial stretch, (Flexcell FX-4000 strain unit, Dunn Labortechnik) for 4 h, 6 h or 24 h. Control, non-stretched cells were subjected to identical conditions however, without stretch being applied.

Experimental stimuli
To determine the effect of TGFβ1, CFs (10,000 cells/cm^2) were serum-starved for 24 hours before incubation with TGFβ1 (1 ng/ml, R&D systems, Minneapolis, USA) for 4 h or 24 h. To investigate the effect of Piezo1 activity, CF were treated with the Piezo1 agonist Yoda1 (10 µM, Tocris, Bristol, UK) for 4 h.

Piezo1 gene silencing
CFs (10,000 cells/cm^2) were plated on bioflex plates (6-well Bioflex plates, precoated with collagen-I, Flexcell Dunn Labortechnik) in CF culture medium. The next day the medium was changed to DMEM. After 4 h CFs were transfected with 10 nM Piezo1-specific Silencer Select Pre-Designed siRNA (4390771, siRNA s107968, Life Technologies, Carlsbad, USA) or Silencer Select Negative Control No. 1 siRNA (4390843, Life Technologies) using Lipofectamine RNAiMAX reagent (Life Technologies) in Opti-MEM (Gibco) according to the manufacturer's instructions. The next day medium was changed again to DMEM. After 48 h CFs were exposed to the stretch protocol described above.

Gene expression analysis
Total RNA was isolated from cells using an RNA isolation kit (micro elute RNA kit, Omega Biotek, Norcross, USA) and reversed transcribed into cDNA using the iScript cDNA synthesis kit (Biorad, Hercules, USA) according to the manufacturer's instructions. Real-time PCR was performed on

a CFX96 Touch Real-Time PCR Detection System (Biorad) using SYBR-Green Supermix (Biorad) [3]. Gene expression levels of Piezo1 and cartilage intermediate layer protein 1 (Cilp1) were normalized using the housekeeping gene Cyclophilin-A (Cyclo) and their relative expression was calculated using the comparative threshold cycle (Ct) method by calculating $2^{\Delta Ct}$ (e.g. $2^{(\text{Cyclophilin Ct} - \text{Cilp1 Ct})}$). The gene expression values were multiplied by 1000 (formula $1000 * 2^{\Delta Ct}$), to enhance readability. The sequences of the specific primers used are provided below (table 1).

Table 1. Gene-specific primer sequences used for quantitative real-time PCR

Gene	Forward primer	Reverse Primer
Piezo1	TTGCGTACGTTCACGAAGGA	TTCGCTCACGTAAAGCTGGT
Cilp1	GAGTACTTCTGTAAGGCGCAG	GGCATTCTGGAAGCAATCATG
Cyclophilin-A (Cyclo)	CAAATGCTGGACCAAACACAA	TTCACCTTCCCAAAGACCACAT

Statistics

Data are presented as mean or individual data points and were analyzed with Wilcoxon matched pairs test or Friedman test, with Dunn selected columns posthoc test where appropriate. Differences were considered statistically significant when $p<0.05$.

Results

Stretch reduces CF Cilp1 expression after 24 h

Mechanical stimulation of CFs in the form of 10% cyclic stretch at 1 Hz significantly reduced Cilp1 mRNA expression after 24 h, but not after 4 h (figure 1A). Treatment of unstretched CFs with TGFβ1 gave a significant induction of Cilp1 mRNA expression after 4 h, but not after 24 h (figure 1B).

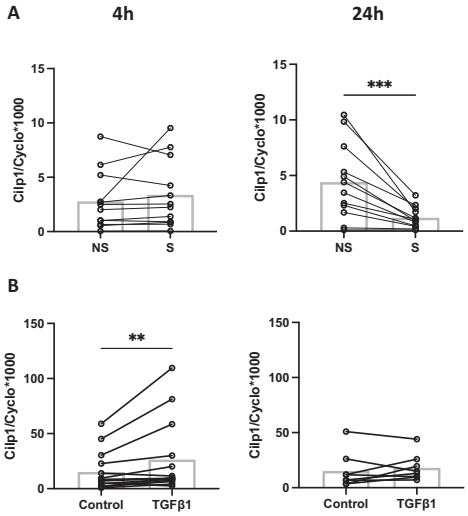

Figure 1. Relative mRNA expression levels of Cilp1 in CFs exposed to 10% cyclic (1 Hz) stretch (S) or non-stretched (NS) conditions for 4 h (n=12) or 24 h (n=12)(A). Relative mRNA expression levels of Cilp1 in CFs after stimulation with TGFβ1 after 4 h (n=8) and 24 h (n=8)(B). ** $p < 0.01$; *** $p < 0.001$. Bar indicates mean.

Yoda1 lowers Cilp1 expression after 4 h

In unstretched CFs treatment with the Piezo1 agonist Yoda1 significantly decreases Cilp1 expression after 4 h (figure 2).

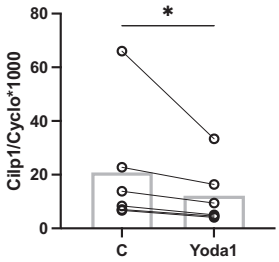

Figure 2. Relative mRNA expression levels of Cilp1 in CFs after stimulation with Piezo1 agonist Yoda1 for 4 h (n=6). * $p < 0.05$. Bar indicates mean.

Piezo1 silencing increases CF Cilp1 expression

Piezo1 silencing, which was shown earlier [13](Chapter 2) to lower Piezo1 mRNA levels by 80%, significantly increased the mRNA expression of Cilp1, an effect that was not observed when using scrambled SI (figure 3).

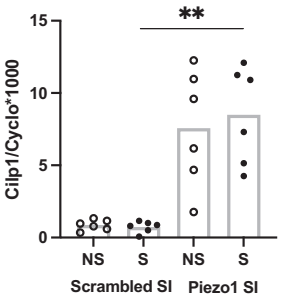

Figure 3. Relative mRNA expression of Cilp1 in CFs exposed to 10% cyclic (1 Hz) stretch for 6h (S) or non-stretched (NS) conditions after transfection with either control siRNA (Scrambled SI) or Piezo1-specific siRNA (Piezo1 SI) (n = 6). ** $p < 0.01$. Bar indicates mean.

Discussion

The present study shows that Cilp1 gene expression in CFs significantly decreased after exposure to 24 h of 10% cyclic stretch (figure 4 [18]). In addition, stimulation of the mechanosensitive Piezo1 by Yoda reduced Cilp1 mRNA expression levels while and silencing Piezo1 increased expression in both stretch and unstretched conditions.

Our finding of Cilp1 downregulation by cyclic stretch in CFs is supported by previous research in human nucleus pulposus cells, exposed to cyclic tensile strain [11] as well as in bovine nucleus pulposus cells exposed to different loading protocols [19]. Mechanosensitivity of Cilp1 was first shown in nucleus pulposus cells, but depending on the type of mechanical loading Cilp1 expression either increased or decreased [11]. This two-way response of Cilp1 is something we also see when stimulating CFs with TGFβ1 and stretch, leading to an increased or downregulation of Cilp1, respectively. Suggesting that depending on the type of stimulation, Cilp1 might react contradictory. Piezo1 activity can lead to increased calcium levels in the cell, which previously has been shown to induce IL-6 expression via p38 MAPK [12] or can lead to activation of integrin– focal adhesion kinase signaling without the need of calcium [20]. The p38 MAPK has been implicated as important regulator in cardiac remodeling [21] and important for Acta2 expression in rat CFs [22, 23]. The Cilp1 stretch-induced downregulation might be regulated via p38 MAPK, while the TGFβ1 induced induction of Cilp1 is regulated via integrin– focal adhesion kinase signaling. Further research is necessary to delineate Piezo1 downstream signaling in CF and to investigate the precise role of Cilp1 in cardiac disease, where mechanical stimuli and increased TGFb1 activity might be simultaneous.

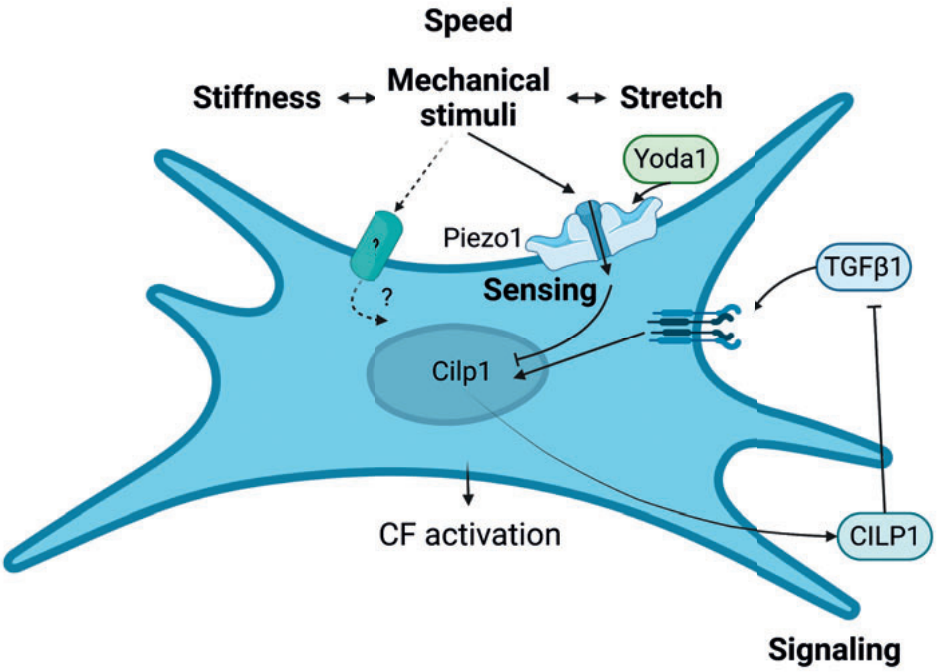

Figure 4. Schematic of proposed mechanism on Piezo1 mechanosignaling and TGFβ1 stimulation of CF on Cilp1 mRNA expression and how this could lead to CF activation and differentiation, ultimately leading towards fibrosis. Stretch and Yoda1 stimulation downregulates Cilp1 mRNA expression and most likely Piezo1 is the mechanotransducer in this process, however there might be other receptors or channels involved. TGFβ1 stimulation leads to increased expression of Cilp1 mRNA expression. TGFβ1 can also be released from ECM activation, as it is stored within the ECM in inactive form. Previous work from our group already showed that CILP1 inhibits TGFβ1 [3].

Stimulation of CFs with Yoda1 gave a significant reduction of Cilp1 mRNA expression after 4 h, similar as the effect of 24 h 10% cyclic stretch. Possibly the difference between onset of the effect might be that direct stimulation of Piezo1 by Yoda1 is a stronger stimulus than the cyclic stretch [13]. The similar response of Cilp1 expression in CF to stretch or Yoda1 stimulation suggests that Piezo1 is involved as mechanotransducer in the stretch-induced downregulation of Cilp1. This is supported by the increased Cilp1 mRNA following Piezo1 silencing. In the scrambled (control) condition, Piezo1 is present and might have a baseline activity due to the stiffness of the substrate (bottom of the plate). The fact that decreasing Piezo1 leads to increased Cilp1 gene expression in CF indicates that activation of this mechanosensitive channel inhibits Cilp1 gene expression. We have previously reported the effect of Piezo1 silencing conditions causing increased mRNA expression of Acta2 and Tnc, already discussing that stiffness of the culture plate might have an influence. The Bioflex plates used for the stretch experiments are 100 times stiffer than myocardial tissue. Both CFs [24, 25] and Piezo1 expression and activity [20, 26] are under the influence of substrate stiffness. Piezo1 might suppress Cilp1 mRNA expression under control conditions, then

when Piezo1 levels decrease after siRNA treatment, this suppression disappears causing an increase in Cilp1 mRNA expression. The regulation of Cilp1 by mechanical stimuli and the role of Piezo1 and the substrate stiffness as possible underlying mechanisms still needs further investigation. For this CF cultures with physiological stiffness are essential. Another difference between the culture plates was the collagen type 1 coating on the Bioflex plates, which was absent in the regular plastic culture plates. Pilot studies, in which coated regular plastic culture plates with collagen type 1 showed no differences compared to Bioflex and non-coated plastic plates.

Cyclic stretch for 6h in control (scrambled siRNA) or Piezo1-silenced (Piezo1 siRNA) showed no further effect. This supports our results of 4 h cyclic stretch. The downregulation of Cilp1 was seen only after 24 h of cyclic stretch. Ideal set up to investigate the role of Piezo1 in stretch-induced downregulation of Cilp1 mRNA expression would be to apply 24 h cyclic stretch in both scrambled and siRNA of Piezo1 conditions. Further research is necessary to investigate whether Piezo1 is involved as the mechanotransducer for stretch-induced downregulation of Cilp1.

CF showed an increased Cilp1 mRNA expression after 4 h treatment with TGFβ1. However, we have previously shown a reduction of Cilp1 expression in rat CFs after treatment with TGFβ1 after 24 h [3]. The timepoint could be of influence, however the current results do not show a reduction in Cilp1 mRNA expression after 24 h. The discrepancy between these contradicting results might be caused by lower baseline expression of Cilp1 in CFs in the present study. A low baseline CILP1 expression was found in human atrial fibroblasts where the induction by TGFβ1 was 20-fold [3]. Our finding of increased Cilp1 expression after TGFβ1 stimulation is supported by research in human cardiac fibroblasts [27] and chondrocytes [28]. Maybe the level of CF activation and differentiation influences the regulation of CILP1 by TGFβ1.

We have confirmed the mechanosensitivity of Cilp1 in CFs and the reduction in Cilp1 mRNA expression after 24 h of 10% cyclic stretch. Piezo1-agonist Yoda1 reduced, while Piezo-silencing increased Cilp1 mRNA expression. Taken together, we conclude that cyclic stretch downregulates Cilp1 mRNA expression and that Piezo1 is most likely involved as mechanotransducer in this process.

References

1. Tsuruda T, Boerrigter G, Huntley BK, Noser JA, Cataliotti A, Costello-Boerrigter LC, et al. Brain natriuretic Peptide is produced in cardiac fibroblasts and induces matrix metalloproteinases. Circ Res. 2002;91(12):1127-34.
2. Daniels A, van Bilsen M, Goldschmeding R, van der Vusse GJ, van Nieuwenhoven FA. Connective tissue growth factor and cardiac fibrosis. Acta Physiol (Oxf). 2009;195(3):321-38.
3. van Nieuwenhoven FA, Munts C, Op 't Veld RC, Gonzalez A, Diez J, Heymans S, et al. Cartilage intermediate layer protein 1 (CILP1): A novel mediator of cardiac extracellular matrix remodelling. Sci Rep. 2017;7(1):16042.
4. Seki S, Kawaguchi Y, Chiba K, Mikami Y, Kizawa H, Oya T, et al. A functional SNP in CILP, encoding cartilage intermediate layer protein, is associated with susceptibility to lumbar disc disease. Nat Genet. 2005;37(6):607-12.
5. Zhang CL, Zhao Q, Liang H, Qiao X, Wang JY, Wu D, et al. Cartilage intermediate layer protein-1 alleviates pressure overload-induced cardiac fibrosis via interfering TGF-beta1 signaling. J Mol Cell Cardiol. 2018;116:135-44.
6. Zhang QJ, He Y, Li Y, Shen H, Lin L, Zhu M, et al. Matricellular Protein Cilp1 Promotes Myocardial Fibrosis in Response to Myocardial Infarction. Circ Res. 2021;129(11):1021-35.
7. Keranov S, Dorr O, Jafari L, Troidl C, Liebetrau C, Kriechbaum S, et al. CILP1 as a biomarker for right ventricular maladaptation in pulmonary hypertension. Eur Respir J. 2021;57(4).
8. Park S, Ranjbarvaziri S, Zhao P, Ardehali R. Cardiac Fibrosis Is Associated With Decreased Circulating Levels of Full-Length CILP in Heart Failure. JACC Basic Transl Sci. 2020;5(5):432-43.
9. Wang C, Jian W, Luo Q, Cui J, Qing Y, Qin C, et al. Prognostic value of cartilage intermediate layer protein 1 in chronic heart failure. ESC Heart Fail. 2022;9(1):345-52.
10. Keranov S, Jafari L, Haen S, Vietheer J, Kriechbaum S, Dorr O, et al. CILP1 as a biomarker for right ventricular dysfunction in patients with ischemic cardiomyopathy. Pulm Circ. 2022;12(1):e12062.
11. He J, Feng C, Sun J, Lu K, Chu T, Zhou Y, et al. Cartilage intermediate layer protein is regulated by mechanical stress and affects extracellular matrix synthesis. Mol Med Rep. 2018;17(4):6130-7.
12. Blythe NM, Muraki K, Ludlow MJ, Stylianidis V, Gilbert HTJ, Evans EL, et al. Mechanically activated Piezo1 channels of cardiac fibroblasts stimulate p38 mitogen-activated protein kinase activity and interleukin-6 secretion. J Biol Chem. 2019;294(46):17395-408.
13. Ploeg MC, Munts C, Prinzen FW, Turner NA, van Bilsen M, van Nieuwenhoven FA. Piezo1 Mechanosensitive Ion Channel Mediates Stretch-Induced Nppb Expression in Adult Rat Cardiac Fibroblasts. Cells. 2021;10(7).
14. Chubinskiy-Nadezhdin VI, Vasileva VY, Vassilieva IO, Sudarikova AV, Morachevskaya EA, Negulyaev YA. Agonist-induced Piezo1 activation suppresses migration of transformed fibroblasts. Biochem Biophys Res Commun. 2019;514(1):173-9.
15. Syeda R, Xu J, Dubin AE, Coste B, Mathur J, Huynh T, et al. Chemical activation of the mechanotransduction channel Piezo1. Elife. 2015;4.
16. Turner NA, Porter KE, Smith WHT, White HL, Ball SG, Balmforth AJ. Chronic β2-adrenergic receptor stimulation increases proliferation of human cardiac fibroblasts via an autocrine mechanism. Cardiovascular Research. 2003;57(3):784-92.
17. van Nieuwenhoven FA, Hemmings KE, Porter KE, Turner NA. Combined effects of interleukin-1α and transforming growth factor-β1 on modulation of human cardiac fibroblast function. Matrix Biology. 2013;32(7-8):399-406.
18. Created with BioRender.com.
19. Croft AS, Roth Y, Oswald KAC, Corluka S, Bermudez-Lekerika P, Gantenbein B. In Situ Cell Signalling of the Hippo-YAP/TAZ Pathway in Reaction to Complex Dynamic Loading in an Intervertebral Disc Organ Culture. Int J Mol Sci. 2021;22(24).

20. Emig R, Knodt W, Krussig MJ, Zgierski-Johnston CM, Gorka O, Gross O, et al. Piezo1 Channels Contribute to the Regulation of Human Atrial Fibroblast Mechanical Properties and Matrix Stiffness Sensing. Cells. 2021;10(3).
21. Turner NA, Blythe NM. Cardiac Fibroblast p38 MAPK: A Critical Regulator of Myocardial Remodeling. J Cardiovasc Dev Dis. 2019;6(3).
22. Hu J, Wang X, Wei SM, Tang YH, Zhou Q, Huang CX. Activin A stimulates the proliferation and differentiation of cardiac fibroblasts via the ERK1/2 and p38-MAPK pathways. Eur J Pharmacol. 2016;789:319-27.
23. See F, Thomas W, Way K, Tzanidis A, Kompa A, Lewis D, et al. p38 mitogen-activated protein kinase inhibition improves cardiac function and attenuates left ventricular remodeling following myocardial infarction in the rat. J Am Coll Cardiol. 2004;44(8):1679-89.
24. Landry NM, Rattan SG, Dixon IMC. An Improved Method of Maintaining Primary Murine Cardiac Fibroblasts in Two-Dimensional Cell Culture. Sci Rep. 2019;9(1):12889.
25. Santiago JJ, Dangerfield AL, Rattan SG, Bathe KL, Cunnington RH, Raizman JE, et al. Cardiac fibroblast to myofibroblast differentiation in vivo and in vitro: expression of focal adhesion components in neonatal and adult rat ventricular myofibroblasts. Dev Dyn. 2010;239(6):1573-84.
26. Chen X, Wanggou S, Bodalia A, Zhu M, Dong W, Fan JJ, et al. A Feedforward Mechanism Mediated by Mechanosensitive Ion Channel PIEZO1 and Tissue Mechanics Promotes Glioma Aggression. Neuron. 2018;100(4):799-815 e7.
27. Kalyanasundaram A, Li N, Gardner ML, Artiga EJ, Hansen BJ, Webb A, et al. Fibroblast-Specific Proteotranscriptomes Reveal Distinct Fibrotic Signatures of Human Sinoatrial Node in Nonfailing and Failing Hearts. Circulation. 2021;144(2):126-43.
28. Mori M, Nakajima M, Mikami Y, Seki S, Takigawa M, Kubo T, et al. Transcriptional regulation of the cartilage intermediate layer protein (CILP) gene. Biochem Biophys Res Commun. 2006;341(1):121-7.

Effects of short periods of cyclic stretch on early-gene response and cardiac fibroblast activation

Meike. C. Ploeg[1], Chantal Munts[1], Frits. W. Prinzen[1] and Frans. A. van Nieuwenhoven[1]

[1]Department of Physiology, Cardiovascular Research Institute Maastricht (CARIM), Maastricht University, the Netherlands;

4

Abstract

Background: Cardiac fibroblasts (CFs) modulate the extracellular matrix and are known to be activated by mechanical stimuli such as stretch and differentiate to myofibroblasts under various pathological conditions. Increased cardiac mechanical loading caused by volume or pressure overload commonly exists over a long period of time (years). However, daily activities such as exercise create shorter lasting changes in mechanical loading (hours). The influence of such relatively short-lasting loading changes on CF is incompletely understood. The aim of the present study was to investigate the effect of short-lasting changes in cyclic stretch on gene expression of early response genes and markers of myofibroblast differentiation in cultured rat CFs.

Methods: Primary adult rat CFs were exposed to different durations of cyclic stretch at 1 Hz. Expression of Nppb, Tnc, Hsp70 and Tgfb1 mRNA were measured as markers of early CF activation, whereas mRNA levels of matricellular proteins Ctgf and Cilp1 were measured as late CF activation markers and Acta2 mRNA as marker for myofibroblast differentiation.

Results: 1 h 10% cyclic stretch lead to significant increases in mRNA expression of Nppb, Tnc, Hsp70 and Tgfb1, after 4 h, but these effects largely disappeared after 24 h. No significant changes in expression levels of Acta2, Ctgf or Cilp1 were observed. Shorter intermittent periods of cyclic stretch within a 1 h time frame showed similar results. In a protocol consisting of 24 h 10% cyclic stretch, an increase of stretch amplitude to 20% or reduction to 0% for 1 hour did not lead to any significant changes in gene expression.

Conclusion: periods of cyclic stretch lasting up to 1 hour temporarily activate CF expression of early response genes, but do not lead to sustained CF activation or initiation of CF differentiation.

Introduction

During normal function, myocardial tissue is exposed to continuous oscillations of stress and strain during the cardiac cycle. On top of that, mechanical loading varies during slow and rapid fluctuations originating from changes in posture, physical activity or emotional state [1]. Blood pressure, heart rate, and cardiac output decrease while sleeping [2, 3] and increase rapidly after waking up [4-6] or physical activity [7, 8]. Chronically increased mechanical load of the myocardial wall is caused by conditions like hypertension and valvular disease and often leads to structural changes such as hypertrophy and fibrosis [9, 10]. Besides mechanical load, neurohormonal activation also plays an important role in cardiac remodeling (3). Together, these stressors modulate the properties of the cells in cardiac tissue [11]. In cardiac tissue, cardiac fibroblasts (CFs) are key cell types for the regulation of extracellular matrix (ECM) function [12-14]. CFs produce the various components of the ECM [15, 16] and are therefore important for maintaining the integrity of the ECM [17, 18]. In addition to producing ECM proteins, CFs also produce ECM-regulatory proteins, which can modulate or degrade the ECM [17, 19] resulting in control of the cardiac ECM turnover [18, 19].

Under various pathological conditions such as hypertension and myocardial infarction, quiescent CFs become activated and transform into myofibroblasts, that show both contractile activity for wound contraction and increased production of ECM proteins like collagen [20]. The expression of α smooth muscle actin (Acta2 gene) is a marker for myofibroblasts [21]. We and others showed previously that in vitro stretch of CFs can lead to activation of marker genes of myofibroblast differentiation [22-24].

In this in vitro setting, CFs exposed to 4 hours of cyclic stretch already increased mRNA expression of several genes related to fibroblast activation [22] and fibrosis [25] but that 24 hours of cyclic stretch are required to significantly increase Acta2 mRNA expression [22]. In the present study, we aimed at investigating the effect of shorter fluctuations (1 hour) in mechanical loading on the fibroblast activation. To this purpose we studied gene expression of primary adult rat CFs in vitro, after a variety of periods of cyclic stretch. To gain insight in CF activation state, we measured a set of “early response” genes including transforming growth factor b1 (Tgfβ1), tenascin C (Tnc), heat-shock protein 70 (Hsp70) and brain natriuretic peptide (Nppb). We also investigate genes known to have slower response following mechanical stimulation of CF, including connective tissue growth factor (Ctgf), cartilage intermediate layer protein 1 (Cilp1) and myofibroblast marker (Acta2).

Materials & methods

Isolation and culture of primary rat cardiac fibroblasts (CFs)

CFs were isolated from cardiac ventricles (combined left and right) of adult surplus rats (n = 20) from any age, weight, sex or breed. Most of the rats used were from the Lewis strain and aged between 5 and 14 weeks. Rat ventricular fibroblasts were isolated and cultured as previously described [26-28] in Dulbecco's modified eagles medium (DMEM; no. 22320, Gibco, Invitrogen, Breda, the Netherlands) supplemented with 10% (v/v) fetal bovine serum (FBS, Gibco) and gentamicin (50 µg/mL, Gibco)(CF culture medium). These primary fibroblasts were used between passage 1-3. CFs (10,000 cells/cm^2) were plated on bioflex plates (6-well Bioflex plates, precoated with collagen-I, Flexcell Dunn Labortechnik, Asbach, Germany) in CF culture medium. The next day, CF culture medium was replaced by DMEM supplemented with gentamicin (50 µg/mL, Gibco) (CF Experimental medium). After 24 h, the fibroblasts were subjected to cyclic (1 Hz) equibiaxial stretch, (Flexcell FX-4000 strain unit, Dunn Labortechnik) up to 29 h. Control, non-stretched cells were subjected to identical conditions however, without stretch being applied.

Intermittent cyclic stretch (1 Hz) protocols

All stretch protocols were performed with the Flexcell system (Flexcell Dunn Labortechnik, Asbach, Germany) and consisted of cyclic equibiaxial stretch with a frequency of 1 Hz. First, protocols were investigating the effects of 1 h 10% cyclic stretch (1 Hz) compared to non-stretch controls. Then the effect of smaller periods of cyclic stretch within 1 h was investigated by applying 2x 20-minute 10% stretch (with 1x20 minute interruption of stretch), 3x 12 minutes 10% stretch (with 2x 12 minutes interruption of stretch) and finally 4x 8 minutes 10% stretch (with 3x8 minutes interruption of stretch) was investigated. In both short-term experimental set-ups, a 4 h waiting period was implemented to allow mRNA expression measurements. Secondly, protocols were set up to investigate the effect of increasing the amplitude of the cyclic stretch to 20% or interrupting stretch (to 0%). Since physiologically, CFs experience continuous cyclic stretch during the cardiac cycle, a protocol was designed of 24 h 10% stretch, then 1 h of 20% stretch (increasing) or no stretch (interrupting), followed by another 4 h of 10% stretch. The idea is setting a baseline of 10% stretch, which is then interrupted or increased for 1 h and then coming back to baseline for a short period, to investigate whether this 1 h time period has an additional effect. The intermittent protocols were compared with data on continuous 10% cyclic stretch (1 Hz, 24 h) as published previously [22](Chapter 2 & 3). Detailed figures of each protocol are provided in the results section.

Gene expression analysis

Total RNA was isolated from cells using an RNA isolation kit (Omega Biotek, Norcross, GA, USA) and reversed transcribed into cDNA using the iScript cDNA synthesis kit (Biorad, Hercules, CA, USA) according to the manufacturer's instructions. Real-time PCR was performed on an CFX96 Touch Real-Time PCR Detection System (Biorad) using SYBR-Green Supermix

(Biorad)[26]. Gene expression levels of Alpha-smooth muscle actin (Acta2), Connective tissue growth factor (Ctgf), Transforming growth factor beta 1 (Tgfb1), Tenascin C (Tnc), Brain Natriuretic Peptide (Nppb), Cartilage intermediate layer protein 1 (Cilp1) and Heat shock protein 70 (Hsp70) were normalized using the housekeeping gene Cyclophilin-A (Cyclo), and their relative expression was calculated using the comparative threshold cycle (Ct) method by calculating $2^{\Delta Ct}$ (e.g., $2^{(\text{Cyclophilin Ct} - \text{Acta2 Ct})}$). The gene expression values were multiplied by 1000 (formula $1000 * 2^{\Delta Ct}$), to enhance readability. The sequences of the specific primers used are provided below (Table 1).

Table 1. Gene-specific primer sequences used for quantitative real-time PCR

Gene	Forward primer	Reverse Primer
Alpha-smooth muscle actin (Acta2)	AAGGCCAACCGGGAGAAAAT	AGTCCAGCACAATACCAGTTGT
Connective tissue growth factor (Ctgf)	CACAGAGTGGAGCGCCTGTTC	GATGCACTTTTTGCCCTTCTTAATG
Transforming growth factor, beta 1 (Tgfb1)	GCACCATCCATGACATGAAC	GCTGAAGCAGTAGTTGGTATC
Tenascin C (Tnc)	TCTGTCCTGGACTGCTGATG	TGGCCTCTCTGAGACCTGTT
Brain Natriuretic Peptide (Nppb)	AGACAGCTCTCAAAGGACCA	CTATCTTCTGCCCAAAGCAG
Cartilage intermediate layer protein 1 (Cilp1)	GAGTACTTCTGTAAGGCGCAG	GGCATTCTGGAAGCAATCATG
Heat shock protein 70 (Hsp70)	CGCTCGAGTCCTATGCCTTC	TCTTTCTCAGCCAGCGTGTT
Cyclophilin-A (Cyclo)	CAAATGCTGGACCAAACACAA	TTCACCTTCCCAAAGACCACAT

Statistics

Data are presented as mean or individual data points and were analyzed with Wilcoxon matched pairs test, Friedman test or Kruskall-Wallis test, with Dunn posthoc test where appropriate. Differences were considered statistically significant when $p < 0.05$.

Results

One-hour cyclic stretch activates “early gene” response in CF

Figure 1A shows that 1 h 10% cyclic stretch period significantly increased Nppb, Tnc and Tgfb1 mRNA after 4 h, when compared to non-stretch (NS) controls. However, these effects on Nppb, Tnc and Tgfb1 mRNA expression disappeared after 24 h, moreover no effect was found on Acta2, Ctgf and Cilp1 mRNA expression (figure 1B). Indicating that 1 h 10% cyclic stretch activates CFs briefly, but that this is not sufficient to keep CFs activated for 24 h .

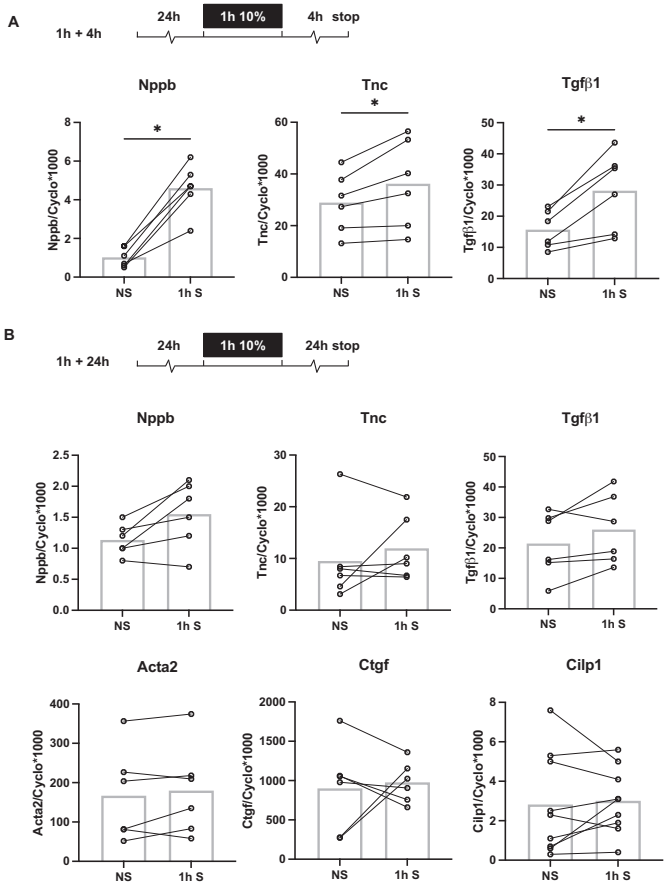

Figure 1. Effect of 1 h 10% cyclic stretch on CF gene expression after 4 h or 24 h. Schematic of the stretch protocol applying 1 h 10% cyclic stretch after 24 h serum starvation period and harvesting 4 h afterwards. Relative mRNA expression levels of Nppb, Tnc and Tgfb1in rat CFs exposed to 1 h of 10% cyclic stretch (1 h S) or non-stretched (NS) conditions after 4 h (n=6) (a). Schematic of the protocol applying 1 h 10% cyclic stretch after 24 h serum starvation period and harvesting 24 h afterwards. Relative mRNA expression levels of Nppb, Tnc, Tgfb1, Acta2, Ctgf, and Cilp1 in CFs exposed to 1 h of 10% 1 Hz cyclic stretch (1 h S) or non-stretched (NS) conditions after 2 4h (n=6-9) (b). * $p < 0.05$. Bar indicates mean.

Effect of 1 h period of intermittent 10% cyclic stretch on CF gene expression

To further determine the minimal stretch period needed to activate CF gene expression the effect of 1 h cyclic stretch was compared to that of several shorter periods of cyclic stretch indicated in the upper panel of figure 2A. The lower panels indicate that the expression of Nppb, TGFb, Tnc and Hsp70 are similar after the four different stretch protocols, since no significant differences were found when comparing the intermittent protocols to the continuous 1 h 10% cyclic stretch (figure 2B). Therefore, also shorter periods of stretch during an hour activate CFs similarly as 1 h continuous 10% cyclic stretch.

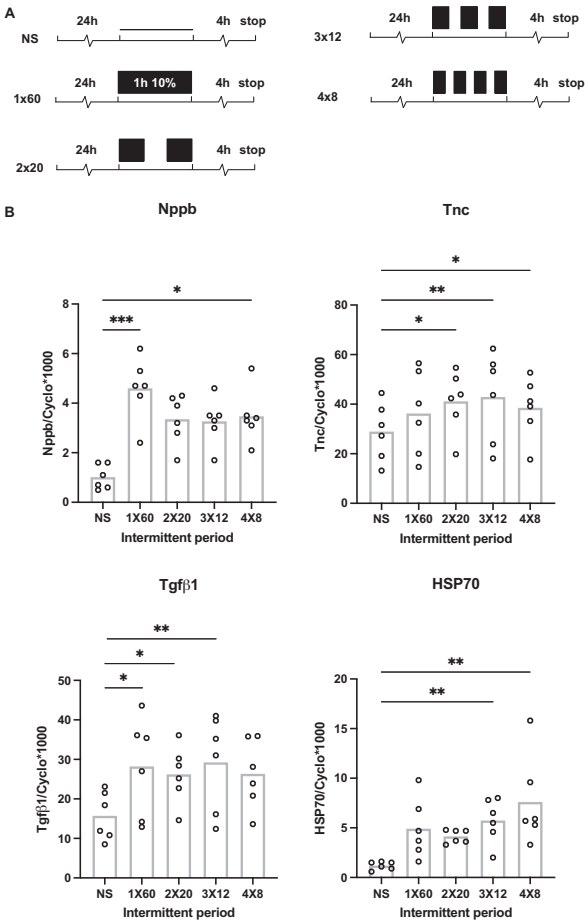

Figure 2. Schematic overview of the intermittent stretch protocols. The 1 h cyclic stretch has been divided into 4 groups: 60 minutes (1 h) 10% cyclic stretch (1x60); 2 times 20 minutes 10% cyclic stretch (2x20); 3 times 12 minutes 10% cyclic stretch (3x12); 4 times 8 minutes 10% cyclic stretch (4x8). Stretch was applied after 24 h serum starvation period and measurements were taken 4h afterwards (a). Relative mRNA expression levels of Nppb, Tgfb, Tnc and HSP70 in rat CFs exposed to shorter periods of 10% cyclic stretch (2x 20min/3x 12 min/4x 8 min) or 1 h of 10% cyclic stretch (1x 60 min) and non-stretched (NS) conditions after 4 h (n=6)(b). * $p < 0.05$; ** $p < 0.01$; *** $p < 0.001$. Bar indicates mean. Paired analysis.

Effect of cyclic stretch amplitude on CF gene expression

In the previous parts we used non-stretch as control condition. Because the beating heart undergoes cyclic stretch, even under resting conditions, we now investigated the effect of modulating the amplitude of cyclic stretch, using continuous 10% cyclic stretch as baseline condition (figure 3A). Changing cyclic stretch amplitude for 1 hour to 0 or 20% during the 24 h period of cyclic 10% stretch did not lead to any significant changes in mRNA expression compared to historical data on 24 h continuous 10% cyclic stretch (figure 3B).

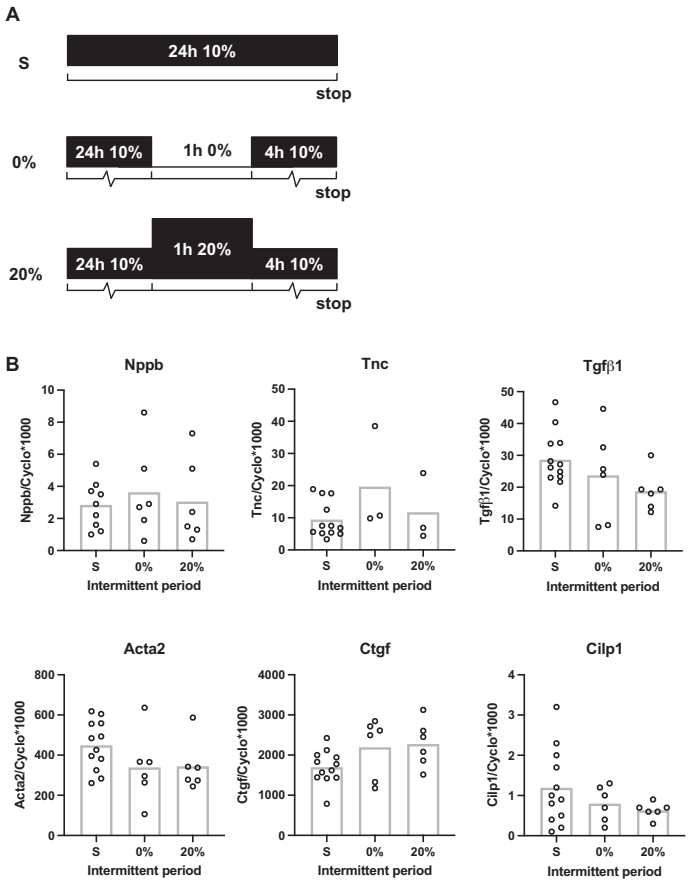

Figure 3. Schematic of the different protocols applied: 24 h continuous cyclic stretch (S), 24 h 10% cyclic stretch, 1 h interruption (0%) or 1 h 20% cyclic stretch (20%) followed by 4 h 10% cyclic stretch (a). Relative mRNA expression levels of Nppb, Tnc, Tgfb, Acta2, Ctgf and Cilp1 in CFs exposed to 24 h 10% stretch, then temporarily 1 h of interrupting (0%) stretch or increasing (20%) stretch conditions followed by 4 h 10% cyclic stretch, compared to 24 h continuous 10% cyclic stretch (S) conditions (n=3-12)(b). Bar indicates mean. No paired analysis.

Discussion

To the best of our knowledge this is the first study showing that one-hour cyclic stretch is a sufficient stimulus for cardiac fibroblast activation of expression of early response genes, even when this period is divided into 2-4 shorter periods of stretch. However, such stretching is not sufficient for sustained fibroblast activation. Also, a change in stretch amplitude to 20% for 1 h did not lead to significantly sustained changes on gene expression.

Short periods of stretch temporarily activates "early response" genes

Our finding that 1 h cyclic stretch leads to increased levels of "early response" genes (Tgfb1, Nppb, Tnc) after 4 h shows that this short duration leads to effects of gene transcription. Our results on increased mRNA expression of Tnc after 1 h of 10% cyclic stretch is supported by Maier et al. also showing an induction of Tnc in immortalized mouse fibroblasts after 1 h cyclic stretch (10%, 0.3 Hz)[29]. Of note, Maier et al. do not specify if there was time between ending the 1 h experiment and measuring mRNA expression via Northern blot, where we left 4 h in between end of the experiment and harvesting the CFs. Contrary to our result Chiquet et al. showed no effect of 1 h cyclic stretch followed by a 5h rest period on Tnc mRNA expression in chick skin fibroblasts [30]. Increased mRNA levels of early response genes peak at 4-6 hours following a stimulus [31, 32], while phosphorylation of targets can be observed much sooner (minutes). Nishimura et al. show changes in AKT and BAD phosphorylation when alternating between 5 minutes of 10% stretch and 2 minutes of no stretch, compared to continuous 10% stretch within the course from 0 to 70 minutes [33]. Effects of cyclic stretch on phosphorylation were measured as early as 15 minutes [34], giving a first implication cyclic stretch is a strong mechanical stimulus. However, 15 minutes cyclic stretch is not sufficient for mRNA or protein levels to be significantly increased [35]. Effect of a cellular stimulus can be measured at different levels, a first effect might be the influx of ions after ion channel activation measurable in (milli)seconds [36, 37], phosphorylation can be detected after minutes [33, 34] while gene expression changes reflected on mRNA levels are measured after hours [22, 29]. Ultimately, changes in protein levels will take further time to develop. The gene chosen to study is important, since early response genes like HSP, Tgfb1, Nppb and Tnc are more likely to give an early response, than late responding genes like Acta2 or collagen 1 which will take a longer time. Together, these results suggest that the shortest mechanical stimulus resulting in an effect on mRNA expression levels after 4 h lays somewhere between 15 minutes and 1 h.

In our hands intermittent cyclic stretch or 1 h cyclic stretch does not lead to sustained CF activation compared to static controls after 24 h, which is supported by a study using fibrin gels with entrapped neonatal human dermal fibroblasts [34]. This study showed that intermittent stretch (5% cyclic stretch 0,5 Hz for 15 minutes following 6h rest, repeat up to 48 h) doesn't have an effect on Collagen 1 mRNA expression [34]. Similarly, Grünheid et al. exposed human gingival fibroblast-like cells for 45 minutes per day to 10% cyclic stretch at 1 Hz, for a total of 10 days, and did not find an effect on collagen 1 protein expression compared to static controls [38]. However, Xu et al. showed that 48 h intermittent cyclic stretch (5%, 1 Hz), for 15 min/h decreased procollagen 1 mRNA expression in fetal lung fibroblasts compared to static controls [39]. These previous studies show that shorter periods of cyclic stretch do not seem to stimulate fibroblasts into producing collagen 1. This is in line with our gene expression data showing only a temporary effect of 1 h cyclic stretch. A longer stimulus seems necessary to induce sustained activation or differentiation of CF.

Short term changes in stretch amplitude don't have an effect on CF gene expression
We did not find an effect of changing the amplitude for 1 h within the 24 h 10% baseline stretch protocol (fig 3b). The lack of CF activation by increasing stretch amplitude to 20% seems in line with findings by Howard et al. who studied periodontal ligament fibroblasts. These investigators found no changes in collagen 1 expression when increasing cyclic stretch amplitude from 5% to 10% (0.5 Hz for 24 h) in compared to static controls [40].

Gilbert et al. studied several cyclic stretch amplitudes (5%, 10% or 15%) and frequencies (0.1, 0.3 or 0.5 Hz) for 20 minutes, three times daily at 8-hour intervals for 3 days and showed no effect of amplitude on Acta2 and Tnc mRNA expression in NIH 3T3 fibroblasts within a decellularized ECM construct compared to static controls [41]. These short activation periods of cyclic stretch mimic the "lower" frequency changes in the heart, as presumably caused by exercise and emotions, these changes create some activation, however mild and short lasting, likely not leading to differentiation. The latter studies corroborate our lack of gene expression changes following a 1 h change in stretch amplitude.

Similar to previous studies by other groups, we used static, non-stretched controls [24, 36, 42] this may not be physiological because fibroblasts are likely to be stretched each heartbeat. Using continuous cyclic stretch is a more physiological control, which has been published before [34]. We have set up a model resembling the in vivo situation in which CFs are always subjected to stretch and then small changes appear by exercise, which we have modeled by changing the amplitude of stretch for 1 h within a period of 24 h cyclic stretch. Our results indicate that 1 h change of amplitude within a period of 24 h cyclic stretch does not lead to sustained CF activation. These 24 h of cyclic stretch might not be sufficient to set baseline conditions for CFs. Previous studies have set up in vitro models for in vivo diseases like hypertension [43], hypertrophy [44, 45], wound healing [46] or traumatic brain injury [47] using mechanical stimulation in the form of stretch. Mechanical stimulation is also used for modeling a more physiological relevant environment in vitro for endothelial cells [48]. Here we have tried developing an in vitro model for CFs in a more physiological relevant environment being under constant mechanical stimuli in the form of cyclic stretch and use this to model the small daily fluctuations in mechanical loading caused by exercise or emotional state. Improving this model might lead to a better in vitro model in which results better represent the in vivo situation. The 24 h time period might not have been sufficient and longer periods of intermittent or incremental stretch might induce myofibroblast differentiation, as indicated by Schmidt et al. who show an increase in collagen content after 2 weeks of incremental stretch, compared to continuous stretch [34].

In conclusion, our results show that short (< or = 1 hour) duration of cyclic stretch creates a temporary early gene response in CFs, but does not lead to sustained CF activation or CF differentiation.

References

1. Chen-Izu Y, Izu LT. Mechano-chemo-transduction in cardiac myocytes. J Physiol. 2017;595(12):3949-58.
2. Degaute JP, van de Borne P, Linkowski P, Van Cauter E. Quantitative analysis of the 24-hour blood pressure and heart rate patterns in young men. Hypertension. 1991;18(2):199-210.
3. Portaluppi F, Tiseo R, Smolensky MH, Hermida RC, Ayala DE, Fabbian F. Circadian rhythms and cardiovascular health. Sleep Med Rev. 2012;16(2):151-66.
4. Rana S, Prabhu SD, Young ME. Chronobiological Influence Over Cardiovascular Function: The Good, the Bad, and the Ugly. Circ Res. 2020;126(2):258-79.
5. Stern N, Beahm E, McGinty D, Eggena P, Littner M, Nyby M, et al. Dissociation of 24-hour catecholamine levels from blood pressure in older men. Hypertension. 1985;7(6 Pt 1):1023-9.
6. Tuck ML, Stern N, Sowers JR. Enhanced 24-hour norepinephrine and renin secretion in young patients with essential hypertension: Relation with the circadian pattern of arterial blood pressure. The American Journal of Cardiology. 1985;55(1):112-5.
7. Jones WB, Finchum RN, Russell RO, Jr., Reeves TJ. Transient cardiac output response to multiple levels of supine exercise. J Appl Physiol. 1970;28(2):183-9.
8. Weissman ML, Jones PW, Oren A, Lamarra N, Whipp BJ, Wasserman K. Cardiac output increase and gas exchange at start of exercise. J Appl Physiol Respir Environ Exerc Physiol. 1982;52(1):236-44.
9. Grossman W, Jones D, McLaurin LP. Wall stress and patterns of hypertrophy in the human left ventricle. Journal of Clinical Investigation. 1975;56(1):56-64.
10. Toischer K, Rokita AG, Unsold B, Zhu W, Kararigas G, Sossalla S, et al. Differential cardiac remodeling in preload versus afterload. Circulation. 2010;122(10):993-1003.
11. Abramochkin DV, Lozinsky IT, Kamkin A. Influence of mechanical stress on fibroblast-myocyte interactions in mammalian heart. J Mol Cell Cardiol. 2014;70:27-36.
12. Pellman J, Zhang J, Sheikh F. Myocyte-fibroblast communication in cardiac fibrosis and arrhythmias: Mechanisms and model systems. J Mol Cell Cardiol. 2016;94:22-31.
13. Baudino TA, Carver W, Giles W, Borg TK. Cardiac fibroblasts: friend or foe? Am J Physiol Heart Circ Physiol. 2006;291(3):H1015-26.
14. Souders CA, Bowers SL, Baudino TA. Cardiac fibroblast: the renaissance cell. Circ Res. 2009;105(12):1164-76.
15. M E. Cardiac Fibroblasts: Function, Regulation of Gene Expression, and Phenotypic Modulation. Basic Res Cardiol. 1992;87:183-9.
16. Porter KE, Turner NA. Cardiac fibroblasts: at the heart of myocardial remodeling. Pharmacol Ther. 2009;123(2):255-78.
17. Fan D, Takawale A, Lee J, Kassiri Z. Cardiac fibroblasts, fibrosis and extracellular matrix remodeling in heart disease. Fibrogenesis Tissue Repair. 2012;5(1):15.
18. van Nieuwenhoven FA, Turner NA. The role of cardiac fibroblasts in the transition from inflammation to fibrosis following myocardial infarction. Vascul Pharmacol. 2013;58(3):182-8.
19. Moore L, Fan D, Basu R, Kandalam V, Kassiri Z. Tissue inhibitor of metalloproteinases (TIMPs) in heart failure. Heart Fail Rev. 2012;17(4-5):693-706.
20. Lighthouse JK, Small EM. Transcriptional control of cardiac fibroblast plasticity. J Mol Cell Cardiol. 2016;91:52-60.
21. Mayer DC, Leinwand LA. Sarcomeric gene expression and contractility in myofibroblasts. J Cell Biol. 1997;139(6):1477-84.
22. Ploeg MC, Munts C, Prinzen FW, Turner NA, van Bilsen M, van Nieuwenhoven FA. Piezo1 Mechanosensitive Ion Channel Mediates Stretch-Induced Nppb Expression in Adult Rat Cardiac Fibroblasts. Cells. 2021;10(7).

23. Watson CJ, Phelan D, Xu M, Collier P, Neary R, Smolenski A, et al. Mechanical stretch up-regulates the B-type natriuretic peptide system in human cardiac fibroblasts: a possible defense against transforming growth factor-beta mediated fibrosis. Fibrogenesis Tissue Repair. 2012;5(1):9.
24. Blaauw E, Lorenzen-Schmidt I, Babiker FA, Munts C, Prinzen FW, Snoeckx LH, et al. Stretch-induced upregulation of connective tissue growth factor in rabbit cardiomyocytes. J Cardiovasc Transl Res. 2013;6(5):861-9.
25. Gan W, Li T, Ren J, Li C, Liu Z, Yang M. Serum-glucocorticoid-regulated kinase 1 contributes to mechanical stretch-induced inflammatory responses in cardiac fibroblasts. Mol Cell Biochem. 2018;445(1-2):67-78.
26. van Nieuwenhoven FA, Munts C, Op 't Veld RC, Gonzalez A, Diez J, Heymans S, et al. Cartilage intermediate layer protein 1 (CILP1): A novel mediator of cardiac extracellular matrix remodelling. Sci Rep. 2017;7(1):16042.
27. Turner NA, Porter KE, Smith WHT, White HL, Ball SG, Balmforth AJ. Chronic β2-adrenergic receptor stimulation increases proliferation of human cardiac fibroblasts via an autocrine mechanism. Cardiovascular Research. 2003;57(3):784-92.
28. van Nieuwenhoven FA, Hemmings KE, Porter KE, Turner NA. Combined effects of interleukin-1α and transforming growth factor-β1 on modulation of human cardiac fibroblast function. Matrix Biology. 2013;32(7-8):399-406.
29. Maier S, Lutz R, Gelman L, Sarasa-Renedo A, Schenk S, Grashoff C, et al. Tenascin-C induction by cyclic strain requires integrin-linked kinase. Biochim Biophys Acta. 2008;1783(6):1150-62.
30. Chiquet M, Sarasa-Renedo A, Tunc-Civelek V. Induction of tenascin-C by cyclic tensile strain versus growth factors: distinct contributions by Rho/ROCK and MAPK signaling pathways. Biochim Biophys Acta. 2004;1693(3):193-204.
31. Wang JH, Thampatty BP, Lin JS, Im HJ. Mechanoregulation of gene expression in fibroblasts. Gene. 2007;391(1-2):1-15.
32. Yang Y, Creer A, Jemiolo B, Trappe S. Time course of myogenic and metabolic gene expression in response to acute exercise in human skeletal muscle. J Appl Physiol (1985). 2005;98(5):1745-52.
33. Nishimura K, Blume P, Ohgi S, Sumpio BE. Effect of different frequencies of tensile strain on human dermal fibroblast proliferation and survival. Wound Repair Regen. 2007;15(5):646-56.
34. Schmidt JB, Chen K, Tranquillo RT. Effects of Intermittent and Incremental Cyclic Stretch on ERK Signaling and Collagen Production in Engineered Tissue. Cell Mol Bioeng. 2016;9(1):55-64.
35. Jagodzinski M, Hankemeier S, van Griensven M, Bosch U, Krettek C, Zeichen J. Influence of cyclic mechanical strain and heat of human tendon fibroblasts on HSP-72. Eur J Appl Physiol. 2006;96(3):249-56.
36. Blythe NM, Muraki K, Ludlow MJ, Stylianidis V, Gilbert HTJ, Evans EL, et al. Mechanically activated Piezo1 channels of cardiac fibroblasts stimulate p38 mitogen-activated protein kinase activity and interleukin-6 secretion. J Biol Chem. 2019;294(46):17395-408.
37. Matthews BD, Thodeti CK, Tytell JD, Mammoto A, Overby DR, Ingber DE. Ultra-rapid activation of TRPV4 ion channels by mechanical forces applied to cell surface beta1 integrins. Integr Biol (Camb). 2010;2(9):435-42.
38. Grunheid T, Zentner A. Extracellular matrix synthesis, proliferation and death in mechanically stimulated human gingival fibroblasts in vitro. Clin Oral Investig. 2005;9(2):124-30.
39. Xu J, Liu M, Post M. Differential regulation of extracellular matrix molecules by mechanical strain of fetal lung cells. Am J Physiol. 1999;276(5):L728-35.
40. Howard PS, Kucich U, Taliwal R, Korostoff JM. Mechanical forces alter extracellular matrix synthesis by human periodontal ligament fibroblasts. J Periodontal Res. 1998;33(8):500-8.
41. Gilbert TW, Stewart-Akers AM, Sydeski J, Nguyen TD, Badylak SF, Woo SL. Gene expression by fibroblasts seeded on small intestinal submucosa and subjected to cyclic stretching. Tissue Eng. 2007;13(6):1313-23.

42. Wahlsten A, Rutsche D, Nanni M, Giampietro C, Biedermann T, Reichmann E, et al. Mechanical stimulation induces rapid fibroblast proliferation and accelerates the early maturation of human skin substitutes. Biomaterials. 2021;273:120779.
43. Sil P, Gupta S, Young D, Sen S. Regulation of myotrophin gene by pressure overload and stretch. Mol Cell Biochem. 2004;262(1-2):79-89.
44. Sadoshima J, Jahn L, Takahashi T, Kulik TJ, Izumo S. Molecular characterization of the stretch-induced adaptation of cultured cardiac cells. An in vitro model of load-induced cardiac hypertrophy. Journal of Biological Chemistry. 1992;267(15):10551-60.
45. Blaauw E, van Nieuwenhoven FA, Willemsen P, Delhaas T, Prinzen FW, Snoeckx LH, et al. Stretch-induced hypertrophy of isolated adult rabbit cardiomyocytes. Am J Physiol Heart Circ Physiol. 2010;299(3):H780-7.
46. Junker JP, Kratz C, Tollback A, Kratz G. Mechanical tension stimulates the transdifferentiation of fibroblasts into myofibroblasts in human burn scars. Burns. 2008;34(7):942-6.
47. Morrison B, 3rd, Cater HL, Benham CD, Sundstrom LE. An in vitro model of traumatic brain injury utilising two-dimensional stretch of organotypic hippocampal slice cultures. J Neurosci Methods. 2006;150(2):192-201.
48. Estrada R, Giridharan GA, Nguyen MD, Roussel TJ, Shakeri M, Parichehreh V, et al. Endothelial cell culture model for replication of physiological profiles of pressure, flow, stretch, and shear stress in vitro. Anal Chem. 2011;83(8):3170-7.

Culturing of cardiac fibroblasts in Engineered Heart Matrix reduces myofibroblast differentiation but maintains their response to cyclic stretch and transforming growth factor β1

Meike. C. Ploeg[1], Chantal Munts[1], Tayeba Seddiqi[1], Tim J.L. ten Brink[2], Jonathan Breemhaar[3], Lorenzo Moroni[2], Frits. W. Prinzen[1] and Frans. A. van Nieuwenhoven[1]

[1]Department of Physiology, Cardiovascular Research Institute Maastricht (CARIM), Maastricht University, the Netherlands; [2]MERLN, Institute for Technology-Inspired Regenerative Medicine, Maastricht University, the Netherlands; [3]MosaMeat, Maastricht, the Netherlands.

Bioengineering. 2022 Oct 14;9(10):551.

5

Abstract

Background: Isolation and culturing of cardiac fibroblasts (CF) induces rapid differentiation toward a myofibroblast phenotype, which is partly mediated by the high substrate stiffness of the culture plates.

Methods and results: In the present study, a 3D model of Engineered Heart Matrix (EHM) of physiological stiffness (Youngs modulus ~ 15 kPa) was developed using primary adult rat CFs and a natural hydrogel collagen type 1 matrix. CFs were equally distributed, viable and quiescent for at least 13 days in EHM and baseline gene expression of myofibroblast-markers alfa-smooth muscle actin (Acta2), and connective tissue growth factor (Ctgf) was significantly lower, compared to CFs cultured in 2D monolayers. CF baseline gene expression of transforming growth factor-beta1 (Tgfβ1) and brain natriuretic peptide (Nppb) was higher in EHM-fibers compared to the monolayers. EHM stimulation by 10% cyclic stretch (1 Hz) increased gene expression of Nppb (3.0-fold), Ctgf (2.1-fold), Tgfβ1 (2.3-fold) after 24 h. Stimulation of EHM with TGFβ1 (1 ng/ml, 24 h) induced Tgfβ1 (1.6-fold) and Ctgf (1.6-fold).

Conclusion: Culturing CF in EHM of physiological stiffness reduces myofibroblast marker gene expression, while the CF response to stretch or TGFβ1 is maintained, indicating that our novel EHM structure provides a good physiological model to study CF function and myofibroblast differentiation.

Introduction

The cardiac extracellular matrix (ECM) is a network of structural proteins, mostly collagen fibers, which provides structural stability, tensile strength but also alignment cues, biochemical signals, and mechanical support to surrounding cells [1-3]. Cardiac fibroblasts (CFs) are the cells producing the structural and regulating components of the ECM [4, 5] and are therefore important for maintaining the integrity of the ECM [6, 7]. In response to injury CFs become activated, then differentiate to so called myofibroblasts [8, 9] showing special morphological and functional characteristics, like the expression of alpha smooth muscle actin (αSMA, encoded by the ACTA2 gene) [9, 10]. Myofibroblasts are key players in cardiac structural remodeling [11-14], producing excessive collagen, resulting in cardiac fibrosis and increased myocardial stiffness [15, 16].

CFs can be isolated from the heart and cultured to study their function in vitro. For many years, these studies have been performed in monolayers (defined as 2 dimensional (2D)-cultures). In this model, cells attach to a flat surface and cell-matrix attachments are restricted to one plane, while in vivo these attachments are present all around the cells [17-19]. 2D culture conditions also limit cell-cell interactions, as cells grow in monolayers [20]. In addition, culturing CFs on hard plastic cell culture plates promotes CF activation and differentiation into myofibroblasts [21, 22]. Stiffness is an important stimulus in this process [23], shown in cardiac fibroblasts [24] but also other types of fibroblasts [25-27]. Therefore, several groups started generating 3D culture systems to allow in vitro investigation of the cell-matrix interactions in a more physiologically relevant environment [17-19].

The aim of the present study is the development of a 3D cell culture model of engineered heart matrix (EHM) of physiological stiffness and to compare CF function in EHM structures vs 2D monolayers and their response to TGFβ1 and mechanical stimulation. To this purpose primary adult rat CFs were cultured in a natural collagen type 1 hydrogel and stiffness was determined. To gain insight in CF activation state, we measured gene expression of genes related to CF activation and myofibroblast differentiation: alfa-smooth muscle actin (Acta2)[28], connective tissue growth factor (Ctgf)[29] transforming growth factor beta 1 (TGFβ1)[30, 31] and brain natriuretic peptide (Nppb) [32]. Baseline gene expression levels of these genes in EHM cultures were compared with CF cultured in 2D monolayers both on cell culture plastic and on Bioflex silicone bottom plates. Finally, EHM responses to cyclic stretch (10%, 1 Hz) and TGFβ1, both established stimuli for CF-activation, were determined.

Materials & Methods

Isolation and culturing of CFs

CFs were isolated from cardiac ventricles (combined left and right) of adult surplus rats from any age, weight, sex or breed (n=48). Most of the rats used were either from the Lewis or

Wistar strain and aged between 5 and 52 weeks. Rat cardiac ventricular fibroblasts were isolated and cultures as previously described [33-35] in Dulbecco's modified eagles medium (DMEM; no. 22320, Gibco, Thermo Fisher Scientific, Waltham, MA, USA) supplemented with 10% (*v/v*) fetal bovine serum (FBS, Gibco), gentamicin (50 µg/ml, Gibco), 1% (*v/v*) Insulin-Transferrin-Selenium-Sodium Pyruvate (ITS-A, Gibco), basic fibroblast growth factor (1 ng/mL, Gibco) and vitamin C (500 uM, Sigma Aldrich, Saint Louis, MO, USA) (CF growth medium, CFGM) on standard cell culture flasks (Cellstar, Greiner Bio-One, Frickenhausen, Germany). The vast majority of these cells are fibroblast-like cells and these primary fibroblasts were used between passage 1–3. Experiments were performed with approval of the Animal Ethical Committee of Maastricht University (DEC-2007-116, July 31st, 2007) and conform to the national legislation for the protection of animals used for scientific purposes.

Assembly of the ring formation molds

Sylgard-184 silicone elastomer base and curing agent (Dow Chemical, Midland, MI, USA) were mixed together and poured into a well of a 12-well culture plate. Custom made 3D-printed casts (Mosa Meat, Maastricht, The Netherlands) were used to provide the shape with an outer diameter of 22 mm. An area with a 12 mm diameter was created to load 250 uL of gel. A 2 mm central pole creates the ring shape (figure 1). The mold was allowed to cure at room temperature for 3 days after which the 3D-printed casts were removed. The custom-made molds were cleaned and sterilized by autoclavation.

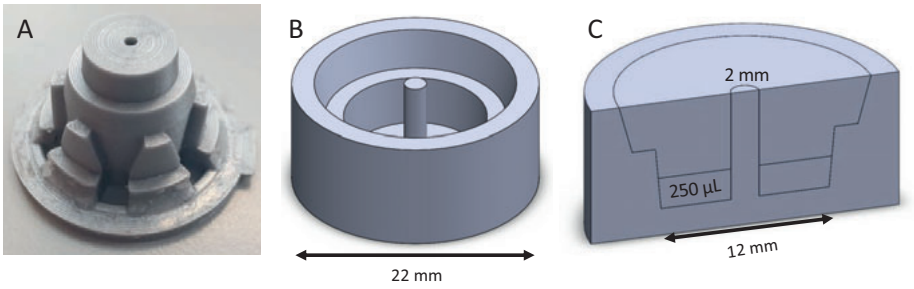

Figure 1. Silicone mold design. Custom made 3D-printed casts to provide the shape for the silicone mold (A). The mold has a diameter of 22mm (B) and a centrally placed post 2mm (C). Initial gel volume is 250 µL, after gelation 500 µL medium was added on top.

Collagen hydrogel

Collagen type 1 from rat tail (5 mg/ml, Ibidi, Gräfelfing, Germany) was diluted with sterile water, 10x DMEM, 20x NaHCO3 and CFs until desired final collagen concentration (between 1-3 mg collagen/ml) and cell density, with the final gel containing 1x DMEM.

Engineered Heart Matrix ring (EHM-ring) formation

CFs were grown in CFGM on Cellstar cell culture flasks to about 80-90% confluency, detached using trypsin-EDTA (Gibco) and taken up in CFGM**.** Cells were centrifuged at 1500 rpm for

5 minutes and then resuspended in CFGM to reach a concentration of 10 million cells/mL. The cells were diluted to 1 million cells/mL into the hydrogel mixture. The hydrogel-cell mixture (250 µL) was reverse pipetted into the molds and put into a 5% CO2 incubator at 37°C. After approximately 1-hour, to polymerize the gel, 500 µL of CF maintenance medium (CFMM, consisting of CFGM with 1% FBS) was added on top of the gels.

Engineered Heart Matrix fiber (EHM-fiber; Flexcell tissue train)

Using the optimized EHM-ring protocol longitudinal EHM-fibers were formed in the Flexcell Tissue Train system. This was achieved by pipetting 200 µL of the hydrogel-cell mixture between the two collagen-1 coated anchors of the Tissue Train culture plates (6-well plates, Flexcell Dunn Labortechnik, Asbach, Germany) atop of the Trough Loaders (figure 2). After approximately 1-hour of polymerization of the gel, 4 mL of CFGM was added on top of the gels. The next day the CFGM was replaced by CFMM. Subsequently, gels were subjected to cyclic stretch (10%, 1 Hz), (Flexcell FX-5000 strain unit, Dunn Labortechnik) for 4 h or 24 h. Control, non-stretched gels were subjected to identical conditions however, without stretch being applied.

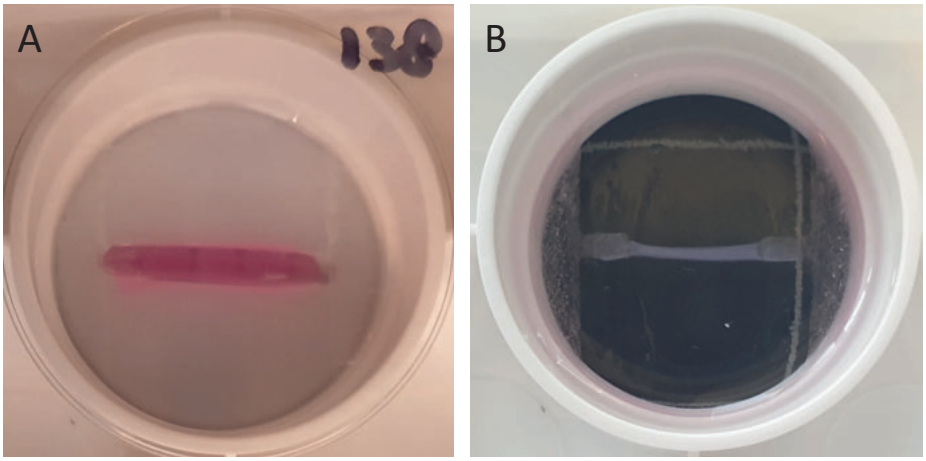

Figure 2. Images of EHM-fibers in Flexcell Tissue Train culture plates. Image (A) shows the (pink) gel after pipetting in the 6 well Flexcell Tissue Train culture plate, still in the Trough Loader (white bottom) providing the mold for the gel. Image (B) shows the EHM-fiber between the two anchors after polymerization of the gel. The black and white grid underneath represents 3 cm by 3 cm. The diameter of the well is 3.5 cm.

Measurement of EHM stiffness

To determine the stiffness of the EHM-ring, mechanical analysis was performed using an Electroforce-3200 Series III multiaxial tensile tester (TA Instruments, Asse, Belgium) combined with a 1000gf (10N) load cell (1 kg/cm2), as previously described [36, 37]. Test setups and data acquisition were directed through the WinTest 7 operational software (TA Instruments). The displacement mode of loading materials was controlled through

vertical, axial movement with a motorized extension arm (DispE, -40/40mm). The EHM-ring was locked into place using a custom-made Radial Tensile Strength tool (MERLN, Institute for Technology-Inspired Regenerative Medicine, Maastricht University, Maastricht, The Netherlands), based on previous research [38, 39].

Uniaxial displacement was applied at a rate of 1% strain per second (0.04 mm/sec.) until EHM-ring failure. Load (N) and displacement (mm) were recorded over time at a rate of 20 points/second. The obtained raw datasets were processed in Microsoft excel and converted to dataset representing exerted stress (σ, kPa) over strain (ε, %). Noise within the stress/strain curve was reduced using a moving average analysis, where the interval average was set at 20 points to equalize all measured data points per second. Young's moduli were calculated from the slope of 15% strain residing within the elastic region of the stress/strain curve.

Histology and immunohistochemistry (IHC)

EHM-rings or fibers were washed in PBS (Thermo Fisher), fixed in 4% paraformaldehyde (Klinipath) for 20 minutes, stained in eosin (J.T.Baker) for 1h and stored overnight in 70% ethanol (Sigma Aldrich). Finally, the EHM-ring or fiber was embedded into paraffin wax. Sections of 5 µm were cut using a rotary microtome.

Hematoxylin and eosin (H&E) staining was performed to gain insight in the cellular distribution and the extracellular matrix (ECM) structure. After rehydration, the slides were placed in Hematoxylin (5 min), washed with running tap water (10 min), placed in eosin (1 min) and washed with demi water. Dehydration steps were performed and the slides were closed with Entallan. Images were obtained using a Leica Microscope (5x, 10x or 20x magnification).

Vimentin and CNA35 IHC was performed to visualize vimentin-positive cells, implicated on being CFs and/or collagen matrix. Slides were stained with vimentin antibody (1/150 dilution, ab92547, Abcam, Cambridge, UK) followed by appropriate secondary antibody (1/500 dilution) or adding CNA35 (1/100 dilution)[40, 41]. Sections were further incubated in 4',6'-diamidino-2-phenylindole (DAPI)-containing mounting medium (Vector Laboratories, Burlingame, USA) to stain nuclei. Images were obtained using a Leica fluorescent microscope (40x magnification) or a Leica SPE confocal microscope (63x magnification).

Gene expression analysis

Total RNA was isolated from cells using an RNA isolation kit (Omega Biotek, Norcross, GA, USA) and reversed transcribed into cDNA using the iScript cDNA synthesis kit (Biorad, Hercules, CA, USA) according to the manufacturer's instructions and previously described [32]. Real-time PCR was performed on an CFX96 Touch Real-Time PCR Detection System using iQ SYBR-Green Supermix (Biorad). Gene expression levels of Alpha-smooth muscle actin (Acta2), Connective tissue growth factor (Ctgf), Transforming growth factor, beta 1 (Tgfβ1) and Brain Natriuretic Peptide (Nppb) were normalized using the housekeeping gene

Cyclophilin-A (Cyclo), and their relative expression was calculated using the comparative threshold cycle (Ct) method by calculating $2^{\Delta Ct}$ (e.g., $2^{(\text{Cyclophilin Ct} - \text{Nppb Ct})}$). The gene expression values were multiplied by 1000 (formula $1000 * 2^{\Delta Ct}$), to enhance readability. The sequences of the specific primers used are provided below (Table 1).

Table 1. Gene specific primer sequences used for real-time qPCR

Gene	Forward primer	Reverse Primer
Alpha-Smooth muscle actin (Acta2)	AAGGCCAACCGGGAGAAAAT	AGTCCAGCACAATACCAGTTGT
Connective tissue growth factor (Ctgf)	CACAGAGTGGAGCGCCTGTTC	GATGCACTTTTTGCCCTTCTTAATG
Transforming growth factor, beta 1 (Tgfβ1)	GCACCATCCATGACATGAAC	GCTGAAGCAGTAGTTGGTATC
Brain Natriuretic Peptide (Nppb)	AGACAGCTCTCAAAGGACCA	CTATCTTCTGCCCAAAGCAG
Cyclophilin-A (Cyclo)	CAAATGCTGGACCAAACACAA	TTCACCTTCCCAAAGACCACAT

Statistics

Data are presented as average, average ± standard deviation or individual data points (indicating separate CF isolations) and were analyzed with Wilcoxon matched pairs test or Kruskal-Wallis test, with Dunn posthoc test where appropriate (Graphpad PRISM V9). Differences were considered statistically significant when $p < 0.05$.

Results

Optimizing CF cell density in EHM-rings

Different CF cell densities were cultured in EHM-rings using a hydrogel collagen concentration of 1 mg/mL in CFMM. EHM-ring formation (compaction) was clearly less in the 2 lower cell densities (figure 3). The two higher cell densities showed considerably more compaction leading to an EHM-ring with a wall thickness of approximately 1.3 mm when using 2000 cells/µL, while using 400 cells/µL leads to a wall thickness of approximately 2.1 mm. HE staining also showed the distribution of cells throughout the gel (figure 6A & B).

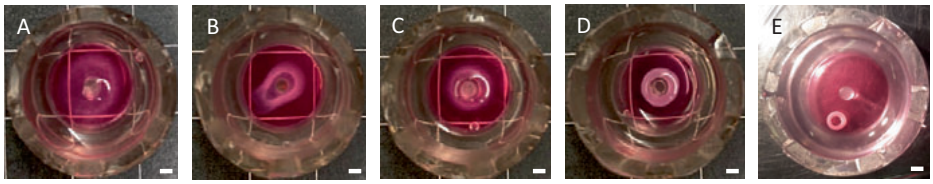

Figure 3. Images of EHM-rings taken 24 h after casting the gel using different cell densities (A-D): 100; 200; 400 and 2000 CF cells/µL using a 1 mg/mL collagen concentration. The images show the top view of the EHM-rings within the clear silicone mold on a black background with white grid (1 cm by 1 cm). Surrounding the central pole is a light pink circle, most left vaguely showing, becoming clearer with increasing the cell density. The final image (E) shows the EHM-ring (8000 cells/µl, 1 mg/mL collagen concentration) after 7 days of culturing, next to the central pole. The EHM-ring has been taking of the central pole manually to enhance visibility. Bars represent 2 mm.

Optimizing the EHM initial hydrogel collagen concentration

Two different initial hydrogel collagen concentrations (1 and 3 mg/ml) were used to vary the stiffness of the EHM-ring [42]. Gel compaction of the 3 mg/mL collagen EHM-ring was reduced resulting in an increased wall thickness compared to EHM-ring of 1 mg/mL collagen (4.9 ± 0.9 mm vs 1.8 ± 0.6 mm, n=3)(figure 4A & B). This is reflected by the HE staining (figure 5) where the cell density was lower in the 3 mg/mL collagen compared to the 1 mg/mL collagen EHM-ring (65 ± 5 vs 205 ± 25 CFs/mm^2, n=2). RNA isolation from the 3 mg/mL collagen EHM-ring resulted in a lower RNA yield when compared to the 1 mg/mL collagen EHM-ring (figure 5). Moreover, qPCR analyses revealed increased mRNA expression of Acta2 and Ctgf in the 3 mg/ml collagen EHM-ring, indicating processes towards myofibroblast differentiation, while there was no effect on Tgfβ1 mRNA expression (figure 5). Based on these results, an optimal collagen concentration of 1.5 mg/ml was chosen for further experiments. Using these conditions, we have cultured EHM-rings up to 13 days, average RNA yield 9.6 pg/cell, measured at day 1, 6, 10 and 13, indicating consistency in viable and quiescent cells over the culturing period. Both histological and immunohistological analysis showed evenly CF distribution and structural alignment within the EHM-structure (figure 6)

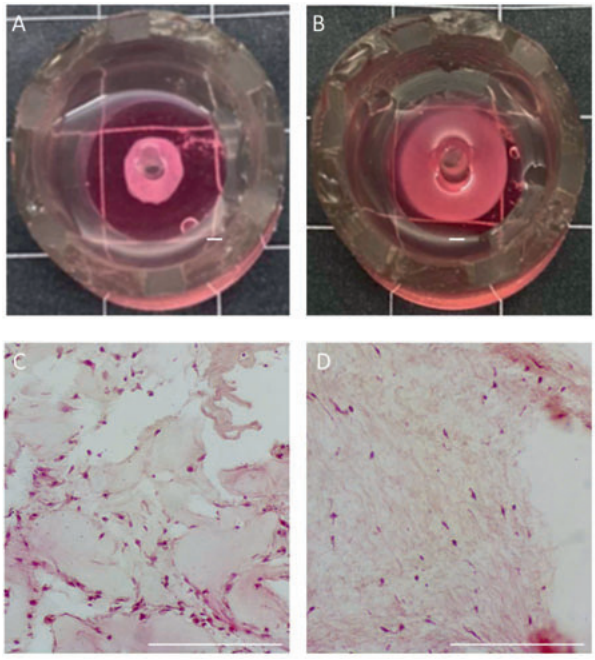

Figure 4. Effect of initial collagen concentration on EHM compaction. EHM-rings using 1 mg/ml (A) or 3 mg/ml (B) initial collagen concentrations (2000 cells/μL) in 250 uL gel after 24 h. Images are taken on the black and white grid of 1 x 1 cm. Shown is the silicone mold, the central pole containing the ring in light pink tones, surrounded by CFMM. Bars represent 2 mm. HE staining of the EHM-ring after 24 h using 1 mg/ml (C) and 3 mg/ml (D) initial collagen concentrations (2000 cells/μL in 250 uL gel) showing the cell density difference between the two collagen concentrations. Magnification 20x. Bars represent 200 μm.

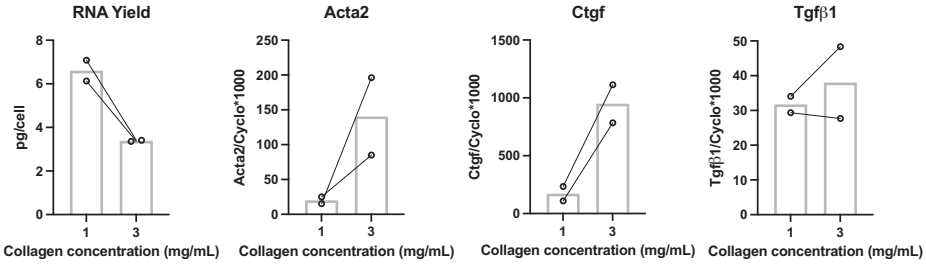

Figure 5. Effect of initial collagen concentration on RNA yield per cell (pg/cell) and gene expression of Acta2, Ctgf and Tgfβ1 of the EHM-rings after 24 h of culture (2000 cells/μL in 250 μL gel) (n=2). Bar represents mean.

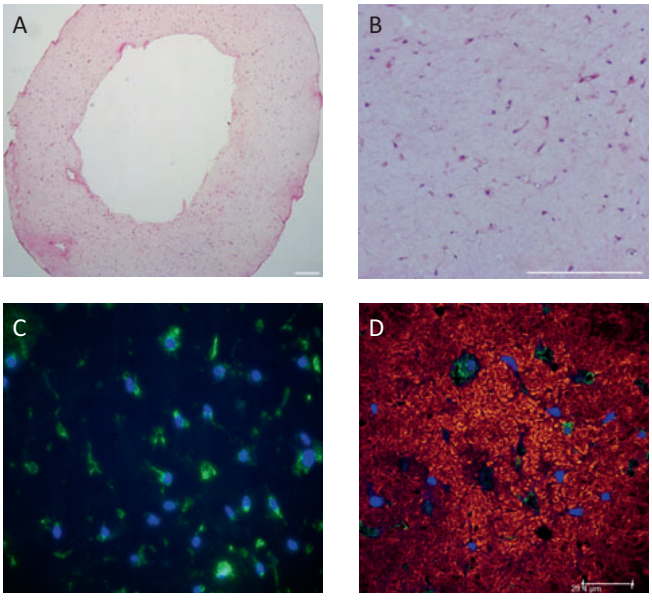

Figure 6. Histological and immunohistological analysis of EHM-rings. HE staining of an EHM-ring showing evenly distribution of the cells throughout the EHM-ring structure. EHM-ring was formed using 1.5 mg/mL collagen concentration and 1000 CF cells/μL gel and was fixed and stained 24 h after casting. Darker dots implicate CFs. Magnification 5x (A) or 20x (B). Bars represent 200 μm. Vimentin (green) and DAPI (blue) staining (C) and Z-stack image of CNA35 (red) and Vimentin (green) staining nuclei are blue (DAPI) (D)(bar represents 29.4μm).

EHM stiffness

EHM stiffness was measured at two different timepoints: 24 h and 48 h after casting the ring structures. The EHM-ring was locked into place using a custom-made Radial Tensile Strength tool. The EHM ring was stretched, starting at slack length (0% elongation, figure 7A) and stretched until break (figure 7B). The Stress Strain (σ/ε) curve of the moving average showing the elastic region, from which the Young's modulus is calculated, followed by the

plastic region and breaking point (figure 7D). After 24 h the average Young's modulus was 15 kPa and increased to 25 kPa after 48 h (figure 7C). These results indicate that the stiffness of our EHM-rings are in the same order of magnitude as the passive stiffness of myocardial tissue in vivo, which is described to be around 10 kPa [43-45]. For comparison, the Bioflex plates are estimated to have a stiffness of ~1000 kPa and plastic culture plates have a stiffness in the gigapascal range [45].

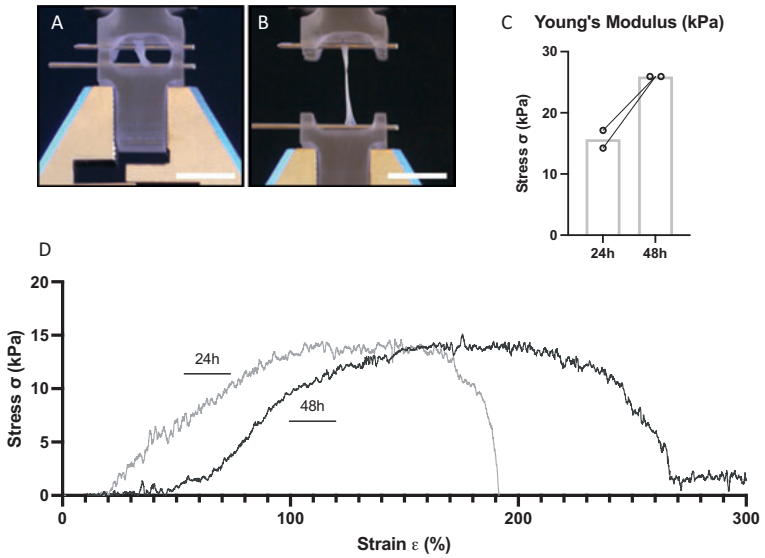

Figure 7. Stiffness measurements of EHM-ring (1.5 mg/mL collagen concentration; 1.000 cells/µl gel) at two different timepoints (24 h and 48 h). Images of tensile analysis at 0% elongation (A) and at elongation at break (B). Bar represents 10 mm. Tensile stiffness displayed as Young's Modulus (n=2)(C). Stress Strain (σ/ε) curve of the moving average (20 points/strain value)(n=1) after 24 h and 48 h (D).

Baseline CF gene expression in 3D (EHM) and 2D (monolayer) culture

Gene expression of Nppb and Tgfβ1, was higher in EHM compared to both regular hard plastic cell culture plates and Bioflex cell culture plates (figure 8). The opposite is true for the gene expression of Ctgf and Acta2, were expression was much lower in EHM fibers compared to both hard plastic and Bioflex cell culture plates (figure 8). The mRNA expression of Ctgf and Acta2 decreases with decreasing stiffness of the culture substrate.

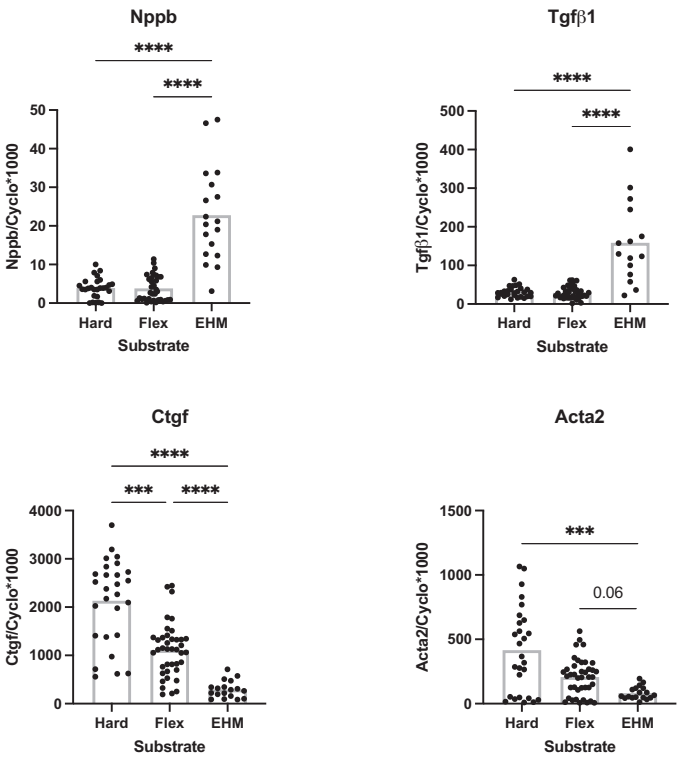

Figure 8. Baseline gene expression levels of Nppb, Tgfβ1, Ctgf and Acta2 in CF cultured on the different substrates: 2D monolayer on hard plastic cell culture plates (Hard), 2D monolayer on Bioflex cell culture plates (Flex) and 3D EHM-fibers (EHM). Data are presented as relative mRNA levels normalized to house-keeping gene cyclophylin (n=15-40). * $p < 0.05$; ** $p < 0.01$; *** $p < 0.001$; **** $p < 0.0001$. Bar indicates mean.

Stretch of EHM-fibers in the Flexcell Tissue Train system

Rat CFs in EHM-fibers exposed to 4 h cyclic stretch (10%, 1 Hz) showed a significantly higher gene expression (2.2-fold) of Nppb compared to non-stretched controls (figure 9A, EHM). Since similar experiments have previously been performed in 2D CF monolayers on Bioflex plates [32], the effects of cyclic stretch were also compared between Bioflex plates and EHM fibers. No effect of 4 h cyclic stretch (10%, 1 Hz) was found on gene expression of Tgfβ1, Ctgf and Acta2 in the EHM-fibers. In EHM-fibers exposed to 24 h of cyclic stretch (10%, 1 Hz) the increase of Nppb remained (3.0-fold). In addition, there was an increased mRNA expression of Ctgf (2.1-fold) and Tgfβ1 (2.3-fold) compared to non-stretched controls (figure 9B, EHM). Acta2 gene expression showed a 1.6-fold increase after 24h, but this difference did not reach statistical significance. Baseline gene expression differences as indicated in figure 8 are also seen when com-paring the non-stretch conditions of flex plates and EHM culture conditions.

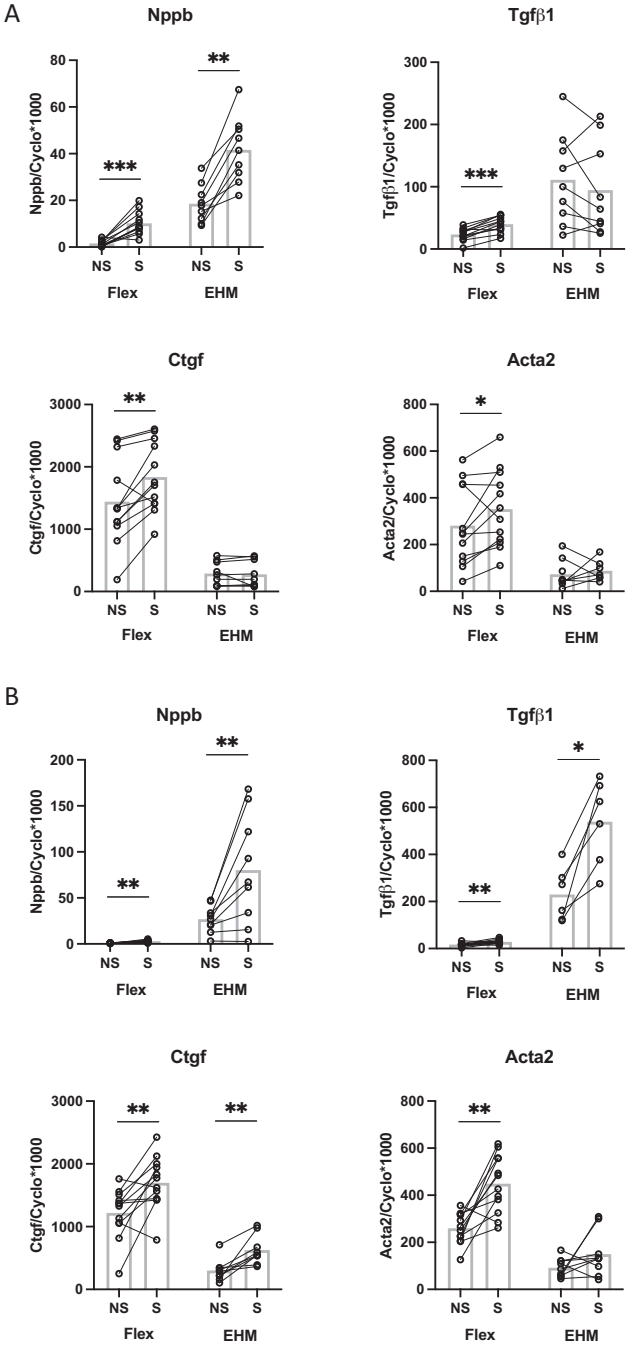

Figure 9. The effect of 4 h (A) and 24 h (B) cyclic stretch (10%, 1 Hz) on gene expression in CF cultured on 2D monolayer Bioflex plates (Flex) (data from [32]) or 3D EHM-fibers (EHM) conditions. Presented are the relative gene expression levels of Nppb, Tgfβ1, Ctgf and Acta2 in 2D (n = 5–12) and 3D (n=6-9) in stretch (S) and non-stretch (NS) conditions. * $p < 0.05$; ** $p < 0.01$; *** $p < 0.001$. Bar indicates mean.

Effect of TGFβ1 stimulation on CF gene expression in 2D (monolayer) and 3D (EHM) cultures

TGFβ1-stimulation (1ng/ml) for 24 h of CFs in 2D monolayers on hard plates showed a significant reduction in Nppb gene expression, no effect on Tgfβ1 gene expression and a significant induction of Acta2 and Ctgf gene expression (figure 10A, Hard). Similar effects of TGFβ1 stimulation on Nppb, Tgfβ1, Ctgf and Acta2 gene expression were observed in 2D monolayers on Bioflex plates (figure 10A, Flex). Stimulation with TGFβ1 in 3D EHM-rings showed no effect on Nppb expression, although as described above Nppb baseline expression levels were higher in the EHM than in 2D cultures. TGFβ1 stimulation in EHM significantly increased Tgfβ1 gene expression (1.6-fold) (figure 10A, EHM). In addition, Ctgf showed 1.6-fold increased expression upon TGFβ1 stimulation, although this did not reach statistical significance (Figure 10B). No clear effect of TGFβ1 stimulation on Acta2 and Nppb was observed in EHM (Figure 10). These results indicate that although the baseline gene expression levels are different in 3D EHM cultures, CFs are still capable of responding to TGFβ1 in a similar way as they would in 2D monolayers.

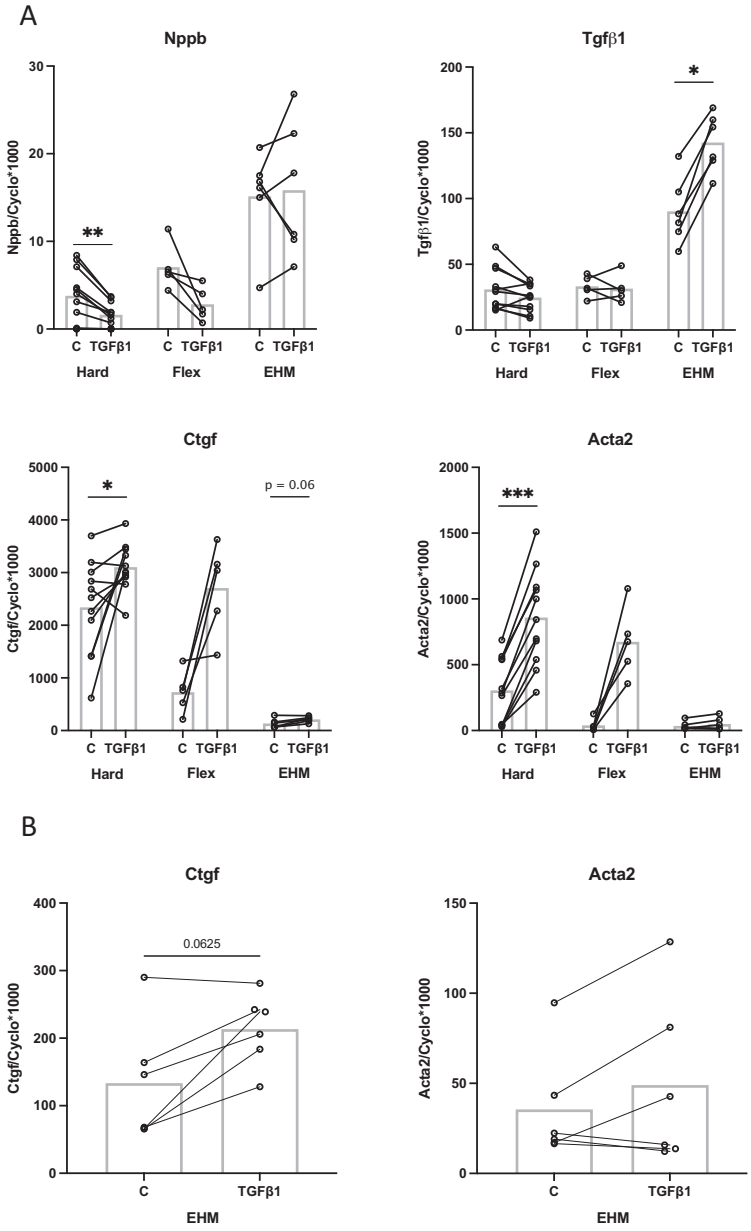

Figure 10. The effect of 24 h stimulation with TGFβ1 in rat CFs on different substrates. Presented are the relative gene expression levels of Nppb, Tgfβ1, Ctgf and Acta2 after stimulation with TGFβ1 (TGFβ1) or control (C) conditions for 24 h in 2D hard plastic cell culture plates (Hard, n = 11), 2D Bioflex plates (Flex, n = 5) and 3D EHM (EHM, n=6)(A). Graphs of the relative gene expression levels of Ctgf and Acta2 in EHM were enhanced to improve readability (B). * $p < 0.05$;*** $p < 0.001$. Bar indicates mean.

Discussion

In this study we designed self-assembling EHM-rings and EHM-fibers composed of rat tail collagen 1 and adult rat ventricular CFs, as models for 3D culturing. Stiffness of our EHM-rings was ~15 kPa. Comparison of CF gene expression between 2D monolayers and 3D EHM revealed reduced gene expression of Acta2 and Ctgf in EHM, indicating a more quiescent CF state. Cyclic stretch and TGFβ1 stimulation of EHM-structures showed CF activation, comparable to 2D cultures of CF. These data indicate that the EHMs provide a more physiological model to study CF function.

Influence of substrate stiffness on baseline CF gene expression

Our finding of lower baseline gene expression of Acta2 and Ctgf in 3D EHM cultures compared to 2D monolayers are in line with results from other studies showing that culturing CFs on hard plastic cell culture plates promotes myofibroblast differentiation [45-47]. Also, human CFs cultured in low stiffness GelMA gels also show a reduced expression of ACTA2 [48]. A more quiescent state of fibroblasts cultured in 3D was also found in human fetal lung fibroblasts [49] and tendon fibroblasts [50]. Therefore, both cardiac and non-cardiac CFs respond to 3D culturing in a similar way. Taken together, fibroblasts appear to remain in a more quiescent state, i.e. , less prone to differentiate into myofibroblasts, when cultured in EHM compared to 2D monolayers. Given the large difference in stiffness between the EHM (~15 kPa) and culture plates (>1000 kPa), it is likely that the quiescent state of CF in EHM, results from the more physiological stiffness of the 3D culture substrates [46, 51].

Possible influence of culture medium differences on baseline CF gene expression

Aside from differences in stiffness between EHM and 2D monolayers, also differences due to the use of different culture media cannot be excluded, and may affect baseline CF gene expression. The EHM fibers were cultured in CFMM, containing 1% fetal bovine serum (FBS), while the experiments in 2D monolayers were performed in serum-free conditions. FBS is known to have an effect on expression of many genes [35]. However, for Acta2 it is known that culturing in the presence of serum increases the expression [24, 35], while we showed a lower Acta2 expression in our EHM-fibers (CFMM, 1% serum), compared to 2D monolayers, indicating that this lower Acta2 mRNA expression is unlikely to be caused by serum. Galie et al. investigated the effect of serum conditions (5% or 10% FBS) on Tgfβ1 expression in rat cardiac fibroblasts cultured in 3D collagen matrix. Culturing the gels for 24 h resulted in a lower Tgfβ1 mRNA expression in 10% serum compared to 5% serum, measurements during other timepoints (6, 48 and 120 h) showed no difference between 5% or 10% serum on Tgfβ1 mRNA expression [24]. These results implicate that the higher Tgfβ1 mRNA expression we show in EHM-fibers is most likely not caused by the 1% serum used in those culture conditions. Important to note here that our FBS-percentage of 1% is much lower than those used by Galie and colleagues [24].

Effect of cyclic stretch and TGFβ1 on CF gene expression

Cyclic stretch for 24 h increased the gene expression of Nppb, Tgfβ1 and Ctgf in both the 2D monolayer and 3D EHM. Acta2 expression was significantly increased in stretched 2D monolayers, but the 1.6-fold increase in EHM was not statistically significant ($p = 0.20$). This lack of significance is most likely caused by low statistical power and large individual variation. Taken together these data indicate that stretch initiates fibroblast activation, ultimately leading to myofibroblast differentiation. Our results showing an increased mRNA expression of Acta2 in EHM after exposure to cyclic stretch is supported by previous research in NIH 3T3 fibroblasts [52] and marrow-derived progenitor cells [53], using a collagen and fibrin 3D construct, respectively. Primary murine dermal fibroblasts within a collagen 3D construct exposed to 24 h cyclic stretch, support our results in showing an increased expression of Tgfβ1 and Ctgf [54]. However, rat cardiac fibroblast-seeded collagen gels exposed to 5% cyclic strain showed a decrease in Tgfβ1 mRNA expression compared to controls [55]. Differences could be attributed by the type of mechanical stimulation applied, compression vs cyclic stretch. We have previously shown Nppb as being a sensitive marker for stretch in 2D monolayers [32], this statement is reinforced when showing a similar strong increase of Nppb gene expression in EHM-fibers, both after 4 h and 24 h of cyclic stretch.

Gene expression of Nppb and Tgfβ1 in EHM is higher in both stretch and non-stretch conditions compared to the 2D monolayers, in both 4 and 24 h conditions. The opposite is true for the expression of Acta2 and Ctgf, suggesting a quiescent state, which has been previously shown [48]. Although expression of Nppb and Tgfβ1 in non-stretch conditions are higher, CFs in EHM are still able to respond to the stimulus of cyclic stretch by even further increasing the expression of Nppb and Tgfβ1, an interesting finding which merits further investigation.

Stimulation of EHM-rings with TGFβ1 showed increased gene expression of Tgfβ1 and Ctgf similar as seen in the 2D cultures. No effect of TGFβ1 stimulation on Acta2 and Nppb expression was found. Our results of increased Ctgf expression after TGFβ1 stimulation is supported by previous research in human cardiac fibroblasts [56], adult rabbit cardiac fibroblasts [29] and human lung fibroblasts [57]. TGFβ1 induced Tgfβ1 expression in CFs is something we [29] and others [58] have shown previously. TGFβ1 is a well-known stimulus for myofibroblast differentiation [59-61], and our finding of TGFβ1–induced increase in Acta2 mRNA expression in 2D cultures therefore fits into the literature [35, 62]. This is further supported by Bracco Gartner et al. [48] in 3D cultures. By contrast, our EHM cultures did not show a clear TGFβ1-mediated induction of Acta2. Possibly this lack of effect indicates that the cells are less prone to TGFβ1-induced myofibroblast differentiation when cultured in EHM. This discrepancy warrants further investigation. Another possible explanation could be the high baseline expression of Nppb in EHM cultures. We have previously shown that BNP inhibits the expression of TGFβ1 induced Acta2 expression [32]. It could be that the high baseline expression of Nppb translates to high levels of BNP within the culture media, inhibiting the TGFβ1 induced Acta2 expression in EHM, hence the lack of effect we see here.

Future research is necessary to investigate the role of Nppb within EHM culture. Taken together, CFs remain quiescent in EHM, but exhibit a clear response after stimulation with stretch or TGFβ1.

Conclusion

In the present study, we describe the development of 3D engineered heart matrix (EHM) ring and fiber structures, with viable and quiescent CFs embedded in a type1 collagen gel of physiological stiffness. Markers of CF differentiation toward myofibroblasts were lower in EHM, compared to 2D cultures, while CF-activation by stretch or TGFβ1 was maintained, indicating that these EHM structures are a good model to study the process of CF activation and differentiation toward myofibroblasts.

References

1. Ariyasinghe NR, Lyra-Leite DM, McCain ML. Engineering cardiac microphysiological systems to model pathological extracellular matrix remodeling. Am J Physiol Heart Circ Physiol. 2018;315(4):H771-H89.
2. Walker CA, Spinale FG. The structure and function of the cardiac myocyte: A review of fundamental concepts. The Journal of Thoracic and Cardiovascular Surgery. 1999;118(2):375-82.
3. Ross RS, Borg TK. Integrins and the myocardium. Circ Res. 2001;88(11):1112-9.
4. M E. Cardiac Fibroblasts: Function, Regulation of Gene Expression, and Phenotypic Modulation. Basic Res Cardiol. 1992;87:183-9.
5. Porter KE, Turner NA. Cardiac fibroblasts: at the heart of myocardial remodeling. Pharmacol Ther. 2009;123(2):255-78.
6. Fan D, Takawale A, Lee J, Kassiri Z. Cardiac fibroblasts, fibrosis and extracellular matrix remodeling in heart disease. Fibrogenesis Tissue Repair. 2012;5(1):15.
7. van Nieuwenhoven FA, Turner NA. The role of cardiac fibroblasts in the transition from inflammation to fibrosis following myocardial infarction. Vascul Pharmacol. 2013;58(3):182-8.
8. Powell DW, Mifflin RC, Valentich JD, Crowe SE, Saada JI, West AB. Myofibroblasts. I. Paracrine cells important in health and disease. Am J Physiol. 1999;277(1):C1-9.
9. Tsuruda T, Boerrigter G, Huntley BK, Noser JA, Cataliotti A, Costello-Boerrigter LC, et al. Brain natriuretic Peptide is produced in cardiac fibroblasts and induces matrix metalloproteinases. Circ Res. 2002;91(12):1127-34.
10. van den Borne SW, Diez J, Blankesteijn WM, Verjans J, Hofstra L, Narula J. Myocardial remodeling after infarction: the role of myofibroblasts. Nat Rev Cardiol. 2010;7(1):30-7.
11. Brown RD, Ambler SK, Mitchell MD, Long CS. The cardiac fibroblast: therapeutic target in myocardial remodeling and failure. Annu Rev Pharmacol Toxicol. 2005;45:657-87.
12. Camelliti P, Borg TK, Kohl P. Structural and functional characterisation of cardiac fibroblasts. Cardiovasc Res. 2005;65(1):40-51.
13. Banerjee I, Yekkala K, Borg TK, Baudino TA. Dynamic interactions between myocytes, fibroblasts, and extracellular matrix. Ann N Y Acad Sci. 2006;1080:76-84.
14. Pedrotty DM, Klinger RY, Kirkton RD, Bursac N. Cardiac fibroblast paracrine factors alter impulse conduction and ion channel expression of neonatal rat cardiomyocytes. Cardiovasc Res. 2009;83(4):688-97.
15. Creemers EE, Pinto YM. Molecular mechanisms that control interstitial fibrosis in the pressure-overloaded heart. Cardiovasc Res. 2011;89(2):265-72.
16. Jalil J. Structural vs. contractile protein remodeling and myocardial stiffness in hypertrophied rat left ventricle. Journal of Molecular and Cellular Cardiology. 1988;20(12):1179-87.
17. Li Y, Asfour H, Bursac N. Age-dependent functional crosstalk between cardiac fibroblasts and cardiomyocytes in a 3D engineered cardiac tissue. Acta Biomater. 2017;55:120-30.
18. Abbott A. Cell culture: biology's new dimension. Nature. 2003;424(6951):870-2.
19. Baker BM, Chen CS. Deconstructing the third dimension: how 3D culture microenvironments alter cellular cues. J Cell Sci. 2012;125(Pt 13):3015-24.
20. Hinz B, Gabbiani G. Cell-matrix and cell-cell contacts of myofibroblasts: role in connective tissue remodeling. Thromb Haemost. 2003;90(6):993-1002.
21. Landry NM, Rattan SG, Dixon IMC. An Improved Method of Maintaining Primary Murine Cardiac Fibroblasts in Two-Dimensional Cell Culture. Sci Rep. 2019;9(1):12889.
22. Santiago JJ, Dangerfield AL, Rattan SG, Bathe KL, Cunnington RH, Raizman JE, et al. Cardiac fibroblast to myofibroblast differentiation in vivo and in vitro: expression of focal adhesion components in neonatal and adult rat ventricular myofibroblasts. Dev Dyn. 2010;239(6):1573-84.

23. Hinz B. Tissue stiffness, latent TGF-beta1 activation, and mechanical signal transduction: implications for the pathogenesis and treatment of fibrosis. Curr Rheumatol Rep. 2009;11(2):120-6.
24. Galie PA, Westfall MV, Stegemann JP. Reduced serum content and increased matrix stiffness promote the cardiac myofibroblast transition in 3D collagen matrices. Cardiovasc Pathol. 2011;20(6):325-33.
25. Chen JH, Chen WL, Sider KL, Yip CY, Simmons CA. beta-catenin mediates mechanically regulated, transforming growth factor-beta1-induced myofibroblast differentiation of aortic valve interstitial cells. Arterioscler Thromb Vasc Biol. 2011;31(3):590-7.
26. Liu F, Mih JD, Shea BS, Kho AT, Sharif AS, Tager AM, et al. Feedback amplification of fibrosis through matrix stiffening and COX-2 suppression. J Cell Biol. 2010;190(4):693-706.
27. Olsen AL, Bloomer SA, Chan EP, Gaca MD, Georges PC, Sackey B, et al. Hepatic stellate cells require a stiff environment for myofibroblastic differentiation. Am J Physiol Gastrointest Liver Physiol. 2011;301(1):G110-8.
28. Mayer DC, Leinwand LA. Sarcomeric gene expression and contractility in myofibroblasts. J Cell Biol. 1997;139(6):1477-84.
29. Blaauw E, Lorenzen-Schmidt I, Babiker FA, Munts C, Prinzen FW, Snoeckx LH, et al. Stretch-induced upregulation of connective tissue growth factor in rabbit cardiomyocytes. J Cardiovasc Transl Res. 2013;6(5):861-9.
30. Tarbit E, Singh I, Peart JN, Rose'Meyer RB. Biomarkers for the identification of cardiac fibroblast and myofibroblast cells. Heart Fail Rev. 2019;24(1):1-15.
31. Swaney JS, Roth DM, Olson ER, Naugle JE, Meszaros JG, Insel PA. Inhibition of cardiac myofibroblast formation and collagen synthesis by activation and overexpression of adenylyl cyclase. Proc Natl Acad Sci U S A. 2005;102(2):437-42.
32. Ploeg MC, Munts C, Prinzen FW, Turner NA, van Bilsen M, van Nieuwenhoven FA. Piezo1 Mechanosensitive Ion Channel Mediates Stretch-Induced Nppb Expression in Adult Rat Cardiac Fibroblasts. Cells. 2021;10(7).
33. Turner NA, Porter KE, Smith WHT, White HL, Ball SG, Balmforth AJ. Chronic β2-adrenergic receptor stimulation increases proliferation of human cardiac fibroblasts via an autocrine mechanism. Cardiovascular Research. 2003;57(3):784-92.
34. van Nieuwenhoven FA, Hemmings KE, Porter KE, Turner NA. Combined effects of interleukin-1α and transforming growth factor-β1 on modulation of human cardiac fibroblast function. Matrix Biology. 2013;32(7-8):399-406.
35. van Nieuwenhoven FA, Munts C, Op 't Veld RC, Gonzalez A, Diez J, Heymans S, et al. Cartilage intermediate layer protein 1 (CILP1): A novel mediator of cardiac extracellular matrix remodelling. Sci Rep. 2017;7(1):16042.
36. van Kampen KA, Fernández-Pérez J, Baker M, Mota C, Moroni L. Fabrication of a mimetic vascular graft using melt spinning with tailorable fiber parameters. Biomaterials Advances. 2022;139.
37. van Kampen KA, Olaret E, Stancu IC, Moroni L, Mota C. Controllable four axis extrusion-based additive manufacturing system for the fabrication of tubular scaffolds with tailorable mechanical properties. Mater Sci Eng C Mater Biol Appl. 2021;119:111472.
38. Geelhoed WJ, Lalai RA, Sinnige JH, Jongeleen PJ, Storm C, Rotmans JI. Indirect Burst Pressure Measurements for the Mechanical Assessment of Biological Vessels. Tissue Eng Part C Methods. 2019;25(8):472-8.
39. Shazly T, Rachev A, Lessner S, Argraves WS, Ferdous J, Zhou B, et al. On the Uniaxial Ring Test of Tissue Engineered Constructs. Experimental Mechanics. 2014;55(1):41-51.
40. de Jong S, van Middendorp LB, Hermans RH, de Bakker JM, Bierhuizen MF, Prinzen FW, et al. Ex vivo and in vivo administration of fluorescent CNA35 specifically marks cardiac fibrosis. Mol Imaging. 2014;13.

41. Baues M, Klinkhammer BM, Ehling J, Gremse F, van Zandvoort M, Reutelingsperger CPM, et al. A collagen-binding protein enables molecular imaging of kidney fibrosis in vivo. Kidney Int. 2020;97(3):609-14.
42. Helary C, Bataille I, Abed A, Illoul C, Anglo A, Louedec L, et al. Concentrated collagen hydrogels as dermal substitutes. Biomaterials. 2010;31(3):481-90.
43. Berry MF, Engler AJ, Woo YJ, Pirolli TJ, Bish LT, Jayasankar V, et al. Mesenchymal stem cell injection after myocardial infarction improves myocardial compliance. Am J Physiol Heart Circ Physiol. 2006;290(6):H2196-203.
44. Engler AJ, Carag-Krieger C, Johnson CP, Raab M, Tang HY, Speicher DW, et al. Embryonic cardiomyocytes beat best on a matrix with heart-like elasticity: scar-like rigidity inhibits beating. J Cell Sci. 2008;121(Pt 22):3794-802.
45. Herum KM, Lunde IG, McCulloch AD, Christensen G. The Soft- and Hard-Heartedness of Cardiac Fibroblasts: Mechanotransduction Signaling Pathways in Fibrosis of the Heart. J Clin Med. 2017;6(5).
46. Herum KM, Choppe J, Kumar A, Engler AJ, McCulloch AD. Mechanical regulation of cardiac fibroblast profibrotic phenotypes. Mol Biol Cell. 2017;28(14):1871-82.
47. Kong M, Lee J, Yazdi IK, Miri AK, Lin YD, Seo J, et al. Cardiac Fibrotic Remodeling on a Chip with Dynamic Mechanical Stimulation. Adv Healthc Mater. 2019;8(3):e1801146.
48. Bracco Gartner TCL, Deddens JC, Mol EA, Magin Ferrer M, van Laake LW, Bouten CVC, et al. Anti-fibrotic Effects of Cardiac Progenitor Cells in a 3D-Model of Human Cardiac Fibrosis. Front Cardiovasc Med. 2019;6:52.
49. Hackett TL, Vriesde N, Al-Fouadi M, Mostaco-Guidolin L, Maftoun D, Hsieh A, et al. The Role of the Dynamic Lung Extracellular Matrix Environment on Fibroblast Morphology and Inflammation. Cells. 2022;11(2).
50. Taylor SE, Vaughan-Thomas A, Clements DN, Pinchbeck G, Macrory LC, Smith RK, et al. Gene expression markers of tendon fibroblasts in normal and diseased tissue compared to monolayer and three dimensional culture systems. BMC Musculoskelet Disord. 2009;10:27.
51. Pelham RJ, Jr., Wang Y. Cell locomotion and focal adhesions are regulated by substrate flexibility. Proc Natl Acad Sci U S A. 1997;94(25):13661-5.
52. Lee PY, Liu YC, Wang MX, Hu JJ. Fibroblast-seeded collagen gels in response to dynamic equibiaxial mechanical stimuli: A biomechanical study. J Biomech. 2018;78:134-42.
53. Nieponice A, Maul TM, Cumer JM, Soletti L, Vorp DA. Mechanical stimulation induces morphological and phenotypic changes in bone marrow-derived progenitor cells within a three-dimensional fibrin matrix. J Biomed Mater Res A. 2007;81(3):523-30.
54. Peters AS, Brunner G, Krieg T, Eckes B. Cyclic mechanical strain induces TGFbeta1-signalling in dermal fibroblasts embedded in a 3D collagen lattice. Arch Dermatol Res. 2015;307(2):191-7.
55. Galie PA, Russell MW, Westfall MV, Stegemann JP. Interstitial fluid flow and cyclic strain differentially regulate cardiac fibroblast activation via AT1R and TGF-beta1. Exp Cell Res. 2012;318(1):75-84.
56. Chen MM, Lam A, Abraham JA, Schreiner GF, Joly AH. CTGF expression is induced by TGF- beta in cardiac fibroblasts and cardiac myocytes: a potential role in heart fibrosis. J Mol Cell Cardiol. 2000;32(10):1805-19.
57. Watts KL, Spiteri MA. Connective tissue growth factor expression and induction by transforming growth factor-beta is abrogated by simvastatin via a Rho signaling mechanism. Am J Physiol Lung Cell Mol Physiol. 2004;287(6):L1323-32.
58. Flanders K, Holder MG, Winokur TS. Autoinduction of mRNA and protein expression for transforming growth factor-?s in cultured cardiac cells. Journal of Molecular and Cellular Cardiology. 1995;27(2):805-12.
59. Hinz B. Formation and function of the myofibroblast during tissue repair. J Invest Dermatol. 2007;127(3):526-37.

60. Tomasek JJ, Gabbiani G, Hinz B, Chaponnier C, Brown RA. Myofibroblasts and mechano-regulation of connective tissue remodelling. Nat Rev Mol Cell Biol. 2002;3(5):349-63.
61. Biernacka A, Dobaczewski M, Frangogiannis NG. TGF-beta signaling in fibrosis. Growth Factors. 2011;29(5):196-202.
62. Watson CJ, Phelan D, Xu M, Collier P, Neary R, Smolenski A, et al. Mechanical stretch up-regulates the B-type natriuretic peptide system in human cardiac fibroblasts: a possible defense against transforming growth factor-beta mediated fibrosis. Fibrogenesis Tissue Repair. 2012;5(1):9.

Left atrial remodeling in mitral regurgitation: a combined experimental-computational study

Sjoerd Bouwmeester[1]*, Tim van Loon[2]*, Meike C. Ploeg[3], Thomas P. Mast[1], Nienke J. Verzaal[3], Lars B. van Middendorp[3], Marc Strik[4], Frans A. van Nieuwenhoven[3], Lukas R. Dekker[1,5], Frits W. Prinzen[3], Joost Lumens[2]* and Patrick Houthuizen[1]*

[1]Department of Cardiology, Catharina Hospital Eindhoven, Eindhoven, The Netherlands; [2]Department of Biomedical Engineering, CARIM School for Cardiovascular Diseases, Maastricht University, Maastricht, The Netherlands; [3]Department of Physiology, CARIM School for Cardiovascular Diseases, Maastricht University, Maastricht, The Netherlands; [4]Bordeaux University Hospital (CHU), Cardio-Thoracic Unit, Pessac, France; [5]Department of Biomedical Technology, Eindhoven University of Technology, Eindhoven, The Netherlands

*These authors contributed equally to this work

PLoS One. 2022 Jul 15;17(7):e0271588.

6

Abstract

Aims: Progressive changes to left atrial (LA) structure and function following mitral regurgitation (MR) remain incompletely understood. This study aimed to demonstrate potential underlying mechanisms using experimental canine models and computer simulations.

Methods and results: A canine model of MR was created by cauterization of mitral chordae followed by radiofrequency ablation-induced left bundle-branch block (LBBB) after 4 weeks (MR-LBBB group). Animals with LBBB alone served as control. Echocardiography was performed at baseline, acutely after MR induction, and at 4 and 20 weeks, and correlated with histology and computer simulations.

Results: Acute MR augmented LA reservoir and contractile strain (40±4 to 53±6% and -11±5 to -22±9% respectively, $p<0.05$). LA fractional area-change increased significantly (47±4 to 56±4%, $p<0.05$) while LA end-systolic area remained unchanged (7.2±1.1 versus 7.9±1.1 cm^2 respectively, $p=0.08$). LA strain 'pseudonormalized' after 4 weeks, and decompensated at 20 weeks with both strains decreasing to 25±6% and -3±2% respectively ($p<0.05$) together with a progressive increase in LA end-systolic area (7.2±1.1 to 14.0±6.3 cm2, $p<0.05$). In the LBBB-group, LA remodeling was less pronounced. Histology and gene expression analysis showed a trend towards increased interstitial fibrosis in the LA of the MR-LBBB group versus the LBBB group, without significant change of cardiomyocyte cross-sectional area. Computer simulations demonstrated that the progressive changes in LA structure and function are the result of both eccentric remodeling and fibrosis.

Conclusion: MR augmented LA strain acutely to supranormal values without significant LA dilation. Over time, LA strain gradually decreases (pseudornormal and decompensated) along with LA dilation, presumably due to a combination of LA eccentric remodeling and fibrosis.

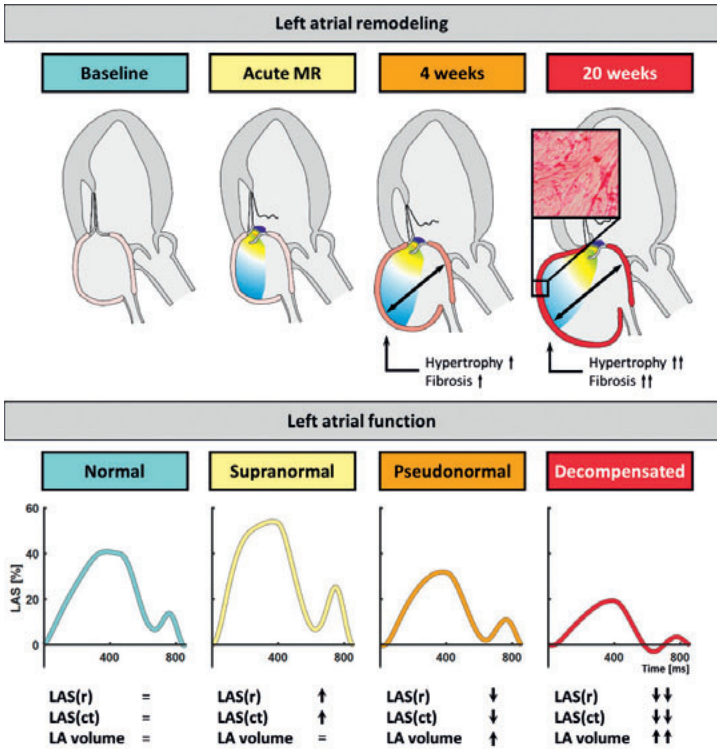

Graphical abstract: Left atrial remodeling after acute primary mitral regurgitation. Introduction of acute MR increases LA reservoir and contractile strain, accompanied by insignificant LA dilation. At 4 and 20 weeks, there is a gradual decrease in both strain values with progressive LA dilation, correlated to LA eccentric hypertrophy and fibrosis.

Introduction

Mitral regurgitation (MR) causes volume overload of both the left ventricle (LV) and left atrium (LA). Although guidelines focus on the impact on LV function to indicate intervention, the LA is the first chamber to receive the volume excess [1]. Not surprisingly, LA dilation, as a marker of LA remodeling, is associated with increased cardiovascular morbidity and mortality irrespective of LV function [2, 3].

Traditionally, standard echocardiographic (LA volume) and Doppler parameters (transmitral and pulmonary vein flow velocities) are used as indirect measures to assess the effects of MR on LA structure and function [4]. However, speckle tracking imaging allows more direct assessment of LA function by myocardial deformation (strain) and may better reflect functional LA changes due to MR [5]. Little is known about the chronological evolution of LA strain from the onset of an acute MR to the chronic phase and what underlying mechanisms contributes to this evolution.

The aim of this study was to provide new insight into the mechanisms of LA structural and functional remodeling after acute MR. The study made use of the same canine models as previously published [6], whose original aim was to investigate the electromechanical effects of LBBB. Two models were used: 1) radiofrequency ablation-induced left bundle-branch block (LBBB group); and 2) severe MR creation followed by LBB ablation after 4 weeks (MR-LBBB group). Changes in LA structure and function were assessed by echocardiography. Furthermore, histology and gene expression analysis were performed, as well as computer simulations to identify potential underlying myocardial disease mechanisms.

Materials & methods

All animal procedures complied with the Dutch Law on Animal Experimentation and the European Directive for the Protection of Vertebrate Animals used for Experimental and Other Scientific Purposes (86/609/EU). The Experimental Animal Committee of Maastricht University approved the study. Dogs were purchased from a commercial party approved by the Dutch Veterinary Inspection.

Study design

All experiments were performed under general anesthesia with continuous infusion of midazolam (0.25 mg/kg/h) and sufentanil (3 μg/kg/h) after induction with thiopental (300 mg). Acute severe MR was induced in 12 adult mongrel dogs using a customized electrophysiology catheter with a hook at the distal tip, which was inserted into the carotid artery and advanced into the LV. After grasping one or more chordae, the hook was cauterized to burn through the chordae. This process was repeated until fluoroscopic and echocardiographic guidance indicated severe MR using the integrative approach according to the European Association for Cardiovascular Imaging (EACVI) recommendations [7]. As the original study aimed to investigate electromechanical effects of left bundle branch block (LBBB), the dogs underwent radiofrequency ablation of the left bundle branch 4 weeks later (MR-LBBB group). During the procedures and at the final day of the protocol, standardized echocardiographic measurements were performed. To distinguish between the effects of MR and LBBB, a second group of 7 dogs with only LBBB (LBBB group) was used as control group (figure 1). Dogs were sacrificed by overdose of anesthetics 16 weeks after induction of LBBB, and atrial tissue was harvested for histology and gene expression analysis.

Echocardiography

Echocardiography was performed in the MR-LBBB group at baseline, directly after induction of MR, and after 4 and 20 weeks. LBBB dogs only underwent echocardiography at baseline and 16 weeks. A Vivid 7 system (GE Vingmed, Horten, Norway) with a 2.5 MHz probe was used with commercially available software to analyze conventional echocardiography parameters (EchoPAC 3.0, GE Vingmed Ultrasound, Horten, Norway). LV end-systolic, end-diastolic volume, and ejection fraction (LVESV, LVEDV, LVEF) were measured on an

apical 4-chamber view by modified single-plane Simpson's rule. LA end-systolic area and LA end-diastolic area expressed in cm^2 were calculated by tracing the LA endocardium in the apical 4-chamber. LA fractional area change (LAFAC) was calculated with the formula: LAFAC (%) = 100% * [(LA end-systolic area – LA end-diastolic area)/LA end-systolic area] [8]. Commercially available software (TOMTEC ARENA, 2D CPA 1.3, TOMTEC Imaging Systems GmbH, Unterschleißheim, Germany) was used to measure LA strain. As recommended by the Taskforce [9], LA strain was measured on a non-foreshortened apical four-chamber view. The LA border was semi-automatically drawn after a 3-point clicking method followed by manual adjustment if required. The zero-strain reference was defined at LV end-diastole (i.e. mitral valve closure). LA reservoir strain (LAS(r)) was measured as difference of the strain value at mitral valve opening minus LV end-diastole. LA contractile strain (LAS(ct)) was calculated as difference of LAS(r) minus the strain value at onset of atrial contraction. Figure 2 shows an example of the echocardiographic assessment of LA strain.

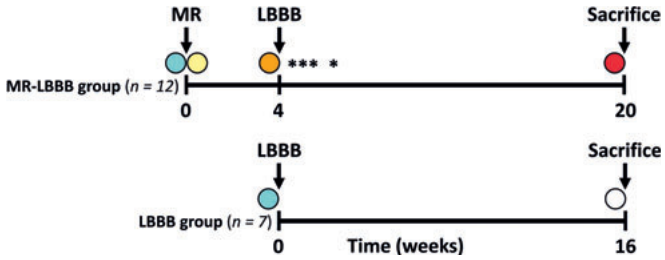

Figure 1. Timeline schematic of the canine experiments. MR-LBBB model: creation of mitral regurgitation at baseline followed by LBBB induction after 4 weeks. LBBB model: LBBB induction after baseline. Circles indicate the time points of echocardiographic and hemodynamic measurements at baseline (blue), acute MR (yellow), 4 weeks (yellow), 16 weeks (white) and 20 weeks (red). The asterisks in the MR-LBBB group indicate death due to heart failure, all within 6 weeks. MR = mitral regurgitation; LBBB = left bundle branch block.

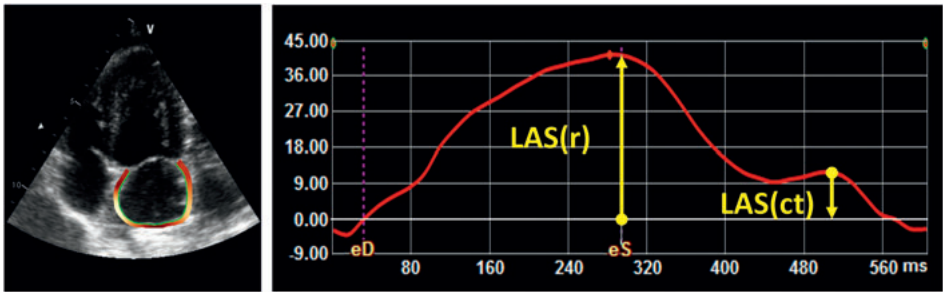

Figure 2. Example of LA strain assessment by 2D speckle-tracking echocardiography at baseline. Four-chamber longitudinal left atrium strain (LAS). Arrows represent reservoir (r) and contractile (ct) phase (42% and -12%, respectively).

Histology and gene expression analysis

Cryosections of 7 µm were cut from the LA of each dog at − 22 °C. Antigen fixation was performed by submerging slides in ice-cold acetone for 10 min. The degree of fibrosis was determined in tissue sections stained with 0.1% Sirius Red. The percentage of collagen was determined using ImageJ in 8 separate pictures (200x magnification, Leica Microscope) per atrial section.

Area of atrial cardiomyocytes was determined at the level of the nucleus using ImageJ (200x magnification, Leica Microscope) in tissue sections stained with hematoxylin-eosin (HE). For each atrium, an average of 56 individual cardiomyocytes were analyzed.

Total RNA was isolated from atrial tissue using an RNA isolation kit (Omega Biotek, Norcross, GA, USA) and reversed transcribed into cDNA using the iScript cDNA synthesis kit (Biorad, Hercules, CA, USA) according to the manufacturer's instructions. Real-time PCR was performed on CFX96 Touch real-time PCR detection system using iQ SYBR-Green Supermix (Biorad). Gene expression level of Alpha-smooth muscle actin (Acta2), Connective tissue growth factor (Ctgf), Collagen type 1 (Col1a1), Atrial Natriuretic Peptide (Nppa), and Brain Natriuretic Peptide (Nppb) were normalized using the housekeeping gene cyclophilin-A (Cyclo), and their relative expression was calculated using the comparative threshold cycle (Ct) method by calculating $2^{\Delta Ct}$ (e.g., $2^{(\text{Cyclophilin Ct} - \text{Col1a1 Ct})}$). The mRNA expression of Acta2, Ctgf and Col1a1 were measured as these genes are known to be involved in fibroblast activation and fibrosis. The mRNA expression of Nppa and Nppb was measured as markers for stretch activation in cardiac tissue and pathological cardiac hypertrophy. The sequences of the specific primers used are provided below (table 1).

Table 1. Gene-specific primer sequences used for quantitative real-time PCR

Gene	Forward primer	Reverse primer
Alpha-smooth muscle actin (Acta2)	CTGGTGTGTGACAACGGCTC	CCCACCATCACTCCCTGATGT
Collagen type 1 (Col1a1)	AGAGCATGACCGACGGATTC	ACGCTGTTCTTGCAGTGGTA
Connective tissue growth factor (Ctgf)	CACAGAGTGGAGCGCCTGTTC	GATGCACTTTTTGCCCTTCTTAATG
Atrial Natriuretic peptide (Nppa)	GCTGGATTTCAAGAACTTGCT	CTTGGGGAGACTCGGCTTC
Brain Natriuretic Peptide (Nppb)	TGCACAAGTCAGGGTGCTTT	CAGGGGGCTGCTGAAGAATC
Cyclophilin-A (Cyclo)	CCCACCGTGTTCTTCGACAT	CCAGTGCTCAGAGCACGAAA

Computer model simulations

Computer simulations of LA and LV myocardial deformation were performed to identify potential underlying pathophysiological substrates underlying the echocardiographic and histological findings in the canine experiments. In addition, simulations allow for the differentiation between the effects of MR and LBBB to LA function, by simulating these pathologies in isolation.

The open source CircAdapt model of the human heart and circulation was used (www.circadapt.org) [10], as previous studies have demonstrated the potential of this model to simulate cardiovascular mechanics and hemodynamics during valve regurgitation [11, 12], dyssynchrony [13] and the combination of both [14]. A reference simulation representing a healthy cardiovascular system under baseline conditions was used as a starting point (see Supplemental Material for a detailed description of model initialization). Acute MR was simulated by increasing mitral effective regurgitant orifice area (EROA) from 0 to 0.40 cm^2. To represent the compromised hemodynamics status after MR, systemic flow and mean arterial pressure (MAP) were reduced from 5.1 to 3.6 L/min and 92 to 75 mmHg, respectively, as previously published [11]. These changes led to a severe MR as characterized by a mitral regurgitant fraction (RF) >50%. All other model parameters were left unchanged compared to the reference simulation.

LA eccentric hypertrophy and interstitial fibrosis are known structural changes caused by MR [15]. To differentiate the possible effects of both LA (patho-)physiological alterations on echocardiographic parameters, two LA myocardial tissue substrates of various severities were simulated (see Supplemental Material for a detailed description of the simulation methodology):

1. LA eccentric hypertrophy: gradual simultaneous increase of LA wall mass and area from 100 (normal LA geometry) to 300% in 10% increments;
2. LA passive stiffness: gradual increase of LA myocardial stiffness from 100 (normal compliance) to 600% in 10% increments.

In each simulation, the change in LAA was compared to the reference simulation, and the strain indices LAS(r) and LAS(ct) were quantified, with zero-strain reference set at mitral valve closure.

To demonstrate the contribution of LBBB in the canine MR-LBBB group, we repeated all the above-mentioned simulations with LBBB. As previously published [13], LBBB was simulated by delaying the mean LV free wall activation time from 0 (synchronous activation) to 30 milliseconds (mild electromechanical substrate), and 60 milliseconds (severe electromechanical substrate), relative to the mean septal- and right ventricular free wall activation times. In a previous study, LBBB has been reported to induce LV eccentric hypertrophy [16]. Hence, analogous to simulating LA eccentric hypertrophy, LV wall mass and area were simultaneously increased to 110% and 120% in the mild and severe electromechanical substrate, respectively. All simulations were performed using MATLAB (R2019a, Mathworks, Natick, MA).

Statistics

Continuous variables are expressed as median (interquartile range) or mean (standard deviations) when appropriate. Normality of distribution was assessed with the Kolmogorov-Smirnov test. The paired sample Wilcoxon rank-sum test was used to compare hemodynamic and echocardiographic differences between different time points. Continuous variables

between MR-LBBB and LBBB groups were compared with the Student's t test or Mann-Whitney U test as appropriate. Statistical analyses were performed using SPSS version 25 (IBM Corporation, Armonk, NY) and Graphpad PRISM. Statistical significance was assigned at $p<0.05$.

Results

All procedures were successfully performed in the MR-LBBB (n=12) and LBBB (n=7) group, however 4 MR-LBBB animals died because of severe heart failure (Figure 1), all within 2 weeks after LBBB induction on top of the MR. The LBBB group had no premature deaths nor development of MR. Baseline data were comparable for both groups (Table 2).

Time course of LA dilation and function

Table 2 summarizes the time course of echocardiographic and hemodynamic LA and LV parameters. In MR-LBBB dogs, no significant LA dilation (as quantified by LA end-systolic area) was present directly after MR induction with respect to baseline (7.4 [6.3-7.8] cm^2 versus 8.0 [7.1-8.9] cm^2, respectively). However, progressive LA dilation was observed in weeks 4 to 20 post-MR (13 [8.6-15.8] cm^2 and 11.6 [10.1-20.7] cm^2, respectively). Moreover, LAFAC increased significantly from 47 [44-50]% at baseline to 55 [53 – 59]%, immediately after MR was induced, and decreased progressively to 41 [39–44]% at week 4 and 33 [25-42]% at week 20. The combination of progressive LA dilation with decreasing LAFAC suggests LA functional deterioration. This is corroborated by the observation and shown in Figure 3 (left panels), in which both LAS(r) and LAS(ct) augmented to supranormal values acutely after MR was induced (40 [37-42] to 51 [48-56]% and -10 [-8;-12] to -21 [-21;-25]%, respectively), whereas in weeks 4 to 20 a significant decline in both strain indices was observed (32 [30-35] to 29 [18-29] % and -7 [-2; -10] to -2 [-1; -5]%, respectively).

No significant LA dilation was present in the LBBB-group, LAFAC, LAS(r), and LAS(ct) did decrease over time (Figure 3, right panels). However, the MR-LBBB group showed a significantly larger decrease in LAFAC, LAS(r), and LAS(ct) compared to the LBBB-group.

Time course of LV dilation and function

Significant LV dilation and increased (hyperdynamic) LVEF was observed after MR induction in the MR-LBBB group compared to baseline (42 [34-45] to 53 [42-57] ml and 54 [50-60] to 61 [61-69]%, respectively). At 4 weeks, progressive LV dilation (65 [39-75] ml) was accompanied by an insignificant increase in LVEF (64 [59-67]%) followed by further LV dilation (82 [50-106] ml), and accompanied by a LVEF pseudo-normalization at 20 weeks (55 [47-57]%). In the LBBB group a significant decrease in LVEF without LV dilation was observed at 16 weeks compared to baseline (50 [48-52] to 34 [24-49]% and 44 [39-45] to 47 [30-51] ml).

Table 2. Overview of echocardiographic and hemodynamic measurements at baseline, acute, subacute, and chronic phase

	MR-LBBB				LBBB	
	n=12			n=8	n=7	
Phase:	Baseline	Acute-MR	4 weeks	20 weeks	Baseline	16 weeks
Heart rate – bpm	82 ± 26	101 ± 37	86 ± 25	73 ± 24	75 ± 40	79 ± 38
Echocardiographic LA parameters						
LA end-systolic area - cm^2	7.4 [6.3 – 7.8]	8.0 [7.1 – 8.9]	13 [8.6 – 15.8]†	11.6 [10.1 – 20.7]†	7.9 [5.4 – 9.2]	8.5 [7.0 – 8.6]
LAFAC - %	47 [44 – 50]	55 [53 – 59]†	41 [39 – 44]†	33 [25 – 42]†	46 [45 – 48]	43 [42 – 46]
LAS(r) - %	40 [37 – 42]	51 [48 – 56]†	32 [30 – 35]†	29 [18 – 29]†	42 [37 – 43]	39 [36 – 40]†
LAS(ct) - %	-10 [-8; -12]	-21 [-21; -25]†	-7 [-2; -10]†	-2 [-1 ;5]†	-8 [-7; -12]	-7 [-4; -8]†
Echocardiographic LV parameters						
LVEDV - ml	42 [34 – 45]	53 [42 – 57]†	65 [39 – 75]†	82 [50 – 106]†	44 [39 – 45]	47 [30 – 51]
LVEF - %	54 [50 – 60]	61 [61 – 69]†	64 [59 – 67]†	55 [47 – 57]	50 [48 – 52]	34 [24 – 49]†

Legend: Data are given as mean ± standard deviation. † $p < 0.05$ compared to baseline; EDV = end-diastolic volume; EF = ejection fraction; ESA = end-systolic area; LA = left atrial; LV = left ventricle; [IQR] = interquartile range.

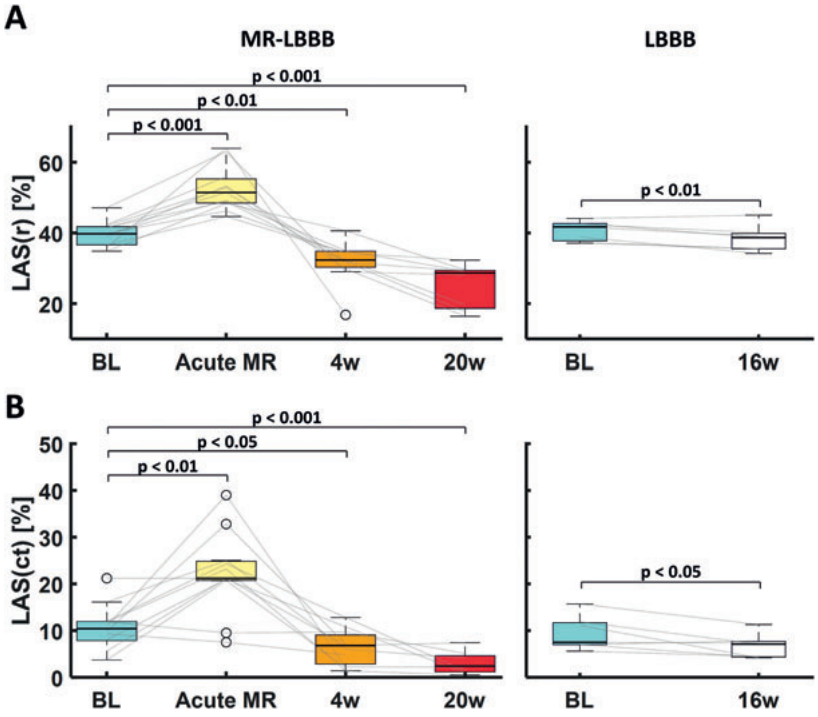

Figure 3. Chronological changes of left atrial strain. Time course of LA reservoir (LAS(r)) (A) and contractile (LAS(ct)) (B) strain for each group (presented as boxplots and lines for individual animals). Statistical significance was assigned at $p < 0.05$. BL = baseline; LAS(r) = left atrial reservoir strain; LAS(ct) = left atrial contractile strain; LBBB = left bundle branch block, MR = mitral regurgitation; w = weeks.

Collagen fractional area and gene expression analysis

Compared with the LBBB group, LA tissue from the MR-LBBB group showed a trend towards increased interstitial LA fibrosis ($p = 0.07$) and Col1A expression ($p = 0.18$)(Figure 4), providing histological confirmation of LA structural remodeling in this group. No significant difference was found in mRNA expression of Ctgf, Acta2 and Nppb between the LBBB and MR-LBBB group. The mRNA expression of Nppa was significantly lower ($p = 0.03$) in the MR-LBBB group compared to the LBBB group (data not shown).

Cardiomyocyte area

There was no significant difference in cardiomyocyte area of the LA between chronic MR-LBBB to LBBB (figure 5).

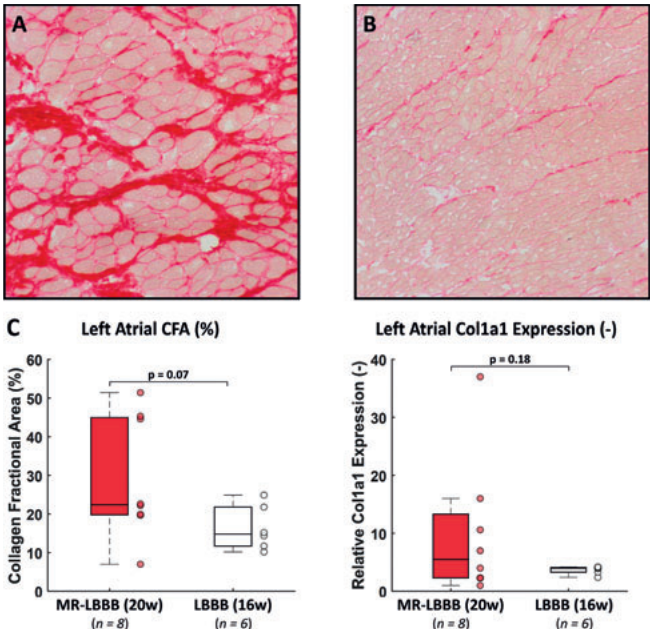

Figure 4. Histological and gene expression analysis of LA tissue. Representative examples of 0.1% Sirius Red stained LA tissue sections of the (A) MR-LBBB group and (B) LBBB group at 200x magnification. (C) Comparison of collagen fractional area (CFA) and relative collagen type 1 (Col1a1) expression to Cyclophilin-A for each group (presented as boxplots and scatters for individual animals). A trend towards more interstitial fibrosis and increased Col1a1 expression was found in the MR-LBBB group at 20 weeks, as compared to LBBB group at 16 weeks.

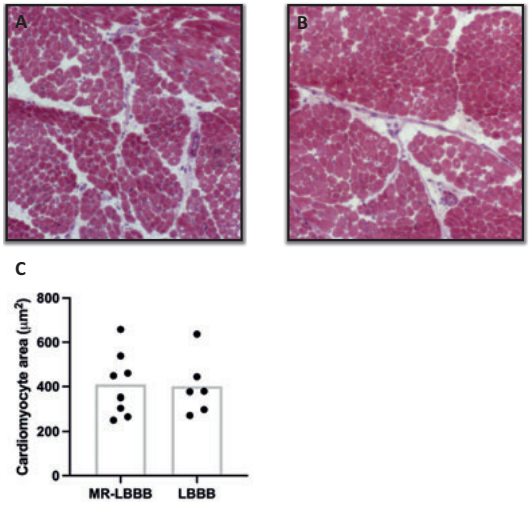

Figure 5. Representative images of HE stained sections the LA of MR-LBBB (A) and LBBB (B) group at 200x magnification. Histological analysis of cardiomyocyte area in LA tissue (C). Data is presented as individual dogs (dots) and mean (bar). No effect on cardiomyocyte area was found in the MR-LBBB group at 20 weeks, as compared to LBBB group at 16 weeks.

Computer simulations

In the CircAdapt model, acute induction of severe MR alone hardly affected LA end-systolic area compared to baseline simulation, while LAFAC, LAS(r) and LAS(ct) increased similarly as observed in the MR-LBBB dogs (Table 3). Simulation of structural LA myocardial remodeling in terms of eccentric remodeling and stiffening in the acute MR simulation resulted in marked changes in strain pattern and LA end-systolic area (Figure 6):

1. An increase in LA eccentric hypertrophy resulted in increased LA end-systolic area together with decreased LAS(r) and LAS(ct);
2. A higher LA passive stiffness led to a decreased LA end-systolic area together with decreased LAS(r) and LAS(ct).

It was observed that none of the LA tissue parameters alone were sufficient to reproduce changes in LA dilation and function as observed in the MR-LBBB-group. Hence, all simulation combinations were considered and two 'best-match' simulations were obtained with LAS(r), LAS(ct), and LA end-systolic area being closest to the average values measured at the 4 and 20 weeks phase. None of the abovementioned changes to the LA myocardium led to a change in LV dilation and function (Table 3).

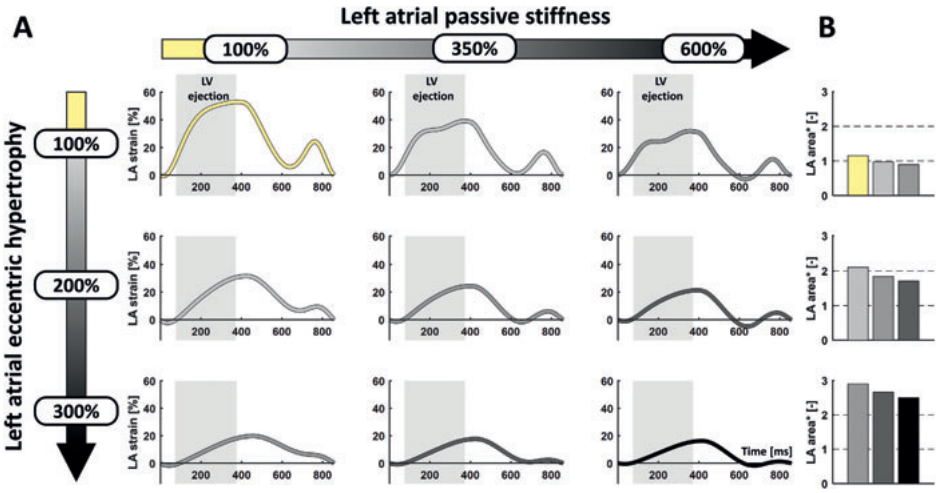

Figure 6. Simulations of LA strain and end-systolic area (LAESA) after acute MR. Simulated changes in (A) LA strain and (B) LA area (i.e. change in LA end-systolic area relative to baseline simulation) of varying severity of LA passive stiffness (left-to-right) and LA eccentric hypertrophy (top-to-bottom) starting from the simulation of the acute severe MR phase (yellow). Vertical gray areas in the strain panels indicate the period of LV ejection.

Table 3. Computer simulation characteristics and derived functional measurements.

	Computer Simulations					
Phase:	Baseline	Acute-MR	4 weeks	20 weeks		
				Synchronous	+30 ms delay	+60 ms delay
Global hemodynamics						
Heart rate – bpm	70	70	70	70	70	70
Systemic flow – L/min	5.1	3.6	3.6	3.6	3.6	3.6
Mean arterial pressure – mmHg	92	75	75	75	75	75
Mitral valve characteristics						
EROA – cm^2	0	0.40	0.40	0.40	0.40	0.40
Regurgitant fraction – %	0	52	52	52	54	56
LA tissue characteristics						
LA eccentric hypertrophy – %	100	100	180	250	250	250
LA passive stiffness – %	100	100	220	530	530	530
LV tissue characteristics						
LV free wall activation delay – ms	0	0	0	0	30	60
LV eccentric hypertrophy – %	100	100	100	100	113	125
Derived LA functional indices						
LA end-systolic area* –	1.00	1.15	1.72	2.00	2.00	2.00
LAFAC – %	61	69	55	45	49	52
LAS(r) – %	41	54	31	19	19	22
LAS(ct) – %	14	26	10	3	0	0
Derived LV functional indices						
LVEDV – ml	130	150	150	150	175	200
LVEF – %	55	72	72	72	65	58

Legend: Overview of computer simulation characteristics, the underlying LA myocardial tissue substrate, and derived echocardiographic measurements of the simulated baseline, acute, 4 and 20 weeks phase. *LA end-systolic area is calculated relative to baseline simulation. EROA = effective regurgitant orifice area; LAFAC = left atrial fractional area change; LAS(ct) = left atrial contractile strain; LAS(r) = left atrial reservoir strain; LVEDV = left ventricular end-diastolic volume; LVEF = left ventricular ejection fraction; MR = mitral regurgitation.

However, adding LBBB to the simulations with severe LA mechanical dysfunction (in accordance with the 20 weeks in-vivo observations) did impair LV function, characterized by LV dilation (i.e. LVEDV), decreased LVEF (Table 3), and heterogeneous longitudinal LV strain (Figure 7).

Concerning the interaction with LBBB, a delayed onset of LV filling was observed with a shorter LV diastolic duration. As a result, LBBB acutely increased LAS(r) and decreased LAS(ct).

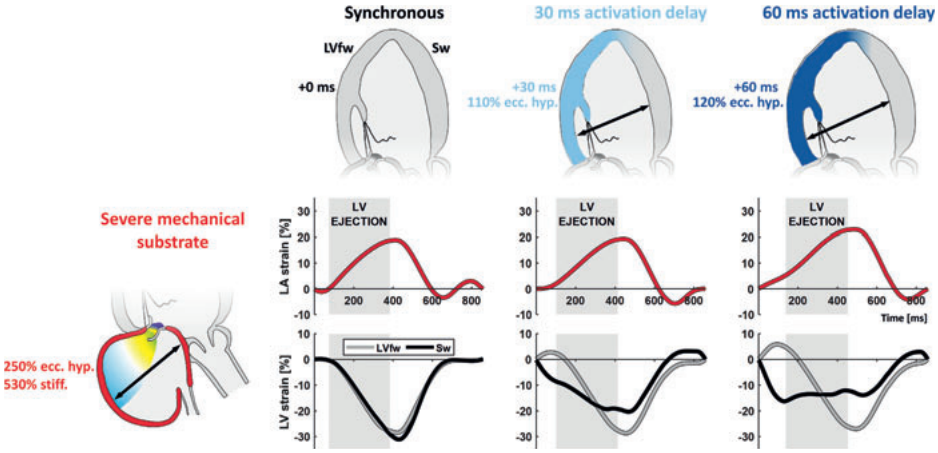

Figure 7. Simulations of LA and LV strain with MR after induction of LBBB. Effect of increasing LV electromechanical activation delay in addition to acute MR. Electromechanical activation delay is characterized by a delayed onset of LV filling, increased LAS(r) and decreased LAS(ct). Vertical gray areas in the strain panels indicate the period of LV ejection. LVfw = left ventricular free wall; Sw = septal wall; ecc. hyp. = eccentric hypertrophy; stiff. = passive stiffness.

Discussion

The present study provides insight on how LA volume and function change after induction of acute MR in a canine model. We demonstrated that acute MR initially increases both LA reservoir and contractile strain function while there is progressive LA dilation with a decrease in LA reservoir and contractile function at later stages. Both histology and computer simulations support the hypothesis that these changes of LA mechanical function are caused by a combination of eccentric hypertrophy and fibrosis. This study also illustrates that LA dysfunction precedes LV failure.

MR acutely augments LA function

In a clinical situation of chronic MR, the volume-overloaded LA has to accommodate the excess in regurgitant volume by dilation in order to protect the pulmonary vasculature from high filling pressures [17, 18]. As LA compliance is limited in acute MR, filling pressures increase and can result in pulmonary edema. In the acute phase of our experiment, there is an instant increase in LA stroke volume together with augmentation of both reservoir and contractile function. Given the absence of LA dilation, the increased strain can only be explained by a small (albeit not-significant) increase in LA end-systolic volume with related stretch-induced increase of LA myocardial contractility (i.e. Frank-Starling length-tension relationship) [19]. This in turn augments the LA booster pump and increases the LAS(ct). Indeed, computer simulation of acute MR confirm this hypothesis of enhanced LA contractile function as LA strain increases without significant LA dilation, while all model parameters related to myocardial tissue behavior were kept constant. Hence, the improved contractility leads to an acute rise in LA stroke volume so that the healthy atrial myocardium is able to compensate for the excess regurgitant volume.

LA decompensation following prolonged volume overload

In later stages, the reduction in LAS(r) and LAS(ct) together with progressive LA dilation indicate that the LA myocardium cannot cope with the chronic volume overload caused by MR. Simulations have shown that this progressive LA failure, cannot be explained by LA dilation alone, as both eccentric hypertrophy and fibrosis were needed to reproduce the in-vivo LA volume and strain observations (Figure 6).

It is known that the LA responds to the excess volume load with a range of adaptive and ultimately maladaptive processes. These include myocyte growth, hypertrophy, and finally, apoptosis and necrosis [5, 15]. Together with excessive fibroblast proliferation, myolysis is enhanced and, consequently, the contractile apparatus is affected [20]. These findings correspond to the progressive increase in LA eccentric hypertrophy and fibrosis as shown by the computer simulations and by the histological examination. The lack of change in diameter in combination with increased atrial size indicates eccentric myocyte hypertrophy. Our findings seem in line with data from a mouse model of MR where cardiomyocytes were also elongated [21]. However, these findings in animal studies appear to differ from those in patients with chronic MR and AF, which show increased cardiomyocyte area in the remodeled LA [22, 23]. A possible explanation is the timeline, because the pathologies are likely to exist for a longer time (years) than in the animal studies (weeks-months).

In addition to eccentric hypertrophy, our data indicate a trend for increased fibrosis, shown by increased Col1a1 mRNA expression in the LA of the MR-LBBB group. On the other hand, LA gene expression of markers for (fibroblast) stretch activation (Acta2, Ctgf and Nppb) were similar in MR-LBBB and LBBB animals and Nppa mRNA expression was even decreased in MR-LBBB animals. Possible explanation of this paradoxical observation is that those genes are more related to the acute activation of CFs, as shown in chapter 2, to be as early as 4h

of stretch. Since the present measurements were taken in a chronic setting, expression may have been downregulated by negative feedback systems, which might be related to the reduction in stretch caused by the increased fibrosis.

Our observation that LA strain progresses from supranormal (acute phase) to decompensated values at 20 weeks has also been observed in patients. Cameli et al. [24] have shown that LAS(r) is increased in patients with mild MR. On the other hand, patients with more severe MR showed a progressive impairment of LAS(r). Debonnaire et al. [5] investigated the correlation between the grade of LA fibrosis and LA function in patients with severe MR referred for mitral surgery. They demonstrated a stepwise reduction of LAS(r) with the lowest values in patients with more severe fibrosis at histologic analysis. Although it seems obvious that fibrosis is the cause of reduced LAS(r), we have shown in our computer simulations that LA eccentric hypertrophy alone can also lead to a reduction of LAS(r) (Figure 6). The reduction in LA myocardial function is therefore likely a result of eccentric hypertrophy in combination with fibrosis.

Limitations

The *in vivo* model used in this study was originally created to investigate the electromechanical effects of LBBB and therefore not a primary MR study. As a result, no typical control group was available as LBBB was present in both canine groups. Therefore, we evaluated the effects of MR, LBBB and the combination thereof on LA structure and function using computer simulations. Both *in vivo* experiments as computer simulations suggest that the observed LA dilation and functional deterioration were related to MR rather than LBBB.

Histology and gene expression analysis show great variation. Due to the large variation and low numbers, there may be insufficient statistical power to demonstrate a difference. However, a trend towards interstitial fibrosis formation in the MR-LBBB was demonstrated.

Our experimental data consisted of young and healthy mongrel dogs and do clearly differ from the pathophysiological heterogeneity expected in human patients. The LA was completely normal at baseline, while in clinical practice LA remodeling often has already occurred before onset of MR due to hypertension, atrial fibrillation, other valvular disease and/or heart failure. Our model is more representative of clinical cases for acutely ruptured chordae in patients with pre-existing valve prolapse of during blunt chest trauma. However, the design of the study makes it possible to provide clear insight into the evolution of LA remodeling after acute MR and showed that not only interstitial fibrosis causes decrease in LA function. This study also illustrates that LA dysfunction precedes LV failure.

Conclusion

In a canine model of acute MR, LA reservoir and contractile function augmented to supranormal values in the absence of significant LA dilation. Over time, there is a gradual decrease in both strain values (pseudonormal to decompensated) together with progressive LA dilation. Histology and computer simulations suggest that these functional changes are the result of a combination of LA eccentric hypertrophy and fibrosis. These mechanistic insights in LA pathophysiology may aid in further understanding the effects of LA volume overload in patients with MR and can help to find the optimal timing for surgery.

Funding sources: this research was performed within the framework of CTMM, the Center for Translational Molecular Medicine (www.ctmm.nl), project COHFAR (grant 01C-203), and supported by the Dutch Heart Foundation. J.L. acknowledges support from the Dr. Dekker Program of the Dutch Heart Foundation (grant 2015T082) and the Netherlands Organisation for Scientific Research (NWO- ZonMw, VIDI grant 016.176.340). All authors have reported that they have no other relationships relevant to the contents of this paper to disclose.

References

1. Kihara Y, Sasayama S, Miyazaki S, Onodera T, Susawa T, Nakamura Y, et al. Role of the left atrium in adaptation of the heart to chronic mitral regurgitation in conscious dogs. Circ Res. 1988;62(3):543-53.
2. Grigioni F, Avierinos J-F, Ling LH, Scott CG, Bailey KR, Tajik AJ, et al. Atrial fibrillation complicating the course of degenerative mitral regurgitation. Journal of the American College of Cardiology. 2002;40(1):84-92.
3. Messika-Zeitoun D, Bellamy M, Avierinos JF, Breen J, Eusemann C, Rossi A, et al. Left atrial remodelling in mitral regurgitation--methodologic approach, physiological determinants, and outcome implications: a prospective quantitative Doppler-echocardiographic and electron beam-computed tomographic study. Eur Heart J. 2007;28(14):1773-81.
4. Falk V, Baumgartner H, Bax JJ, De Bonis M, Hamm C, Holm PJ, et al. ESC/EACTS Guidelines for the management of valvular heart disease. Eur J Cardiothorac Surg 2017.
5. Debonnaire P, Leong DP, Witkowski TG, Al Amri I, Joyce E, Katsanos S, et al. Left atrial function by two-dimensional speckle-tracking echocardiography in patients with severe organic mitral regurgitation: association with guidelines-based surgical indication and postoperative (long-term) survival. J Am Soc Echocardiogr. 2013;26(9):1053-62.
6. Strik M, van Middendorp LB, Vernooy K. Animal models of dyssynchrony. J Cardiovasc Transl Res. 2012;5(2):135-45.
7. Lancellotti P, Tribouilloy C, Hagendorff A, Popescu BA, Edvardsen T, Pierard LA, et al. Recommendations for the echocardiographic assessment of native valvular regurgitation: an executive summary from the European Association of Cardiovascular Imaging. Eur Heart J Cardiovasc Imaging. 2013;14(7):611-44.
8. Nakamura K, Osuga T, Morishita K, Suzuki S, Morita T, Yokoyama N, et al. Prognostic value of left atrial function in dogs with chronic mitral valvular heart disease. J Vet Intern Med. 2014;28(6):1746-52.
9. Badano LP, Kolias TJ, Muraru D, Abraham TP, Aurigemma G, Edvardsen T, et al. Standardization of left atrial, right ventricular, and right atrial deformation imaging using two-dimensional speckle tracking echocardiography: a consensus document of the EACVI/ASE/Industry Task Force to standardize deformation imaging. Eur Heart J Cardiovasc Imaging. 2018;19(6):591-600.
10. Walmsley J, Arts T, Derval N, Bordachar P, Cochet H, Ploux S, et al. Fast Simulation of Mechanical Heterogeneity in the Electrically Asynchronous Heart Using the MultiPatch Module. PLoS Comput Biol. 2015;11(7):e1004284.
11. Palau-Caballero G, Walmsley J, Gorcsan J, 3rd, Lumens J, Delhaas T. Abnormal Ventricular and Aortic Wall Properties Can Cause Inconsistencies in Grading Aortic Regurgitation Severity: A Computer Simulation Study. J Am Soc Echocardiogr. 2016;29(11):1122-30 e4.
12. Walmsley J, Squara P, Wolfhard U, Cornelussen R, Lumens J. Impact of abrupt versus gradual correction of mitral and tricuspid regurgitation: a modelling study. EuroIntervention. 2019;15(10):902-11.
13. Lumens J, Ploux S, Strik M, Gorcsan J, 3rd, Cochet H, Derval N, et al. Comparative electromechanical and hemodynamic effects of left ventricular and biventricular pacing in dyssynchronous heart failure: electrical resynchronization versus left-right ventricular interaction. J Am Coll Cardiol. 2013;62(25):2395-403.
14. Lumens J, Fan CS, Walmsley J, Yim D, Manlhiot C, Dragulescu A, et al. Relative Impact of Right Ventricular Electromechanical Dyssynchrony Versus Pulmonary Regurgitation on Right Ventricular Dysfunction and Exercise Intolerance in Patients After Repair of Tetralogy of Fallot. J Am Heart Assoc. 2019;8(2):e010903.

15. Verheule S, Wilson E, Everett Tt, Shanbhag S, Golden C, Olgin J. Alterations in atrial electrophysiology and tissue structure in a canine model of chronic atrial dilatation due to mitral regurgitation. Circulation. 2003;107(20):2615-22.
16. Vernooy K, Verbeek XA, Peschar M, Crijns HJ, Arts T, Cornelussen RN, et al. Left bundle branch block induces ventricular remodelling and functional septal hypoperfusion. Eur Heart J. 2005;26(1):91-8.
17. Sasayama S, Takahashi M, Osakada G, Hirose K, Hamashima H, Nishimura E, et al. Dynamic geometry of the left atrium and left ventricle in acute mitral regurgitation. Circulation. 1979;60(1):177-86.
18. Yoran C, Yellin EL, Becker RM, Gabbay S, Frater RW, Sonnenblick EH. Dynamic aspects of acute mitral regurgitation: effects of ventricular volume, pressure and contractility on the effective regurgitant orifice area. Circulation. 1979;60(1):170-6.
19. Katz AM. Ernest Henry Starling, his predecessors, and the "Law of the Heart". Circulation. 2002;106(23):2986-92.
20. Mary-Rabine L, Albert A, Pham TD, Hordof A, Fenoglio JJ, Jr., Malm JR, et al. The relationship of human atrial cellular electrophysiology to clinical function and ultrastructure. Circ Res. 1983;52(2):188-99.
21. Li S, Nguyen NUN, Xiao F, Menendez-Montes I, Nakada Y, Tan WLW, et al. Mechanism of Eccentric Cardiomyocyte Hypertrophy Secondary to Severe Mitral Regurgitation. Circulation. 2020;141(22):1787-99.
22. Foglieni C, Rusconi R, Mantione ME, Fragasso G, Alfieri O, Maisano F. Early left atrial tissue features in patients with chronic mitral regurgitation and sinus rhythm: Alterations of not remodeled left atria. Int J Cardiol. 2016;219:433-8.
23. Corradi D, Callegari S, Benussi S, Maestri R, Pastori P, Nascimbene S, et al. Myocyte changes and their left atrial distribution in patients with chronic atrial fibrillation related to mitral valve disease. Hum Pathol. 2005;36(10):1080-9.
24. Cameli M, Lisi M, Giacomin E, Caputo M, Navarri R, Malandrino A, et al. Chronic mitral regurgitation: left atrial deformation analysis by two-dimensional speckle tracking echocardiography. Echocardiography. 2011;28(3):327-34.

General discussion

7

Cardiac remodeling is an important process in the pathology of heart failure, that has been and still is topic of intensive research. Fibrosis is one of the main characteristics of cardiac remodeling with cardiac fibroblasts (CFs) and myofibroblast as main players. This thesis aimed to investigate the mechanisms of mechanical activation of CFs.

In **chapter 2** and **3** the role of the mechanosensitive ion channel Piezo1 on stretch-induced expression of Nppb and Cilp1 was investigated in rat CFs. Results showed that Nppb gene expression and BNP secretion was strongly induced by cyclic stretch. Moreover, the stretch-induced Nppb gene expression was mediated by the mechanosensitive ion channel Piezo1 (**chapter 2**). In addition, stretch-induced Tgfβ1 gene expression showed a similar Piezo1 involvement as in Nppb expression (**chapter 2**). Cyclic stretch as well as the Piezo1-agonist Yoda1 downregulated CF Cilp1 gene expression, indicating that Piezo1 is also involved in Cilp1 regulation by mechanical stimuli (**chapter 3**).

In **chapter 4** the influence of duration of mechanical stimulation on CF activation was explored. It was shown that a short 1 h period of stretch can activate CF early-gene response after 4 h, which returned to baseline at 24 h, indicating only temporary activation of CFs by short-term mechanical stimuli.

In **chapter 5** the development of 3D Engineered Heart Matrix (EHM) aimed at a more physiologically relevant environment for CFs was described. Results show that baseline expression of Acta2 and Ctgf is lower in EHM compared to 2D monolayers, indicating decreased myofibroblast differentiation in EHM. The CF-response to cyclic stretch and TGFβ1 stimulation was found to be maintained in EHM.

Finally, in **chapter 6**, the mechanisms underlying atrial fibrosis were investigated in a dog-model of mitral regurgitation (MR). Results showed progressive left atrial (LA) dilation with decrease in LA reservoir and contractile function. Echocardiography, computational modeling, histology and gene expression data support the hypothesis that these changes are likely caused by a combination of eccentric hypertrophy and fibrosis.

CF activation and differentiation (Stretch, Stiffness, Sensing & Signaling)

Cardiac fibrosis is the result of a complex interplay of extracellular matrix (ECM) protein synthesis, degradation and crosslinking. CFs are important in this process as they produce collagen, but also metalloproteinases (MMPs) and tissue inhibitors of MMPs (TIMPs), resulting in control over the ECM turnover [1, 2]. The stretch-induced Nppb gene expression, resulting in increased BNP-protein secretion by rat CFs, has previously been shown in human CFs [3]. The inhibition of profibrotic effects by BNP in CF, namely the inhibition of TGFβ1 induced Acta2 expression, (chapter 2) underscores previous studies showing inhibition of collagen production and fibroblast proliferation [4], and the inhibition of TGFβ-activation of pro-fibrotic and inflammatory genes by BNP in human CFs [5].

The finding of a role for BNP in regulation of CFs by us and by others [3, 4, 6-8] was initially remarkable, because cardiomyocytes (CMs) were considered to be main source of cardiac BNP [7, 9-13] being a marker of cardiac overload. Indeed, the level of Nppb gene expression was clearly lower in CFs as compared to CMs (chapter 2), but yet our experiments indicate a significant role for BNP produced by CFs. The regulation of CFs by BNP likely acts locally in an autocrine or paracrine manner, counteracting the profibrotic effect of TGFβ1. This antifibrotic role of BNP could make BNP an interesting therapeutic target for heart failure [14, 15], by administration of exogenous (recombinant) BNP [16] or by preventing the inactivation of BNP [14]. Indeed, several clinical trials have investigated the effect of BNP, but this was primarily as treatment option for acute decompensated heart failure [17]. In that study, administration of Nesiritide (recombinant BNP) for a maximum of 7 days had no effect on all-cause mortality, cardiovascular death or worsening heart failure, compared to placebo after 180 days [18]. However, this study aimed at the natriuretic effect of BNP during acute heart failure and not on it antifibrotic effect. Such relatively short period of administration cannot be expected to have influenced the slow process of fibrosis. However, a few studies in mice indicate that long-term administration of BNP attenuates cardiac hypertrophy after myocardial infarction [19] and in obese diabetic mice [20].

Our results showed that stretch-induced BNP expression is mediated by Piezo1. Piezo1 is thought to be a primary mechanosensor, meaning that Piezo1 detects mechanical stimulation in the absence of other cofactors [21]. Both cardiac specific deletion or overexpression of Piezo1 in murine models has shown severe consequences for cardiac function, impaired cardiac function and severe heart failure respectively [22]. Apparently, balanced expression and/or activity is key for Piezo1. Mechanotransduction of Piezo1 leads to downstream activation of the p38α MAPK pathway [23]. This same pathway is also activated via TGFβ1 [23]. These results implicate an interesting role for Piezo1 in cardiac remodeling, as modulator but also as a potential therapeutic target.

Based on our finding that silencing of Piezo1 induced Cilp1 mRNA expression (chapter 3), we speculate that Piezo1 is active under our cell culture conditions, inhibiting the expression of Cilp1. When Piezo1 is then inactivated by siRNA, this inhibition is cancelled leading to an increased Cilp1 expression. The mechanism causing the increased Cilp1 expression when Piezo1 is inactivated by siRNA, would need further investigation, not only measuring gene expression but also Piezo1 activity. Administration of Yoda1 induces a similar effect on Acta2, Ctgf, Tnc and Cilp1 as stretch, further supporting the involvement of Piezo1 in the stretch-induced effects.

Another important factor involved in the observed gene expression changes upon silencing of Piezo1 is the stiffness of the cell culture substrate. Our results in EHM (chapter 5) showed that differences in stiffness lead to differences in baseline gene expression. Since Piezo1 is a primary mechanosensitive ion channel, studying the role of Piezo1 on CF cultured on hard plastic plates or Bioflex plates can make a difference, as the stiffness of the Bioflex plates is

1000 times softer than the plastic plates. However, there was no difference between baseline expression of Piezo1 in CFs cultured on hard plates and on Bioflex plates. Unlike expression, Piezo1 activity seems to be affected by the substrate stiffness [24, 25]. In future studies this idea may be further investigated by determining Piezo1 activity in EHM with physiological stiffness and compare this to CFs cultured on hard plastic or Bioflex plates. The induction of Tnc gene expression by Yoda1 in our studies seems to be in line with increased Tnc mRNA and protein levels, in a recent Piezo1 gain of function mutation study in CFs [26].

In conclusion, Stretch, Stiffness, Sensing & Signaling influence the perception of mechanical stimuli by CFs. Figure 1 [27] summarizes the proposed mechanisms by which mechanical stimuli via Piezo1 ultimately lead towards fibrosis. On the one hand fibrosis will lead to a reduction in stretch, which would reduce fibrosis by blocking the stretch-initiated fibrotic processes by a negative feedback system. On the other hand, fibrosis increases ECM stiffness, which in turn activates CFs, leading to more fibrosis through a positive feedback loop. The factor Speed in the title of this thesis will be discussed in the next paragraph.

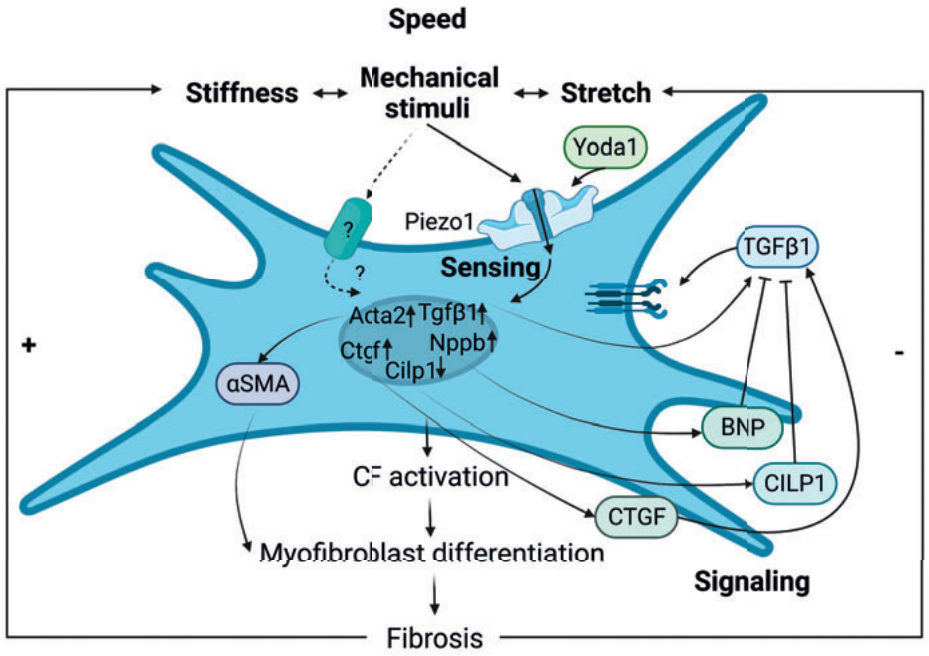

Figure 1. Schematic of proposed mechanism on Piezo1 mechanosignaling in CF and modulation of CF gene expression of Acta2, Ctgf, Cilp1, Nppb and Tgfβ1. The figure shows how mechanical stimuli might lead to CF activation and differentiation, ultimately resulting in fibrosis. Fibrosis increases stiffness on the one side, but decreases stretch on the other side. Stretch and Yoda1 stimulation upregulates all genes, but downregulated Cilp1 gene expression. TGFβ1 is a known stimulus for CF activation. TGFβ1 can also be released after ECM activation, as it is stored within the ECM in inactive form. TGFβ1 is inhibited by BNP (chapter 2) and CILP1 [28]. Whereas it is known that CTGF stimulates TGFβ1 [29, 30].

Duration of mechanical stimuli (Stretch & Speed)

Activation of CFs and the subsequent differentiation towards myofibroblasts is a gradual process [31]. In this thesis, CF activation was defined by the gene expression profile consisting of a group of genes. This selection was based on the speed of which the genes are activated, ranging from early responsive genes (Nppb), intermediate responsive genes (Tnc and Tgfβ1) and late activated genes (Acta2 and Ctgf), some of which are also known to be involved in myofibroblast differentiation: Acta2, Ctgf, Tenascin C (Tnc), Tgfβ1 and Nppb [1, 28, 32-35]. Continuous cyclic stretch (10% 1Hz) for 4 h induces the mRNA expression of Acta2, Ctgf, Tnc, Tgfβ1 and Nppb (Chapter 2). The further increase in mRNA levels of Acta2 and Ctgf after 24 h of cyclic stretch indicates that after 4 hours their induction is still in the rising phase. On the other hand, the gene expression of Nppb and Tgfβ1 is lower after 24 h than after 4 h stretch, suggesting that the peak of expression of these genes is somewhere between 4 h and 24 h. For Tnc the effect of stretch is over after 24 h, expression levels being back to baseline. Figure 2A summarizes the interpretation of these timeframes. Contrary to continuous cyclic stretch, 1 h stretch increases Nppb, Tnc and Tgfβ1 mRNA expression after 4 h, but this effect is over after 24 h (chapter 4). 1-hour stretch did not change gene expression of Ctgf and Acta2 after 24 h at all, as summarized in figure 2B. These results show the importance of the different timeframes (Speed) in which gene expression comes up or fades out, as effects might be missed otherwise.

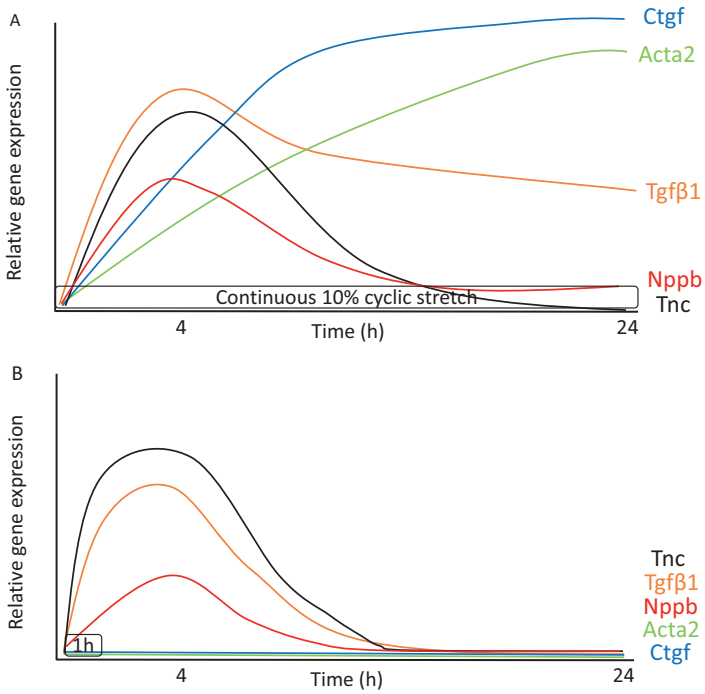

Figure 2. Interpretation of different expression patterns of our gene profile for CF activation after continuous cyclic stretch (A) or 1 h cyclic stretch (B) after 4 h and 24 h for gene expression of Ctgf, Acta2, Tgfβ1, Nppb and Tnc. Y-axis is presented as maximum change (0-100%).

The practical implications of the findings about the minimal duration of mechanical load on CF activation and differentiation may be illustrated by differences between the athlete's heart and that of patients with long-lasting pressure overload, like aortic valve stenosis or hypertension. *In vivo* CFs are mechanically stimulated by fluctuations of stretch amplitude by daily activities, such as exercise [31]. Exercise training, which commonly comprises not more than 1-2 hours exercise per day, leads to dilatation and hypertrophy of the LV and RV within a few weeks [36] but in the absence of fibrosis [37]. The adaptations in the athlete's heart are commonly considered physiological [38, 39]. In contrast, adaptation to chronic pressure overload, is considered pathophysiological [40, 41] because it consists of concentric hypertrophy (increased wall thickness) and excessive ECM deposition [42]. The time course of CF activation, illustrated in figure 2 supports the idea that relatively short-lasting activities, like exercise, do not lead to CF differentiation and fibrosis. This property may, in part explain the physiological nature of remodeling in the athlete's heart.

While chronic volume overload usually does not lead to fibrosis in the ventricles [43, 44], our findings in chapter 6 show that the atrium responds differently to volume overload. This discrepancy between atria and ventricles might be caused of atria being more prone to fibrosis, since the baseline collagen percentage is higher in the atria then in the ventricles [45, 46].

2D vs 3D in vitro models

Our results on CF activation in response to continuous cyclic stretch and TGFb1 stimulation in 2D monolayers (chapter 2 & 3) was confirmed in 3D EHM (chapter 5). One of the main advantages of *in vitro* studies is that properties and behavior of one specific cell type can be investigated apart from other cell types within the tissue and humoral factors in the blood. At the same time this is also the main limitation of this model, because cells are removed from their physiological environment. This is where 3D cultures may be a good compromise. The EHM matrix provides structure for CFs to attach to, leading to compaction of the collagen gel. Gel compaction also leads to elimination of water within the gel, increasing the collagen concentration. A higher concentration also affects the stiffness of the gel, something that can be changed by increasing the initial collagen concentration. Increasing the stiffness of EHM could be used as a model for fibrotic tissue, making EHM a suitable model to compare CF response to different stimuli (mechanical or drug/pharmaceutical) in both physiological and fibrotic matrix. Such difference is difficult to model in 2D monolayers, as plastic culture plates are already stiffer (in the range of 1 Gpa) compared to fibrous tissue (20-100 kPa) [47]. Results from EHM culturing indicated a more quiescent CF state in 3D. The EHM model can be applied using CFs from multiple sources; primary adult CFs, freshly isolated or commercially available [8, 12]. Human CFs can be isolated from cardiac tissue derived from cardiac surgery but recently a limitless source comes from human stem cells [48] or induced pluripotent stem cells (iPSCs)[49].

3D culturing using human CFs

Next steps for using our EHM model would be to implement human derived cells. A pilot study using the EHM-ring was performed combining commercially available human cardiac ventricular fibroblasts (Lonza) with human stem cell derived CMs (3:1 ratio). The EHM-ring showed compaction, similarly as the EHM-ring containing only human CFs or rat CFs (chapter 5). After 6 days of culturing the EHM-rings were harvested and Hoechst staining was added. All EHM-rings showed live cells and cells were evenly distributed throughout the gel. Similar results were obtained when we used CF derived from human induced pluripotent stem cells (hiPSC-CF). Further improvements need to be implemented, as well as optimization of the matrix and the medium to accommodate both CFs and CMs. As human embryonal derived cells are still subject of discussion, iPSC-CF would be a good alternative also enabling the investigation of the influence of patient specific mutations. Future perspectives are on characterizing iPSC-CFs and further optimizing and standardizing of the differentiation protocol. These optimizations would lead to a more stable iPSC-CFs culture, hopefully resulting in a more constant baseline mRNA expression. Ultimately using EHM for a co-culture of iPSC-CFs together with iPSC-CMs for investigating the interplay of these cells. The potential of such a system has been shown recently on pirfenidone, an anti-fibrotic drug which showed promising results in pre-clinical animal models of cardiac fibrosis [50]. The use of iPSCs also creates opportunities to investigate patient derived cells [51] or certain mutations, in either cell type and how these co-cultures respond to stimuli such as stretch. In conclusion, using human derived cells are the future of 3D *in vitro* culturing and most likely will replace 2D monolayers.

Combining different cell types, like CFs with CMs creates options for 3D culturing and this field has been exploding the last decades. Many steps have been made with improving 3D structures. The use of patches, mostly a combination of a biomaterial seeded with cells, has been shown to improve bone [52] or skin healing [53]. However, these patches were not successful in cardiac healing [54]. These patches were invented for direct application, not for investigating or testing purposes; as our EHM is. A 3D model that does have the potential to serve as investigating or drug testing system is the organ on a chip [55]. Organ on a chip can be defined as microfluidic cell-culture system providing a controllable culture microenvironment that contains continuously perfused chambers being inhabited by living human cells arranged in a 3D organization used for modeling physiological functions of tissues and organs [55, 56]. These systems have also been used to model mechanical activation, as a model of hypertrophy [57]. Further developments are needed to design physiological culture systems to study the CF in a natural ECM environment in coculture with other cardiac cell types with appropriate mechanical and electrical stimulation.

From *in vitro* to *in vivo* model

The use of animals for experiments raises ethical concerns in the society at large [58], despite extensive legislation and control and supervision by ethical committees [58, 59]. Our *in vivo* dog model has provided valuable insight in the development of atrial fibrosis. This series of experiments were part of a larger series, primarily aimed at investigating the effect of the conduction abnormality left bundle branch block (LBBB). [60-62]. The dog model was chosen to this purpose, because the conduction system of the dog heart is similar to that of man [63, 64]. Also, the size and heart rate of the dog heart is comparable to that of humans [63, 65]. The comparison between the measurements in the hearts with MR and the simulations in the CircAdapt model shows the potential of using computational modeling, first of all to complement the measurements, but ultimate as replacement of animal experiments.

Worth mentioning is that these *in vivo* experiments were performed in 2010-2011 and that our analysis were possible due to the organized biobank of echocardiographic and hemodynamic data as well as tissue samples, thus still generating publications many years later (chapter 6). In conclusion, although 3D *in vitro* models using human derived cells have the potential to ultimately replace *in vivo* studies, as results in this thesis have shown, *in vivo* models may still add valuable information.

References

1. van Nieuwenhoven FA, Turner NA. The role of cardiac fibroblasts in the transition from inflammation to fibrosis following myocardial infarction. Vascul Pharmacol. 2013;58(3):182-8.
2. Moore L, Fan D, Basu R, Kandalam V, Kassiri Z. Tissue inhibitor of metalloproteinases (TIMPs) in heart failure. Heart Fail Rev. 2012;17(4-5):693-706.
3. Watson CJ, Phelan D, Xu M, Collier P, Neary R, Smolenski A, et al. Mechanical stretch up-regulates the B-type natriuretic peptide system in human cardiac fibroblasts: a possible defense against transforming growth factor-beta mediated fibrosis. Fibrogenesis Tissue Repair. 2012;5(1):9.
4. Tsuruda T, Boerrigter G, Huntley BK, Noser JA, Cataliotti A, Costello-Boerrigter LC, et al. Brain natriuretic Peptide is produced in cardiac fibroblasts and induces matrix metalloproteinases. Circ Res. 2002;91(12):1127-34.
5. Kapoun AM, Liang F, O'Young G, Damm DL, Quon D, White RT, et al. B-type natriuretic peptide exerts broad functional opposition to transforming growth factor-beta in primary human cardiac fibroblasts: fibrosis, myofibroblast conversion, proliferation, and inflammation. Circ Res. 2004;94(4):453-61.
6. Jarai R, Kaun C, Weiss TW, Speidl WS, Rychli K, Maurer G, et al. Human cardiac fibroblasts express B-type natriuretic peptide: fluvastatin ameliorates its up-regulation by interleukin-1alpha, tumour necrosis factor-alpha and transforming growth factor-beta. J Cell Mol Med. 2009;13(11-12):4415-21.
7. Makino N, Sugano M, Satoh S, Oyama J, Maeda T. Peroxisome Proliferator-Activated Receptor-γ Ligands Attenuate Brain Natriuretic Peptide Production and Affect Remodeling in Cardiac Fibroblasts in Reoxygenation After Hypoxia. Cell Biochemistry and Biophysics. 2006;44(1):065-72.
8. Ploeg MC, Munts C, Prinzen FW, Turner NA, van Bilsen M, van Nieuwenhoven FA. Piezo1 Mechanosensitive Ion Channel Mediates Stretch-Induced Nppb Expression in Adult Rat Cardiac Fibroblasts. Cells. 2021;10(7).
9. Morita E, Yasue H, Yoshimura M, Ogawa H, Jougasaki M, Matsumura T, et al. Increased plasma levels of brain natriuretic peptide in patients with acute myocardial infarction. Circulation. 1993;88(1):82-91.
10. Nishikimi T, Yoshihara F, Morimoto A, Ishikawa K, Ishimitsu T, Saito Y, et al. Relationship Between Left Ventricular Geometry and Natriuretic Peptide Levels in Essential Hypertension. Hypertension. 1996;28(1):22-30.
11. Koglin J, Pehlivanli S, Schwaiblmair M, Vogeser M, Cremer P, vonScheidt W. Role of brain natriuretic peptide in risk stratification of patients with congestive heart failure. Journal of the American College of Cardiology. 2001;38(7):1934-41.
12. Blaauw E, van Nieuwenhoven FA, Willemsen P, Delhaas T, Prinzen FW, Snoeckx LH, et al. Stretch-induced hypertrophy of isolated adult rabbit cardiomyocytes. Am J Physiol Heart Circ Physiol. 2010;299(3):H780-7.
13. Nishikimi T, Maeda N, Matsuoka H. The role of natriuretic peptides in cardioprotection. Cardiovasc Res. 2006;69(2):318-28.
14. Ichiki T, Dzhoyashvili N, Burnett JC, Jr. Natriuretic peptide based therapeutics for heart failure: Cenderitide: A novel first-in-class designer natriuretic peptide. Int J Cardiol. 2019;281:166-71.
15. Jhund PS, McMurray JJ. The neprilysin pathway in heart failure: a review and guide on the use of sacubitril/valsartan. Heart. 2016;102(17):1342-7.
16. O'Connor CM, Starling RC, Hernandez AF, Armstrong PW, Dickstein K, Hasselblad V, et al. Effect of nesiritide in patients with acute decompensated heart failure. N Engl J Med. 2011;365(1):32-43.
17. Hernandez AF, O'Connor CM, Starling RC, Reist CJ, Armstrong PW, Dickstein K, et al. Rationale and design of the Acute Study of Clinical Effectiveness of Nesiritide in Decompensated Heart Failure Trial (ASCEND-HF). Am Heart J. 2009;157(2):271-7.
18. Dandamudi S, Chen HH. The ASCEND-HF trial: an acute study of clinical effectiveness of nesiritide and decompensated heart failure. Expert Rev Cardiovasc Ther. 2012;10(5):557-63.

19. He JG, Chen YL, Chen BL, Huang YY, Yao FJ, Chen SL, et al. B-type natriuretic peptide attenuates cardiac hypertrophy via the transforming growth factor-ss1/smad7 pathway in vivo and in vitro. Clin Exp Pharmacol Physiol. 2010;37(3):283-9.
20. Plante E, Menaouar A, Danalache BA, Broderick TL, Jankowski M, Gutkowska J. Treatment with brain natriuretic peptide prevents the development of cardiac dysfunction in obese diabetic db/db mice. Diabetologia. 2014;57(6):1257-67.
21. Stewart L, Turner NA. Channelling the Force to Reprogram the Matrix: Mechanosensitive Ion Channels in Cardiac Fibroblasts. Cells. 2021;10(5).
22. Jiang F, Yin K, Wu K, Zhang M, Wang S, Cheng H, et al. The mechanosensitive Piezo1 channel mediates heart mechano-chemo transduction. Nat Commun. 2021;12(1):869.
23. Turner NA, Blythe NM. Cardiac Fibroblast p38 MAPK: A Critical Regulator of Myocardial Remodeling. J Cardiovasc Dev Dis. 2019;6(3).
24. Blythe NM, Muraki K, Ludlow MJ, Stylianidis V, Gilbert HTJ, Evans EL, et al. Mechanically activated Piezo1 channels of cardiac fibroblasts stimulate p38 mitogen-activated protein kinase activity and interleukin-6 secretion. J Biol Chem. 2019;294(46):17395-408.
25. Emig R, Knodt W, Krussig MJ, Zgierski-Johnston CM, Gorka O, Gross O, et al. Piezo1 Channels Contribute to the Regulation of Human Atrial Fibroblast Mechanical Properties and Matrix Stiffness Sensing. Cells. 2021;10(3).
26. Bartoli F, Evans EL, Blythe NM, Stewart L, Chuntharpursat-Bon E, Debant M, et al. Global PIEZO1 Gain-of-Function Mutation Causes Cardiac Hypertrophy and Fibrosis in Mice. Cells. 2022;11(7).
27. Created with BioRender.com.
28. van Nieuwenhoven FA, Munts C, Op 't Veld RC, Gonzalez A, Diez J, Heymans S, et al. Cartilage intermediate layer protein 1 (CILP1): A novel mediator of cardiac extracellular matrix remodelling. Sci Rep. 2017;7(1):16042.
29. Daniels A, van Bilsen M, Goldschmeding R, van der Vusse GJ, van Nieuwenhoven FA. Connective tissue growth factor and cardiac fibrosis. Acta Physiol (Oxf). 2009;195(3):321-38.
30. Blaauw E, Lorenzen-Schmidt I, Babiker FA, Munts C, Prinzen FW, Snoeckx LH, et al. Stretch-induced upregulation of connective tissue growth factor in rabbit cardiomyocytes. J Cardiovasc Transl Res. 2013;6(5):861-9.
31. van Putten S, Shafieyan Y, Hinz B. Mechanical control of cardiac myofibroblasts. J Mol Cell Cardiol. 2016;93:133-42.
32. Tamura N, Ogawa Y, Chusho H, Nakamura K, Nakao K, Suda M, et al. Cardiac fibrosis in mice lacking brain natriuretic peptide. Proc Natl Acad Sci U S A. 2000;97(8):4239-44.
33. Frangogiannis NG. Matricellular proteins in cardiac adaptation and disease. Physiol Rev. 2012;92(2):635-88.
34. Hinz B. Formation and function of the myofibroblast during tissue repair. J Invest Dermatol. 2007;127(3):526-37.
35. Tomasek JJ, Gabbiani G, Hinz B, Chaponnier C, Brown RA. Myofibroblasts and mechano-regulation of connective tissue remodelling. Nat Rev Mol Cell Biol. 2002;3(5):349-63.
36. Scharhag J, Lollgen H, Kindermann W. Competitive sports and the heart: benefit or risk? Dtsch Arztebl Int. 2013;110(1-2):14-23; quiz 4; e1-2.
37. Scharhag J, Schneider G, Urhausen A, Rochette V, Kramann B, Kindermann W. Athlete's heart. Journal of the American College of Cardiology. 2002;40(10):1856-63.
38. Reindell H, Klepzig H, Steim H, Musshoff K, Roskamm H, Schildge E. Herz, Kreislaufkrankheiten und Sport. Barth, editor. München, Germany1960.
39. Kindermann W, Keul J, Reindell H. Principles of the evaluation of achievement-physiological adaptation. Dtsch Med Wochenschr. 1974;99(25):1372-9.
40. Jurcut R, Giusca S, Ticulescu R, Popa E, Amzulescu MS, Ghiorghiu I, et al. Different patterns of adaptation of the right ventricle to pressure overload: a comparison between pulmonary hypertension and pulmonary stenosis. J Am Soc Echocardiogr. 2011;24(10):1109-17.

41. Garcia D, Pibarot P, Kadem L, Durand L-G. Respective impacts of aortic stenosis and systemic hypertension on left ventricular hypertrophy. Journal of Biomechanics. 2007;40(5):972-80.
42. Heineke J, Molkentin JD. Regulation of cardiac hypertrophy by intracellular signalling pathways. Nat Rev Mol Cell Biol. 2006;7(8):589-600.
43. Grossman W. Cardiac hypertrophy: Useful adaptation or pathologic process? The American Journal of Medicine. 1980;69(4):576-84.
44. Rossi MA, Carillo SV. Cardiac hypertrophy due to pressure and volume overload: distinctly different biological phenomena? International Journal of Cardiology. 1991;31(2):133-41.
45. de Jong S, van Middendorp LB, Hermans RH, de Bakker JM, Bierhuizen MF, Prinzen FW, et al. Ex vivo and in vivo administration of fluorescent CNA35 specifically marks cardiac fibrosis. Mol Imaging. 2014;13.
46. Oken DE, Boucek RJ. Quantitation of collagen in human myocardium. Circ Res. 1957;5(4):357-61.
47. Herum KM, Lunde IG, McCulloch AD, Christensen G. The Soft- and Hard-Heartedness of Cardiac Fibroblasts: Mechanotransduction Signaling Pathways in Fibrosis of the Heart. J Clin Med. 2017;6(5).
48. Mayhall EA, Paffett-Lugassy N, Zon LI. The clinical potential of stem cells. Curr Opin Cell Biol. 2004;16(6):713-20.
49. Takahashi K, Yamanaka S. Induction of Pluripotent Stem Cells from Mouse Embryonic and Adult Fibroblast Cultures by Defined Factors. Cell. 2006;126(4):663-76.
50. Bracco Gartner TCL, Crnko S, Leiteris L, van Adrichem I, van Laake LW, Bouten CVC, et al. Pirfenidone Has Anti-fibrotic Effects in a Tissue-Engineered Model of Human Cardiac Fibrosis. Front Cardiovasc Med. 2022;9:854314.
51. Llucia-Valldeperas A, Smal R, Bekedam FT, Ce M, Pan X, Manz XD, et al. Development of a 3-Dimensional Model to Study Right Heart Dysfunction in Pulmonary Arterial Hypertension: First Observations. Cells. 2021;10(12).
52. Battafarano G, Rossi M, De Martino V, Marampon F, Borro L, Secinaro A, et al. Strategies for Bone Regeneration: From Graft to Tissue Engineering. Int J Mol Sci. 2021;22(3).
53. Nourian Dehkordi A, Mirahmadi Babaheydari F, Chehelgerdi M, Raeisi Dehkordi S. Skin tissue engineering: wound healing based on stem-cell-based therapeutic strategies. Stem Cell Res Ther. 2019;10(1):111.
54. Belien H, Evens L, Hendrikx M, Bito V, Bronckaers A. Combining stem cells in myocardial infarction: The road to superior repair? Med Res Rev. 2022;42(1):343-73.
55. Paloschi V, Sabater-Lleal M, Middelkamp H, Vivas A, Johansson S, van der Meer A, et al. Organ-on-a-chip technology: a novel approach to investigate cardiovascular diseases. Cardiovasc Res. 2021;117(14):2742-54.
56. An F, Qu Y, Liu X, Zhong R, Luo Y. Organ-on-a-Chip: New Platform for Biological Analysis. Anal Chem Insights. 2015;10:39-45.
57. Parsa H, Wang BZ, Vunjak-Novakovic G. A microfluidic platform for the high-throughput study of pathological cardiac hypertrophy. Lab Chip. 2017;17(19):3264-71.
58. Tjarnstrom E, Weber EM, Hultgren J, Rocklinsberg H. Emotions and Ethical Decision-Making in Animal Ethics Committees. Animals (Basel). 2018;8(10).
59. Directive E. 63/EU of the European Parliament and of the Council of 22 September 2010 on the protection of animals used for scientific purposes. Off J Eur Union. 2010;276:33-79.
60. Nguyen UC, Verzaal NJ, van Nieuwenhoven FA, Vernooy K, Prinzen FW. Pathobiology of cardiac dyssynchrony and resynchronization therapy. Europace. 2018;20(12):1898-909.
61. Auricchio A, Fantoni C, Regoli F, Carbucicchio C, Goette A, Geller C, et al. Characterization of left ventricular activation in patients with heart failure and left bundle-branch block. Circulation. 2004;109(9):1133-9.
62. Noheria A, Sodhi S, Orme GJ. The Evolving Role of Electrocardiography in Cardiac Resynchronization Therapy. Curr Treat Options Cardiovasc Med. 2019;21(12):91.

63. Milani-Nejad N, Janssen PM. Small and large animal models in cardiac contraction research: advantages and disadvantages. Pharmacol Ther. 2014;141(3):235-49.
64. Fedorov VV, Glukhov AV, Chang R. Conduction barriers and pathways of the sinoatrial pacemaker complex: their role in normal rhythm and atrial arrhythmias. Am J Physiol Heart Circ Physiol. 2012;302(9):H1773-83.
65. Camacho P, Fan H, Liu Z, He JQ. Large Mammalian Animal Models of Heart Disease. J Cardiovasc Dev Dis. 2016;3(4).

Appendix

Summary

Summary

Cardiac tissue consists of different cell types, like cardiac fibroblasts (CFs) and cardiomyocytes (CMs). These cells reside within a complex structure called the extracellular matrix (ECM). CFs control the ECM turnover, by producing proteins that break down and build up the ECM. Pathological conditions, like cardiac overload and myocardial infarction, induce cardiac fibrosis: the production of excess ECM, in particular collagen. The fibrotic process is initiated when CFs become activated and differentiate into myofibroblasts. Cardiac fibrosis has a functional purpose of healing necrotic myocardium, replacing dead cells and clearing ECM debris, thereby preventing further damage. However, fibrosis also has adverse effects like disturbing impulse conduction and increasing stiffness of the myocardium, hampering cardiac pump function. This thesis investigates the role of mechanical load on the function of CFs. CFs can sense mechanical forces, referred to as mechanosensing. Mechanical forces are then converted into changes in cell function via mechanotransduction.

In response to stretch, cardiac tissue produces brain natriuretic peptide (BNP), which has been suggested to have beneficial effects in heart failure patients. Cartilage intermediate layer protein 1 (CILP1) is a matricellular protein expressed by CFs which recently gained interest as a marker and pathogenic factor in cardiac disease. In this thesis, we explored the mechanism of stretch-induced changes in the genes regulating these proteins (Nppb and Cilp1, respectively).

In chapter 2 we showed that CFs subjected to cyclic stretch (1 Hz, 10%) induces a significant increase in Nppb and BNP expression, as well as induction of genes related to myofibroblast differentiation like Acta2. Myofibroblasts are characterized by the synthesis of α-smooth muscle actin (α-SMA), transcribed from the Acta2 gene. Moreover, recombinant BNP inhibites transforming growth factor (TGFβ1)-induced Acta2 expression. In a next step we were able to find strong indications for a role of Piezo, a recently discovered stretch sensitive ion channel. The effects of stretch were reproduced by stimulation with the Piezo1 agonist Yoda1. Silencing of Piezo1 reduced the stretch-induced Nppb and Tgfβ1 expression in CFs.

Further studies in chapter 3 indicated that cyclic stretch induces a significant reduction in Cilp1 gene expression as did stimulation with Yoda1. Silencing of Piezo1 caused an increased Cilp1 gene expression in both stretch and non-stretch conditions. In conclusion, our study identifies Piezo1 as mediator of stretch-induced Nppb and Tgfβ1 in CFs (chapter 2). Moreover, Piezo1 is involved in the stretch-induced downregulation of Cilp1 in CFs (chapter 3).

Increased cardiac mechanical loading caused by volume or pressure overload commonly exist over a long period of time (years). However, daily activities such as exercise create shorter lasting changes in mechanical loading (hours). The influence of such relatively short-term loading changes on CF is incompletely understood. In chapter 4 we investigated the effect of shorter periods of cyclic stretch on CF activation. Results from these studies

implicate that 1h cyclic stretch is a stimulus causing CF activation as indicated by temporary induction of early response genes: Nppb, Tenascin C, Tgfβ1 and Heat Shock Protein 70 at 4h. However, this is effect has disappeared after 24h and therefore, 1h cyclic stretch is not sufficient for sustained CF activation or initiation of myofibroblast differentiation (chapter 4). Also, a 1 hour change in stretch amplitude to 20%, during a 24 hour 10% stretch protocol did not change gene expression.

Isolation and culturing of CFs induces rapid activation of cell proliferation and differentiation toward a myofibroblast phenotype. Myofibroblast differentiation in cell culture is partly mediated by the non-physiologically high stiffness of the culture plates. In chapter 5 we have developed engineered heart matrix (EHM) by culturing CFs within a natural collagen-1 hydrogel with a physiological stiffness (Youngs modulus of ~15 kPa). Results showed that CFs were evenly distributed throughout the gels and maintain a quiescent phenotype up to 13 days of culturing. Baseline gene expression levels of markers for myofibroblast differentiation, Acta2 and Connective Tissue Growth Factor (Ctgf) were significantly lower in EHM-fibers compared to CFs cultured in 2D monolayers on silicon and hard plastic culture plates. CF baseline gene expression of Tgfβ1 and Nppb were higher in EHM-fibers compared to the monolayers. Importantly the CFs response to stimuli like stretch and TGFβ1 was maintained in EHM.

In chapter 6 we investigated the effect of longer lasting myocardial stretch in an in vivo situation, by studying the change in left atrial (LA) structure and function in a dog model of chronic mitral regurgitation (MR). This chapter was aimed at identifying potential underlying myocardial disease mechanisms using echocardiography, histology and gene expression analysis of the LA as well as computational modeling. Histology and gene expression analysis showed increased fibrosis and increased mRNA expression of collagen type 1 (Col1a1) after chronic MR, while no effect was found on genes related to CF activation and stretch, Acta2, Ctgf and Nppb. The combination of histological and echocardiographic findings along with results from computational modeling implicate that the changes in LA reservoir and contractile function are the result of a combination of eccentric hypertrophy and fibrosis.

Overall, results from this thesis have contributed to understanding the role of Piezo1 in stretch-induced changes in expression of Nppb, Tgfβ1 and Cilp1 in CF. The development of EHM showed that culturing CFs in a physiological environment keeps them quiescent, indicating stiffness is an important factor determining CF function and differentiation. The quiescent state of CFs in our EHM makes it a better model for studying the role of CFs for future research. In the bigger picture of chronic atrial volume overload, the in vivo studies showed the complexity of structural remodeling, involving a combination of eccentric hypertrophy (involving myocytes) and fibrosis (involving CFs).

Appendix

Impact

Impact

The main goal of this thesis was to investigate mechanisms of mechanosensing of cardiac fibroblasts (CFs). To this end we examined the effect of mechanical stimulation in the form of cyclic stretch on CFs, using *in vitro* models and, to study the effect of long-lasting stretch, in an *in vivo* setting of mitral regurgitation in dogs.

Scientific impact

CFs are important during healing after myocardial infarction and in the adaptation of the heart to increased mechanical load. While the repair function of fibrosis by CFs after myocardial injury is clearly beneficial, excess fibrosis causes a stiffer myocardium and conduction disorders, contributing to development of cardiac dysfunction and arrhythmia. Better understanding of the fibrotic processes may help finding ways to avoid the negative and take benefit of positive parts of the fibrotic processes.

Fibrosis, characterized by excess matrix protein deposition, occurs when CFs differentiate into myofibroblasts under the influence of different stimuli like TGFβ1 and mechanical loading.

In this thesis we have unveiled a mechanism of mechanosensing and regulation of CFs involving the mechanosensitive ion channel Piezo1 in both stretch-induced upregulation of the brain natriuretic peptide (BNP) (generally known for expression by cardiomyocytes and as plasma marker of heart failure) and the stretch-induced downregulation of Cilp1 (chapters 2 and 3). These findings may open new doors for pharmacological modulation of fibrosis, for example by stimulation of Piezo1.

Such future studies may also benefit from another part of our research: the development of a novel 3D culture system of Engineered Heart Matrix (EHM), composed of CFs cultured within a collagen-1 matrix gel. We showed that it is possible to culture CFs within the 3D EHM with a stiffness similar to that of normal healthy myocardium and that the use of such physiological stiffness results in a more quiescent CF state when compared with CFs cultured on commonly used hard plastic culture plates.

Societal impact

Heart failure forms a large social and economic burden, because it, accounts for 19% of all cardiac deaths and it required frequent hospitalizations, creating costs of half a billion euros per year in the Netherlands. Fibrosis, involving modifications of CFs, is an important factor in the development of heart failure.

Like in many other research groups, most of the CFs used in cell cultures were derived from rats, therefore involving animal experiments. During the last part of the PhD period we used Induced Pluripotent Stem Cells (iPSC's). These are human derived cells and therefore

creates opportunity to replace animal experiments. Moreover, the human nature of these cells likely increases the clinical relevance of the studies. Moreover, when the cells are taken from patients it also opens the door towards investigating patient specific treatment. The aforementioned Engineered Heart Matrix seems ideal to perform such studies with human iPSC's.

Appendix

Nederlandse samenvatting

Nederlandse samenvatting

Hartweefsel bestaat uit verschillende typen cellen, waaronder bindweefselcellen (fibroblasten) en hartspiercellen (myocyten). Al deze cellen samen bevinden zich in een dynamisch netwerk van bindweefsel dat de extracellulaire matrix (ECM) wordt genoemd. Fibroblasten kunnen eiwitten maken die de ECM afbreken en opbouwen, daarmee controleren fibroblasten het evenwicht in de eigenschappen van de ECM. Pathologische omstandigheden, zoals tijdens overbelasting van het hart of na een hartinfarct, start het proces van verbindweefseling (fibrose), waarbij fibroblasten meer ECM-eiwitten gaan maken, met name collageen. Een belangrijke eerste stap voor fibrose is de activatie van fibroblasten door de omgeving, waarbij fibroblasten zowel van uiterlijk als van functie veranderen en dan myofibroblasten worden genoemd. Fibrose heeft een functioneel doel, namelijk het genezen van het afgestorven weefsel, het vervangen van dode cellen en het opruimen van brokstukken van de ECM. Dit alles zorgt ervoor dat ergere schade aan het hart kan worden voorkomen. Echter, er zijn ook negatieve gevolgen van fibrose, zoals verstoring van de elektrische geleiding en verhoogde stijfheid van het weefsel wat de pompfunctie van het hart belemmert. In dit proefschrift is de rol van mechanische belasting op de functie van fibroblasten in het hart onderzocht. Fibroblasten kunnen namelijk mechanische krachten "voelen" wat met een engels woord "mechanosensing" wordt genoemd. Die mechanosensing leidt tot moleculaire veranderingen, uiteindelijk resulterend in veranderingen in cel functie.

Het doel van dit onderzoek was om te kijken via welke wegen mechanische stimulatie leidt tot moleculaire veranderingen en hoe we die dan eventueel kunnen sturen, zodat uiteindelijk het proces van fibrose kan worden beïnvloed.

Het grootste deel van dit proefschrift betreft onderzoek in gekweekte fibroblasten die in meer of mindere mate onderworpen werden aan rek (doorgaans 1x per seconde 10% rek).

Als gevolg van een dergelijke rek produceren de fibroblasten een aantal eiwitten, zoals "Brain Natriuretic Peptide" (BNP), "Transforming Growth Factor bèta 1" (Tgfβ1) en "Cartilage intermediate layer protein 1" (Cilp1), waarvan bekend is dat ze betrokken zijn bij hartziektes. Daarnaast zagen we verhoogde expressie van genen die gerelateerd worden aan de verandering tot myofibroblast, zoals Acta2. Interessant was dat we zagen dat het toedienen van BNP aan fibroblasten deze verandering richting myofibroblast tegenging.

Ook vonden we bewijs voor een rol voor Piezo1, een recent ontdekt eiwit dat gevoelig is voor rek. Uitschakeling van Piezo1 verhinderde in belangrijke mate de activatie van fibroblasten door rek. Bovendien konden we de effecten van rek ook verkrijgen door de Piezo-agonist Yoda1 aan ongerekte cellen te geven.

Hierop voortbordurend hebben we in hoofdstuk 3 gezien dat rek zorgt voor een verminderde expressie van Cilp1 en dat ook hier Yoda1 weer zorgt voor een identiek effect als rek in

fibroblasten. Uitschakeling van Piezo1 zorgde in dit geval voor een verhoogde expressie van Cilp1 zowel in ongerekte als in gerekte fibroblasten.

Hieruit hebben wij geconcludeerd dat de toename in expressie van BNP en Tgfβ1 door rek via Piezo1 verloopt (hoofdstuk 2). Daarnaast is Piezo1 betrokken bij de verlaging van Cilp1 expressie door rek in fibroblasten (hoofdstuk 3).

Een volgende vraag was hoe snel een toegenomen mechanische belasting leidt tot de veranderingen in de fibroblasten. Overbelasting van het hart door ziekten (hoge bloeddruk) of klepgebreken is vaak jaren aanwezig, terwijl dagelijkse activiteiten, zoals sporten, zorgen voor een korter durende (uren) belasting van het hart. In hoofdstuk 4 hebben we onderzocht naar de effecten van relatief korte rek periodes op fibroblasten. Resultaten van deze studie gaven aan dat een periode van 1 uur cyclische rek een korte activatie van fibroblasten geeft, gebaseerd op meting van verhoogde expressie van vroeg geactiveerde genen (o.a. BNP) maar niet van laat geactiveerde genen (o.a. Acta2). Deze effecten zijn verdwenen na 24 uur. *Dus een periode van 1 uur rek activeert fibroblasten maar leidt niet tot verandering naar myofibroblast*. Ook het veranderen van de sterkte van de rek voor 1 uur, 20% in plaats van 10% rek zorgt niet voor een additioneel effect op genexpressie.

Het kweken en isoleren van fibroblasten zorgt voor een snelle verandering in deze cellen, waardoor ze meer op myofibroblasten gaan lijken. Deze verandering is mede veroorzaakt door de hoge stijfheid van de kweekflessen en plastic kweekplaten die gebruikt worden tijdens de kweek en experimenten. In hoofdstuk 5 laten we de ontwikkeling zien van onze "Engineered Heart Matrix" (EHM) waarbij we fibroblasten kweken in een natuurlijke collageen hydrogel met een meer fysiologische stijfheid. We hebben aangetoond dat fibroblasten gelijk verdeeld zijn in de gel en daarnaast in kweek in leven blijven tot 13 dagen. Basale expressie niveaus van genen die betrokken zijn bij myofibroblast differentiatie zijn lager wanneer fibroblasten in EHM gekweekt vergeleken met fibroblasten gekweekt op hard plastic of siliconen in 2D.

Gebaseerd op dit expressie patroon valt op te maken dat de fibroblasten in EHM-kweek omstandigheden meer in rust stand verkeren dan wanneer ze gekweekt worden op plastic kweekplaten. Ondanks deze verandering in basale expressie niveaus zijn fibroblasten in EHM gekweekte condities nog wel in staat te reageren op stimuli zoals rek.

In hoofdstuk 6 hebben we de lange termijneffecten van rek in een proefdiermodel onderzocht. Hierbij hebben we gekeken naar de veranderingen in linkerboezem-functie en -structuur na chronische mitralisklep-lekkage in honden. We konden gebruik maken van de gegevens van een reeds eerder uitgevoerd onderzoek, zoals echobeelden, histologie en genexpressie in weefselmonsters van de linkerboezem. Daarnaast is gebruik gemaakt van een computermodel. De resultaten van de histologie en genexpressie gaven verhoogde fibrose en expressie van collageen aan in de groep na de chronische kleplekkage. Er was

echter geen effect te zien in de genen die relateren aan fibroblast activatie, zoals Acta2 en BNP. Wanneer de resultaten van de histologie, echodata en het computermodel worden samengevoegd kwamen we tot de conclusie dat *de veranderingen die we zien in de linkerboezem worden veroorzaakt door zowel excentrische hypertrofie als fibrose. De lagere waarden van Acta2 in dit chronisch model duidt op het feit dat de fase van fibroblast activatie inmiddels voorbij is.*

Alle resultaten overziend heeft dit proefschrift bijgedragen aan een beter begrip van de rol van Piezo1 in rek geïnduceerde veranderingen in de expressie van BNP, Tgfβ1 en Cilp1 in fibroblasten. De ontwikkeling van de EHM heeft aangetoond dat het kweken van fibroblasten in een fysiologische omgeving ervoor zorgt dat deze cellen meer fibroblast blijven en niet myofibroblasten worden. Het gegeven dat dit wel gebeurt wanneer ze gekweekt worden op reguliere plastic kweekplaten geeft aan dat stijfheid een belangrijke stimulus is voor fibroblasten. Om de fibroblast goed te kunnen bestuderen in zijn fysiologische staat, is ons EHM-model een beter model voor toekomstig onderzoek. In het grotere perspectief van chronische mitralisklep-lekkage heeft onze honden studie aangetoond dat de complexiteit van de structurele veranderingen in de linker boezem een combinatie zijn van zowel excentrische hypertrofie, waarbij ook myocyten bij betrokken zijn, als fibrose, waarbij met name fibroblasten van belang zijn.

Appendix

Acknowledgements

Acknowledgements

Het is inmiddels 5 jaar geleden dat ik mijn eerste dag had als nieuwe PhD student op de afdeling fysiologie. Cliché maar waar: de tijd vliegt. Met ups en downs is dit proefschrift er gekomen, mede dankzij iedereen die ik hier speciaal nog in het zonnetje wil zetten. Want zonder alle hulp en nodige afleiding was dit proefschrift er niet gekomen. Dus vooraf alvast even: bedankt allemaal!

Als eerste m'n promotieteam:
Prof. Dr. F.W. Prinzen, beste **Frits**. Vanaf het allereerste moment was het "zeg maar gewoon Frits" en dat zette de toon. Je deur stond letterlijk altijd open, voor korte vragen of gewoon even een babbeltje. En als ik dat niet deed, dan kwam je zelf even langs bij m'n kantoor. Je persoonlijke begeleiding, bereikbaarheid en beschikbaarheid zijn eigenschappen die voor jou misschien normaal zijn, maar waarvan ik weet dat het ook anders kan. Ik wil je daarvoor heel erg bedanken.

Dr. F.A. van Nieuwehoven, beste **Frans**. Op m'n allereerste dag heb je mij de afdeling laten zien, me voorgesteld aan iedereen, laten zien waar ik koffie kan halen en me m'n (tijdelijke) kantoor laten zien. Ook bij jou stond letterlijk de deur altijd open, ook als je er zelf niet was. Je was nooit te beroerd om zelf op het lab nog je handen uit de mouwen te steken of om even mee te kijken naar de confluentie van de cellen, ondanks je eigen drukke agenda. Bedankt voor je betrokkenheid.

Frits, Frans, als dit proefschrift over jullie zou gaan zou de titel luiden: Begeleiding, Bereikbaarheid, Beschikbaarheid & Betrokkenheid: promoveren bij Frits & Frans. Dank jullie wel.

Dear members of the reading committee: **Prof. Dr. Uli Schotten**, **Prof. Dr. Blanche Schroen**, **Prof. Dr. Marie-Jose Goumans**, **Dr. Matthijs Blankesteijn** and **Remi Peyronnet, PhD**, thank you so much for your interest in my thesis and participating in the assessment committee. I hope you have read my thesis with great pleasure.

I would also like to thank all of the co-authors who have contributed to the chapters published in this thesis.

Zonder experimenten, geen resultaten en zonder resultaten komt er geen proefschrift. En zonder **Chantal** waren er geen experimenten geweest. Dank je wel voor je oneindige kennis op het lab, over cel kweek, RNA-isolaties, qPCRs, maar bovenal ook je gezelligheid op het lab. Daarnaast wil ik je bedanken voor je handige trucjes, zoals het verplaatsen van een epje nadat je een handeling hebt gedaan, waardoor vergissen niet meer mogelijk was en waardoor menig experiment niet opnieuw hoefde. Dank je wel!

De dag waarop ik niet even een vraag kon stellen is nooit gekomen, **Jolanda**. Dank je wel voor alle hulp! Soms waren het kleine dingen zoals pennen, kladblokken, linialen of post-its die ik nodig had. Soms waren het grotere dingen: waar vind ik bepaalde informatie, het plaatsen van een bestelling of het organiseren van meetings. Groot of klein, niks was te gek en geen vraag raar. Ik ga jou en onze dagelijkse lunch wandelingen ontzettend missen. Ik denk dat het secretariaat het hart van fysiologie is, mede dankzij jou. Ook wil ik graag **Bianca** en **Vivian** bedanken die voor jou, hier hun steentje aan hebben bijgedragen.

We grapten samen dat dit zowel Frits z'n grootste fout als beste beslissing ooit was, maar wat ben ik blij dat ik een kantoor met jou mocht delen, **Nienke**. Dat ze ons gelach konden horen tot aan het secretariaat geeft aan hoe gezellig we het gehad hebben. Dat we beiden onze PhD gehaald hebben geeft aan hoe hard er gewerkt is. De oneindige tripjes naar het ziekenhuis om "lekkere koffie" te halen, met een koekje erbij, we waren inmiddels vaste klant en hoefde onze bestelling al niet meer door te geven. Je bood me een luisterend oor en je kennis als "oudere Phd-student" kwam mij vooral in het begin heel erg van pas. Kennis die ik ook al heb mogen overdragen aan nieuwe PhD studenten. Ook vonden we steun bij elkaar in onze gedeelde smart wat betreft groot proefdieronderzoek, het zat meer tegen dan mee, maar samen zijn we er doorheen gekomen. Ik wil je er allemaal heel erg voor bedanken, maar specifiek nog even voor het feit dat je m'n paranimf bent.

Elisa, I remember looking up at you for being an "older PhD-student" but pretty soon you made me feel like I was part of the group. Being almost neighbors, with only 1 office in between yours (and Billy's) and mine and Nienke's, the three of us became close friends. Signified by our Whatsapp group: Nina, Pinta & Santa Maria. I can't believe I answered the Physiology Pubquiz question wrong about the ships of Christopher Columbus, when our whatsapp group was the correct answer! I still remember that one look we exchanged in the lab, signifying our hectic day at the lab, which at that point made us both laugh. It was a great honor being your paranymph at your defense and thank you for returning the favor. Outside the office we went for drinks, dinners or PhD academy activities for some much-needed relaxation. In the lab I could always count on your help and vice versa. Thank you for everything!

Door corona heb ik een hele tijd een kantoor voor mij alleen gehad, een luxe, maar ik was blij toen daar verandering in kwam, **Uyên**. We hadden al eens eerder samen een kantoor gedeeld, toen ik net begonnen was als PhD student en jij vlak daarna de kliniek in ging. Het wederzijds een spiegel voorhouden heeft mij veel gebracht en ik kijk op hoe jij het allemaal doet: je gezin, de kliniek en de wetenschap. Je doet het allemaal maar als "geluksvogel verkapt als harde werker". Wat ik niet wist is dat dat jij ook **Karin** in ons kantoor zou brengen, als PhD student op jouw Dekkerbeurs. Het klikte gewoon meteen. Met z'n drieën was het een beetje krap op kantoor, maar dat mocht de pret niet drukken. Jullie portemonnees zijn mij misschien iets minder dankbaar, aangezien ik jullie allebei aangestoken heb met het

"Fabienne Chapot-virus". Maar ik wil jullie allebei heel erg bedanken voor de gezelligheid tijdens de laatste maanden van m'n PhD.

Hoewel de varkensexperimenten het niet hebben gered tot in m'n proefschrift wil ik m'n **piggies** toch bedanken. Dat gezegd hebbende wil ook de mensen van CPV proefdiergroot bedanken voor alle goede zorgen en betrokkenheid: **Inger**, **Huub**, **Petra, Saskia** en **Rachelle**. **Marion**, bedankt voor je expertise en operatie skills, het zat niet altijd mee, maar koekjes en chocolade maakte veel goed. **Luuk**, bedankt voor je hulp bij alle proefdier experimenten en bij het assisteren van Marion. Steriel staan was mij niet bekend, maar jou ging het goed af en als een geoliede machine stonden jullie te werken. Ook wil ik **Lars** bedanken voor de data van het hondenmodel.

Er is een nauwe samenwerking tussen de afdeling Fysiologie en **Biomedische Technologie**, waaruit de TRANCE-meeting is gekomen, voorheen CRT-meeting. Ik wil de mensen van BMT heel erg bedanken door met een open blik naar mijn cel werk resultaten te kijken, die resultaten staan toch ver weg van computermodellen of de kliniek, maar ik voelde me altijd gewaardeerd in de groep. Dank voor jullie kritische vragen en opmerkingen op m'n presentaties.

As a PhD student at the department, you're never alone: **Moedi**, **Jolijn**, **Floor**, **Hongxing**, **Philip** and **Mehrdad** thanks for your input during presentations, critical questions but also for chit chat at the coffee machine or "gezelligheid" at the Day Out of the department. And even though I was part of Frits' group and meetings were separated from those from Uli's group we found each other: **Billy**, **Vladimir**, **Zarina**, **Ozan**, **Victor**, **Michal** and **Joris**. With you guys it was mostly fun since we did not share scientific meetings; which resulted in helping each other out at the OR, zooming during the Coffee Break meetings, having vlaai in the coffee room, having lunch together or taking a much needed (coffee or tea) break. Thank you all!

I would like to thank all the students who temporarily joined the department, in particular **Parniyan**, you were the first student I ever had to help me with the EHM project, which was back then still in its infancy. Thank you for making that bold choice, you could have chosen something easier, but this says something about the scientist you are. Thank you for helping me with the steps it took to bring EHM where it is now in this thesis.

Tayeba, niet voor niets verdien jij een plekje in de auteurs lijst van het EHM-hoofdstuk, jouw bijdrage als student zijn van enorme waarde gebleken. Dat door corona je praktische stage deels in het water is gevallen, vergeten we daarom maar even. Dank je wel voor je bijdrage, zowel in de wetenschap als in gezelligheid!

De afdeling fysiologie bestaat uit meer dan alleen het secretariaat en Phd-studenten, die mensen wil ik ook bedanken voor hun bijdrage: **Sander**, **Marc**, **Nynke**, **Daniel**, **Mick**,

Geertje, **Stef, Aaron, Ed**, **Bas**, **Richard, Arne, Ben** en **Andries**. Allemaal hebben jullie je steentje bijgedragen, misschien heel klein zoals het laten zien van hoe de microscoop werkt, m'n paper kritisch lezen, me weer eens wat lenen wat op was op het lab, me een hart onder de riem steken dat dat proefschrift er echt wel komt, gewoon een luchtig gesprek of een grapje hier en daar. Misschien heel klein, maar alle kleine beetjes dragen bij tot wat hier nu ligt. Dank jullie wel.

Ook buiten de afdeling fysiologie zijn er mensen die ik wil bedanken. Als eerste **Annika**, al telt dat niet helemaal want je was zowel onderdeel van de afdeling Cardiologie als Fysiologie. We deelde soms het lab omdat je gebruik maakte van onze cellen en regelmatig hadden we daar samen discussies over, vooral wanneer ze niet groeiden en de confluentie te laag bleef. Omdat je deels bij de afdeling fysiologie zat ging je ook altijd mee op onze uitjes en nam deel aan onze kerstborrels, heel erg gezellig, dank je wel!

We leerde elkaar kennen tijdens de proefdier cursus en het klikte meteen, **Relinde**. Die Brabantse nuchterheid en gezelligheid herkende ik meteen en het voelde eigenlijk alsof we elkaar al langer kende. We spreken elkaar misschien niet zo vaak, maar pakken de draad meteen weer op zodra we elkaar zien. Dank je wel voor al je tips en "maak je niet te druk" support.

Buiten de muren van de UM zijn er ook mensen die ik wil bedanken, sommige die een PhD gedaan hebben, anderen die er geen kaas van gegeten hebben of aangeven dat het "hun pet te boven gaat", maar allemaal stuk voor stuk hebben ze bijgedragen aan wat hier nu staat. Lieve GirlsLoveGirls: **Darlyne**, **Evelyne**, **Simone**, **Eline** en **Vera**. We kennen elkaar nu al meer dan 10 jaar, vanaf het allereerste begin van onze studie in Groningen. Bedankt voor alle feestjes, theetjes, high tea's, gala's, dinertjes, (dierentuin)uitjes en corona skype-gesprekken. Zonder deze afleiding was het allemaal een stuk minder leuk geweest. Ook wil ik **Maeve** bedanken, als "next-generation" hoort ook zij bij de GirlsLoveGirls. Er was geen GirlsLoveGirls geweest zonder de Collegebeesten: **Maarten**, **Huub**, **Laurens**, **Sebastiaan**, **Tim** en **Reinoud** bedankt! Tijdens corona niet zoveel gesproken, maar een reünie bleek zo gepland! Het was weer zoals vanouds gezellig, dank jullie wel.

Lieve **Rian**, **Laura** en **Mariska**, al vriendinnen vanaf de middelbare school: time flies when you're having fun! Dank jullie wel voor de nodige afleiding tussendoor, luisterend oor, de spelletjes avonden, weekendjes naar Brugge, vakanties naar Kos of feestjes in de Groene Schuur. Dank je wel dat jullie er waren, in goede en slechte tijden.

Jesse, **Robin**, **Rick**, **Jelmer**, **Pascale** en **Cetanya**, bedankt voor de gezellige (kroeg)avonden, terrasjes en uitjes samen in Zeewolde, het heeft gezorgd voor de nodige afleiding. De boog kan ten slotte niet altijd gespannen staan.

Support did not only come from the Netherlands, **Jessica**, when I became your roommate in Boston you took me under your wing, showed me around icy and snowy Boston ("did you bring your other winter coat?"), introduced me to all your friends, who I now also consider my friends and we connected over our mutual experience of going abroad. Little did we know that this turned in to a strong friendship. Thank you so much for being a true friend, for supporting me and for always cheering me on. I would also like to thank your family, **Cathi** and **Sarah**, who have shown such love and support to me, it warms my heart. I know I'll always have a place to stay when visiting Boston or in the USA if you ever decide to move somewhere else.

Joop, dank je wel voor je ondersteuning en praktische tips, waardoor ik het mezelf iets makkelijker kon maken. Dank je wel voor die inzichten, mede daardoor ligt hier iets wat misschien niet perfect is, maar dat is oké.

Er zijn vrienden die je al zo lang kent, dat het familie geworden is. Zo iemand ben jij **Anne**, en daarmee ook de rest van jouw gezin: **Lucas**, **Niek** en **Daan**. Dank je wel dat je er altijd voor me bent. Familie de Vries, **Marja** en **Pieter**, maar ook **Sjoerd**, **Fraukje** en **Lynn**, dank jullie wel, voor veel meer dan alleen de betrokkenheid rondom m'n proefschrift.

Roos, we zijn op papier geen familie, maar zo voelt het wel, je bent als een tante voor mij. Mam en jij zijn al vriendinnen sinds de middelbare school, waardoor ik jou al m'n hele leven ken. Jouw onafhankelijkheid is iets waar ik altijd naar heb opgekeken, je dopte altijd zelf je boontjes en had het goed voor elkaar. Dank je wel voor dit voorbeeld.

Dat familie belangrijk was wist ik al, maar is me de afgelopen tijd nog meer duidelijk geworden. Familie Ploeg: **Loek**, **Yvon**, **Douwe**, **Bas** en **Lotte**; Familie Vrancken: **Mike**, **Jeanny**, **Sander**, **Mandy**, **Anouk**, **Dustin**, **Faye**, **Jade** en **Bart**; Familie van Rennes: **Pien**, **Geurt**, **Jan**, **Sharida**, **Tom** en **Nancy**. Voor familie is het misschien vanzelfsprekend, maar als er iets is wat ik geleerd heb is dat niets vanzelfsprekend is dus bij deze: heel erg bedankt allemaal!

Wes(sel), vroeger konden we niet met of zonder elkaar, maar de afgelopen jaren is het vooral met elkaar, twee handen op 1 buik. Ik kan een heel epistel schrijven over hoe blij en dankbaar ik ben, maar dat zal ik je besparen. Want aan een half woord hebben wij al genoeg. Bedankt broer(tje)!

Lieve **Mam**, dank je wel voor alles! De keren dat jij hebt moeten aanhoren dat ik er mee wilde stoppen en het allemaal in de prullenbak wilde gooien zijn niet meer op één hand te tellen, maar goed: we zijn er! Ik zeg we, want mede dankzij jou (en pap) ben ik gekomen waar ik nu ben. Jullie hebben altijd achter m'n keuzes gestaan, ook als ik daar later op terug kwam. Maar door jouw support (en die van pap) ligt hier nu wel iets waarvan ik zeker weet dat je heel trots bent. Dank je wel!

Bij een wetenschappelijk artikel zijn de eerste en de laatste auteur het belangrijkste. De eerste van het proefschrift ben ik zelf, die laatste plek is voor jou, **Pap**. Lieve Pap, dat je er niet bij kan zijn en nooit het eindresultaat van m'n proefschrift hebt kunnen zien, is het grootste gemis dat er is, daar zijn eigenlijk geen woorden voor. Maar wat zou je trots zijn geweest, dat weet ik zeker! Ik ben de belofte die ik tijdens de crematie gedaan heb "ik zal de eerste Dr. Ploeg worden" nagekomen. Hier ligt het bewijs. Dank je wel voor alles pap!

Appendix

About the author

About the author

Meike Christianne Ploeg was born in Zeewolde, The Netherlands, on the 6th of February in 1993. After completing high school at RSG Slingerbos in Harderwijk in 2011, she moved to Groningen to study at the University of Groningen. She successfully finished the bachelors program Biology with a double major in both Biomedical Sciences and Behavior & Neurosciences in 2015.

Subsequently she continued her studies at the University of Groningen where she obtained her Master of Science degree in Biomedical Sciences in 2017. As part of her studies she performed two research internships. The first focused on the effects of pre- and post-natal smoke exposure on SIRT1 expression and inflammation in mouse offspring and was performed at the department of Pathology and Medical Biology (UMC Groningen) under supervision of Dr. Machteld Hylkema. The second project was about setting up a new model using mouse cardiac slices to test cardiotoxicity and to bridge the gap between cell assays and intact animals, which was performed at the Centre for Vascular Biology Research (Harvard Medical School, Beth Israel Deaconess Medical Center, Boston, USA) under supervision of Dr. Ramaswamy Krishnan. For her research at Harvard Medical School Meike was awarded with the "Holland Scholarship for outbound student mobility" by the University of Groningen, which is financed by the Dutch Ministry of Education, Culture and Science and Dutch research universities and universities of applied sciences. Moreover, she was awarded with a "Dekkerbeurs for a non-medical student" by the Dutch Heart Foundation for her research internship at Harvard Medical School. During her second research internship Meike wrote a PhD project proposal under the supervision of Prof. Dr. Janette Burgess (University of Groningen) for which she was awarded The Avril McDonald Award by the Rosalind Franklin Fellows of the University of Groningen. This award is awarded each year to support excellent female scientists in pursuing an academic career.

In 2017, she started her PhD at the department of Physiology (Maastricht University) under the supervision of Prof. Dr. Frits Prinzen and Dr. Frans van Nieuwenhoven. The results of her PhD trajectory are published in this thesis.